



### This is to certify that the

#### dissertation entitled

#### THERMAL AND ELECTRICAL PROPERTIES OF ELECTRIDES

presented by

KEVIN JAMES MOEGGENBORG

has been accepted towards fulfillment of the requirements for

Ph.D. degree in Physical Chemistry

Major professor

Date 1.12-90

MSU is an Affirmative Action/Equal Opportunity Institution

0-12771

LIBRARY Michigan State University

PLACE IN RETURN BOX to remove this checkout from your record. TO AVOID FINES return on or before date due.

DATE DUE	DATE DUE	DATE DUE

MSU is An Affirmative Action/Equal Opportunity Institution c:/circ\datadus.pm3-p.1

### THERMAL AND ELECTRICAL PROPERTIES OF ELECTRIDES

bу

Kevin James Moeggenborg

### **A DISSERTATION**

Submitted to
Michigan State University
in partial fulfillment of the requirements
for the degree of

DOCTOR OF PHILOSOPHY

Department of Chemistry

1990

#### **ABSTRACT**

### THERMAL AND ELECTRICAL PROPERTIES OF ELECTRIDES

#### b y

# Kevin James Moeggenborg

The thermal and electrical properties of electrides were explored. A method to determine the stability and decomposition kinetics of electrides at a single temperature was developed. The method uses Differential Scanning Calorimetry and was applied to two electrides. A sample of Li+(PMPCY)e- underwent a first-order decomposition reaction with a half life of 110 hrs at room temperature while a sample of K+(C222)e- decomposed autocatalytically and was stable for less than 2 days at -57 °C. The results point to two different mechanisms of decomposition in electrides. Visual observations combined with Differential Scanning Calorimetry show color to be a poor indicator of the extent of decomposition of electrides.

The electrical properties of several electrides were investigated through Impedance Spectroscopy and a.c. and d.c. conductivity methods. Instrumentation was computer interfaced through IEEE-488 control busses. Instrumental control and data acquisition

programs were written and were applied through an IBM PC/XT computer.

The electrides investigated exhibited a wide variety of electrical properties. D.C. conductivity studies of K<sup>+</sup>(C222)e<sup>-</sup> indicated a low band gap but high apparent resistivity for the compound. The compound exhibited a marked non-Ohmic behavior. Through the use of impedance spectroscopy, the high apparent resistivity and non-Ohmic behavior were found to be due to a Schottky barrier at the sample-electrode interface of the measurement cell. The use of potassium metal as an electrode material decreased the resistance of the barrier by four orders of magnitude. Four probe a.c. conductivity experiments which used a van der Pauw configuration on a cylindrical sample pellet were These measurements revealed a band gap of 0.086 eV performed. for the compound and placed an upper limit of 0.189  $\Omega$ cm at 130 K on the resistivity of the compound. The band gap of the compound may be due to the activated transfer of electrons across grain boundaries in the polycrystalline samples.

The electrides Cs+(15C5)<sub>2</sub>e<sup>-</sup> and Cs+(18C6)<sub>2</sub>e<sup>-</sup> were shown to exhibit the first ionic conductivity ever seen in electrides. Cs+(15C5)<sub>2</sub>e<sup>-</sup> undergoes a transition from defect electronic conductivity to ionic conductivity, the latter having an activation energy of 0.7 eV. Similar behavior was observed with Cs+(18C6)<sub>2</sub>e<sup>-</sup> which has an activation energy of 1.0 eV for ionic conduction. Both compounds exhibited electrochemical cell behavior when placed between one cesium and one stainless steel electrode. The mechanism of the ionic conductivity is unknown, but is believed to

involve the initial release of the cesium cation from its crown ether cage coupled with its reduction by an electron anion of the compound. Cs<sup>+</sup> is then transferred between anionic sites in the crystal lattice. The apparent semiconductor behavior previously seen in Cs<sup>+</sup>(18C6)<sub>2</sub>e<sup>-</sup> was shown to be due to the doping of the compound with small amounts of ceside which increases the electronic conductivity sufficiently to give semiconductor behavior.

Partial electrical conductivity results on several other compounds were also collected. Li+(PMPCY)e- appears to be an extrinsic semiconductor doped by lithium metal. Results on Li+(TMPAND)e- indicate that it may be the first insulating electride. No measurable conductivity was observed for this compound up to its decomposition point. The d.c. conductivity of Rb+(C222)e-revealed an apparent band gap of only 0.065 eV.

To my wife Maureen who has been forced to learn almost as much chemistry in the past five years as I have and whose constant love and support made this work possible.

#### **ACKNOWLEDGEMENTS**

I would like to express my appreciation to Dr. James L. Dye for his constant support and guidance during the course of this work. I would also like to thank Drs. William P. Pratt, Jr., and Michael Dubson of the Physics Department for their helpful advice on many aspects of this work.

I would also like to thank all the members of the Dye research group with whom I have worked, in particular Rui Huang, Lauren Hill-McMills, Mark Kuchenmeister, Jineun Kim, and especially Judith Eglin for their help, advice, and support. I would like to thank Dr. John Papaioannou for his help in beginning my research. I would also like to express my appreciation to master glassblowers Keki Mistry, Manfred Langer, and Scott Bancroft for the numerous cells that they designed, built, and repaired for me.

Finally, I would like to thank Shiela Kolb who is largely responsible for my interest in chemistry and my decision to pursue it as a career.

I am grateful to have received financial support from the National Science Foundation grants nos. DMR-84-14154 and DMR-87-14751. Additional support from the Michigan State University Center for Fundamental Materials Research is also acknowledged.

# TABLE OF CONTENTS

		Page
	TABLE OF CONTENTS	vii
	LIST OF TABLES	ix
	LIST OF FIGURES	х
I.	Introduction and Background	1
	I.A. Introduction	1
	I.B. Alkalides and Electrides	3
	I.C. Electrical Conductivity	6
	1. Background Information	6
	2. Conductivity of Alkalides and Electrides	11
II.	Experimental	20
	II.A. Synthesis of Doped Electrides	20
	II.B. Magnetic Susceptibility	21
	II.C. Differential Scanning Calorimetry	23
	II.D. Conductivity Methods and Instrumentation	24
	1. Conductivity Cells	24
	a. 2-Probe Cell	24
	b. 4-Probe Cell	26
	c. Impedance Cell	27
	2. Temperature Control and Measurement	27
	3. General Handling	32
	4. Alkali Metal Electrodes	33
	5. Pressed Pellet Formation	33
	6. D.C. Conductivity Methods	35
	7. Impedance Spectroscopy and A.C. Conductivity	40
III	Decomposition of Electrides	42
	III.A. Introduction	
	III.B. Differential Scanning Calorimetry	

	1. Kissinger Method	44
	2. Ozawa Method	45
	3. Isothermal Stability and Kinetics Measurements	47
	III.C. Results and Discussion	48
	1. Li+(PMPCY)e	48
	2. K+(C222)e	54
	III.D. Conclusions	60
IV.	Electrical Properties of Electrides	62
	IV.A. Theory	62
	1. Polycrystalline Conductivity Problems	62
	a. Orientational and Packing Problems	63
	b. Grain Boundary Effects	64
	c. Electrode Effects	65
	2. Van der Pauw Method	73
	3. Impedance Spectroscopy	76
	IV.B. Results and Discussion	86
	1. K+(C222)e	86
	2. Cs+(15C5) <sub>2</sub> e	105
	3. Cs+(18C6) <sub>2</sub> e	118
	4. Miscellaneous	132
	a. Li+(PMPCY)e	133
	b. Li+(TMPAND)e- and Li+(TMPAND)Na	135
	c. Rb+(C222)e	
	d. Others	138
V.	Conclusions and Suggestions for Further Work	140
	V.A. Conclusions	
	V.B. Suggestions for Further Work	143
	APPENDIX	146
	REFERENCES	164

# LIST OF TABLES

1.	Band gaps and references for alkalides and electrides for which conductivity measurements	
	have been attempted.	.17
2.	Conductivity data for electrides studied in this work	41

# LIST OF FIGURES

1	Representative complexants a) 15-crown-5 (15C5) b) cryptand[2.2.2] (C222) c) pentamethylpentacyclen (PMPCY)
2	a) Band structure of a semiconductor at low temperature, E <sub>g</sub> is the band gap between the valence and conduction bands. b) Semiconductor at higher temperatures where some electrons have been excited into the conduction band creating two partially filled bands in which conduction can occur.
3	Simplified band structure showing the effects of  a) p-type doping, and b) n-type doping at non-zero temperatures where excitation has occurred
4	The 2-probe d.c. conductivity cell. Both electrodes are stainless steel, the sample chamber is a glass tube, and the body of the cell is brass. The top electrode is spring loaded to ensure that good pressure contacts between the sample and the electrodes are maintained
5	The 4-probe conductivity cell. The four pogo stick electrodes are arranged in a square configuration to contact the sample pellet near its perimeter27
6	The I.S. cell. The top electrode and bottom plate are both stainless steel, the cell body is brass, and the sample chamber is Delrin. The top electrode is spring loaded to make pressure contacts between the sample and electrodes.
7	The pellet die used to make pellet samples for

	conductivity measurements. The body of the die is hardened steel and the piston is carbide steel	34
8	Li+(PMPCY)e- DSC trace from -40 °C through the	
	decomposition.	49
9	Activation analysis of Li <sup>+</sup> (PMPCY)e <sup>-</sup> , a) Kissinger method, b) Ozawa method	50
10	Li <sup>+</sup> (PMPCY)e <sup>-</sup> first order kinetics, ln(enthalpy) versus time at 23 °C.	53
11	a) DSC trace of K <sup>+</sup> (C222)e <sup>-</sup> showing the large	
	temperature overshoot, and b) disruption of the heating rate.	55
12	Activation energy analysis of K <sup>+</sup> (C222)e <sup>-</sup> , a) Kissinger method, and b) Ozawa method.	57
13	K+(C222)e- long term kinetics at -57 °C, enthalpy of reaction versus time at -57 °C.	59
14	Band diagram for two semiconductor grains and their contact region. a) The grains and their boundary as three isolated materials. b) The contact at thermal equilibrium. c) boundary region under an applied voltage V.	66
15	A) Oxide barrier at thermal equilibrium between two metals. B) Oxide layer under an applied voltage V	68
16	Energy band diagrams of a metal-semiconductor contact. Left: Energy levels before contact, Right: Energy levels and Schottky barrier at thermal equilibrium after contact.	70

17	a) Placement of electrical contacts in the van
	der Pauw method. b) Placement of electrical
	contacts to simplify data reduction in a
	symmetric sample75
18	Representation of the impedance vector Z in
	the complex plane showing the phase angle φ,
	magnitude  Z , and the real and imaginary
	components Z' and Z'', respectively78
19	Representations of a perfect inductor (L),
	capacitor (C), and resistor (R), in the complex plane79
20	a) RC circuit representing an ideal single phase
	material b) The impedance spectrum of that circuit81
21	a) The equivalent circuit for an ideal two phase
	system and b) the impedance spectrum of that circuit83
22	The temperature dependence of the resistance of
	K+(C222)e <sup>-</sup> plotted as ln R versus 1/T88
23	Ohm's law plot for K+(C222)e- showing the extreme
	non-linearity observed in d.c. conductivity data89
	·
24	Impedance arc for K+(C222)e- at -147.5 °C and 20 mV91
	-
25	Impedance arc of K <sup>+</sup> (C222)e <sup>-</sup> at three voltages
	showing the large dependence of the impedance
	on applied voltage92
	••
26	Voltage dependence of the impedance arc of
	K+(C222)e- with gold electrodes at -184.4 °C94
27	K+(C222)e- impedance arc for a sample in contact
	with potassium electrodes at -183 °C95

28	a) Impedance spectrum of K+(C222)K- with steel electrodes at -143 °C. b) Impedance spectrum for K+(C222)K- between potassium electrodes at -169 °C97
29	Ohm's law data from a sample of K <sup>+</sup> (C222)e <sup>-</sup> between one potassium and one stainless steel electrode99
30	Plot of ln (I) versus applied voltage from Ohm's  Law data of K+(C222)e
3 1	Four probe conductivity of K <sup>+</sup> (C222)e <sup>-</sup> 103
32	The impedance spectrum of Cs <sup>+</sup> (15C5) <sub>2</sub> e <sup>-</sup> at -17.2 °C and 20 mV107
33	The d.c. conductivity of Cs <sup>+</sup> (15C5) <sub>2</sub> e <sup>-</sup> showing the low and high temperature activation energies108
34	Ohm's law plot from the high temperature conductivity region of Cs <sup>+</sup> (15C5) <sub>2</sub> e <sup>-</sup> 111
35	Ohm's law plot of data from the electrochemical cell formed by placing Cs+(15C5) <sub>2</sub> e <sup>-</sup> between one cesium and one steel electrode.
36	Ohm's law plot for a sample of Cs <sup>+</sup> (15C5) <sub>2</sub> e <sup>-</sup> between two cesium metal electrodes
37	The d.c. conductivity of Cs <sup>+</sup> (15C5) <sub>2</sub> Cs <sup>-</sup> 117
38	The conductivity of two samples of Cs <sup>+</sup> (18C6) <sub>2</sub> e <sup>-</sup> taken from two different syntheses
39	Ohm's law plot for Cs+(18C6) <sub>2</sub> e <sup>-</sup> at -39.2 °C122

40	Ohm's law plot of Cs <sup>+</sup> (18C6) <sub>2</sub> e <sup>-</sup> between one steel
	and one cesium electrode at -33.4 °C and 60 s on bias123
4 1	Ohm's law plot for Cs <sup>+</sup> (18C6) <sub>2</sub> e <sup>-</sup> between two
	cesium electrodes at -34.4 °C124
42	The conductivity of Cs <sup>+</sup> (18C6) <sub>2</sub> e <sup>-</sup> doped with cesium127
43	Ohm's law plot for a sample of Cs <sup>+</sup> (18C6) <sub>2</sub> e <sup>-</sup> doped with cesium and held between one cesium and one
	steel electrode at -51 °C
44	The conductivity of Cs <sup>+</sup> (18C6) <sub>2</sub> Cs <sup>-</sup> 129
45	The conductivity of Cs <sup>+</sup> (18C6) <sub>2</sub> e <sup>-</sup> doped with sodium133
46	The d.c. conductivity of Li <sup>+</sup> (PMPCY)e <sup>-</sup> showing the
	break in semiconductor behavior attributed to a solid-solid phase transition
47	The d.c. conductivity of Li+(TMPAND)Na- showing the
	onset of conductivity at the solid-solid phase transition137
48	The d.c. conductivity of Rb+(C222)e139

### I. INTRODUCTION AND BACKGROUND

### I.A. Introduction

Since 1864 when Weyl discovered that alkali metals dissolve in liquid ammonia, the study of metal ammonia solutions has been an active area of chemical research. These solutions are blue when dilute (<10-3 M) and metallic bronze at higher metal concentrations. The two major species present in dilute solutions are the solvated electron (e-solv) and the solvated metal cation (M+solv). The formation of these species follows the equation:

$$M_{(s)} + NH_{3(l)} = M^{+}_{solv} + e^{-}_{solv}$$
 (1)

In more concentrated solutions, these species exist as an associated ion pair species held together by the attractive coulomb potential between the ions.<sup>2</sup>

The alkali metals are very soluble in liquid ammonia. The saturation concentration is almost 20 mole percent metal for lithium and 16 mole percent metal for sodium, potassium, and rubidium. Cesium at its melting point is soluble in ammonia in all proportions. As the metal concentration is increased from 3 to 8 mole percent metal, these solutions undergo a non-metal to metal transition. Above 8 mole percent metal, the solutions have a high electrical

conductivity (generally >10<sup>3</sup>  $\Omega^{-1}$ cm<sup>-1</sup>) which in some cases can exceed that of liquid mercury.<sup>3</sup>

In addition to ammonia, alkali metals have limited solubilities in certain amines. As in metal ammonia solutions, the species M<sup>+</sup><sub>solv</sub> and e<sup>-</sup><sub>solv</sub> are present in metal amine solutions. Unlike metal ammonia solutions, metal amine solutions can also contain solvated alkali metal anions whose concentration is dependent upon both the solvent and the metal concentration.

In the late 1960's Pedersen and Lehn developed two new classes of compounds which they called crown ethers<sup>4</sup> and cryptands<sup>5</sup>, respectively. Crown ethers are cyclic polyethers while cryptands are bicyclic polyethers. Both of these classes of compounds were quickly shown to complex metal cations very strongly.<sup>4,6</sup>

Dye and coworkers were the first to use crown ethers and cryptands in metal amine solutions. Through the use of these complexants, it was shown that alkali metals could be solubilized in solvents which would not otherwise dissolve alkali metals.<sup>7,8</sup> The most important equilibria involved in the process of solubilization are:

$$M_s + C \implies M^+C_{solv} + e^-_{solv}$$
 (2)

$$M_s + e_{solv} = M$$

where M is the alkali metal and C is the complexant molecule. It can be seen that the use of excess complexant has the net effect of producing mostly solvated electrons as the anionic species while excess metal tends to favor the formation of the alkali metal anion.

### I.B. Alkalides and Electrides

It was the work on metal amine solutions that led to the current studies of alkalides and electrides. Dye and coworkers were able to precipitate the first alkalide, Na+(cryptand[2.2.2])Na-, from an ethylamine solution of sodium and cryptand[2.2.2] (C222) in 1974.9,10 Na+(C222)Na- was the first solid to contain an alkali metal anion in its structure. By careful control of stoichiometry Dye was later able to synthesize Cs+(18-crown-6)<sub>2</sub>e- in which stoichiometric amounts of trapped electrons serve as the anion in the structure. This was the first member of a new series of crystalline compounds, the electrides.

Since 1974, over 30 alkalides and 8 electrides have been synthesized. It is necessary to complex the cations in alkalides and electrides to prevent their reduction by the unique anions of these systems. The complexants that have been used are crown ethers, cryptands, and more recently, aza analogs of crown ethers<sup>12</sup> and cryptands.<sup>13</sup> In addition, it is possible, in some cases, to make simple alkalides by using small amines and diamines as complexants.<sup>14</sup> The structural formulas of three typical complexants, 15-crown-5, cryptand[2.2.2], and pentamethylpentacyclen are shown in Figure 1.

Alkalides and electrides are very air, temperature, and moisture sensitive. Because of this, these compounds must be handled and stored at low temperatures and under inert atmosphere

or vacuum conditions.<sup>15,16</sup> Although the extent of thermal instability varies, alkalides tend to be more stable than electrides. A few alkalides and electrides are stable at room temperature for short periods of time in vacuo. Typically, however, alkalides and electrides must be handled below -20°C to avoid thermal decomposition. For long term storage, alkalides are normally kept below -70°C while most electrides are stored at liquid nitrogen temperature (77 K).

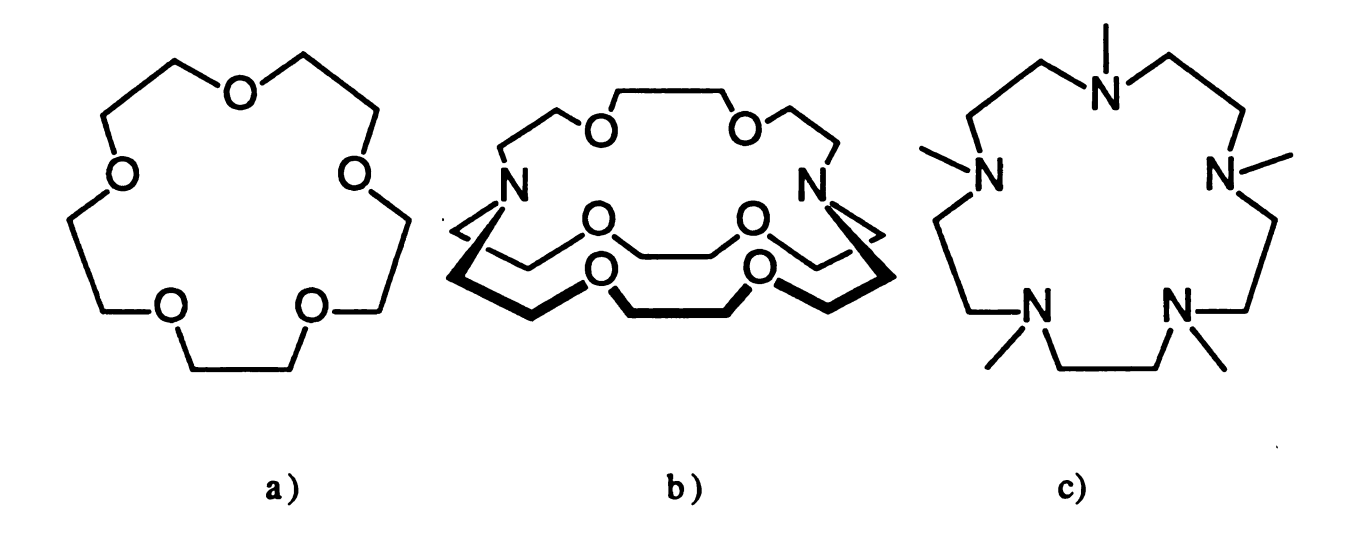


Figure 1. Representative complexants a) 15-crown-5 (15C5) b) cryptand[2.2.2] (C222) c) pentamethylpentacyclen (PMPCY).

Attempts to synthesize more stable alkalides and electrides have utilized the aza complexants mentioned above. Compared to crown ethers and cryptands, aza compounds tend to be more resistant to reductive decomposition.<sup>17</sup> These compounds do have smaller complexation constants toward alkali metal cations which means that alkalides and electrides made by using aza

complexants tend to decomplex when warmed. One such complexant, hexamethylhexacyclen (HMHCY) has been shown to form several fairly stable alkalide compounds. Two of these compounds, K+(HMHCY)Na- and Cs+(HMHCY)Na-, decomplex only slowly (about 4 days) in vacuo at room temperature. Results with other aza complexants indicate that further stability may be achieved by complete encapsulation of the cation in a tightly fitting complexant molecule. 17,19

Synthesis of alkalides and electrides would be straightforward were it not for the inherent reactivities of both the reactants and the products. This problem requires that syntheses be carried out under vacuum and low temperature conditions. The synthesis of alkalides and electrides has been described in detail elsewhere<sup>20,21</sup> so only a brief description will be given here. Alkalide and electride synthesis involves the introduction of the proper ratios of alkali metal(s) and complexant into a reaction cell in a helium glove box. The metal is then distilled to produce a metal mirror.<sup>22</sup> A solvent, such as dimethylether, is then added to dissolve the complexant and then the metal. The desired product can then be obtained by removal of the solvent or by addition of a less polar cosolvent, such as trimethylamine, to precipitate the crystalline alkalide or electride.

Despite their reactivities and associated handling and storage problems, alkalides and electrides have been extensively studied. Characterization methods include solution NMR,<sup>23,24</sup> MAS-NMR,<sup>25,26</sup> EPR,<sup>27</sup> X-ray crystallography,<sup>28,29</sup> optical absorbtion of thin films by solvent evaporation,<sup>30,31</sup> or vapor deposition,<sup>32,33</sup> magnetic susceptibility,<sup>27,34</sup> photoluminescence spectroscopy,<sup>35</sup> and electrical

conductivity.<sup>36</sup> Studies of these unique compounds have yielded information on the nature of trapped electrons and alkali metal anions.<sup>37,38</sup>

# I.C. Electrical Conductivity

### I.C.1 Background Information

Ignoring superconductors as a special case, solids can classified by their electrical properties as either metals, semiconductors, or insulators. From a physical standpoint, semiconductors and insulators are identical except for the fact that semiconductors have a smaller band gap which gives rise to a higher conductivity at nonzero temperatures.

In a metal, the electrical conductivity is very high, typically  $10^4$  to  $10^6$  ohm- $^1$ cm- $^1$ . In addition, their conductivity decreases nearly linearly with temperature. The reason for these properties becomes apparent when we look at the band structure of a metal. The highest occupied electronic band of a metal (the valence band) is only partially filled with electrons. Because of this, there are empty states nearby in energy for an electron in the band to move through under the influence of an electric field, thus giving rise to conductivity.

The conductivity of a metal follows the law:

$$\sigma(T) = ne^2 \tau/m \tag{4}$$

where  $\sigma$  is conductivity, n is the density of carriers, -e is the charge of an electron, m is the electron mass, and  $\tau$  is the relaxation time for an electron in the valence band. Since n, e, and m are temperature independent, the temperature dependence of the conductivity depends on  $\tau$ . The relaxation time,  $\tau$ , is the time between scattering events for an electron in the metal. For a pure sample, scattering is due only to the phonon vibrations of the crystal lattice. As temperature is increased, the number of phonons also increases, leading to a decrease in the relaxation time and, therefore, the conductivity.

The main difference between metals and semiconductors or insulators is that for a semiconductor or insulator at absolute zero temperature all electronic bands are either completely filled or completely empty. In addition, there is a separation in energy (the band gap) between the valence band and the lowest unoccupied band, the conduction band. Because of this, there are no nearby empty states into which electrons may move under the influence of an electric field and conductivity is not possible.

At temperatures above 0 K, electrons can be thermally excited from the valence band into the conduction band as shown in Figure 2. The excitation of valence band electrons to the conduction band creates empty states (holes) in the band through which conduction can occur. The conduction band electrons also have nearby empty states available for conduction. Thermal excitation of electrons from valence to conduction bands follows the Boltzmann law. Since the conductivity is proportional to the number of electrons which are

excited, conductivity in a semiconductor or insulator also follows a Boltzmann type law:

$$\sigma = \sigma_{\infty} \exp \left( \frac{-E_g}{2k_b T} \right) \tag{5}$$

where  $\sigma_{\infty}$  is the conductivity extrapolated to infinite temperature,  $E_g$  is the band gap,  $k_b$  is Boltzmann's constant, and T temperature. The factor of 2 in the denominator of equation 5 is due to the fact that two conduction sites are created for each electron excited across the band gap. Because of this, the activation energy measured for conductivity in an intrinsic semiconductor is one-half of the band gap.

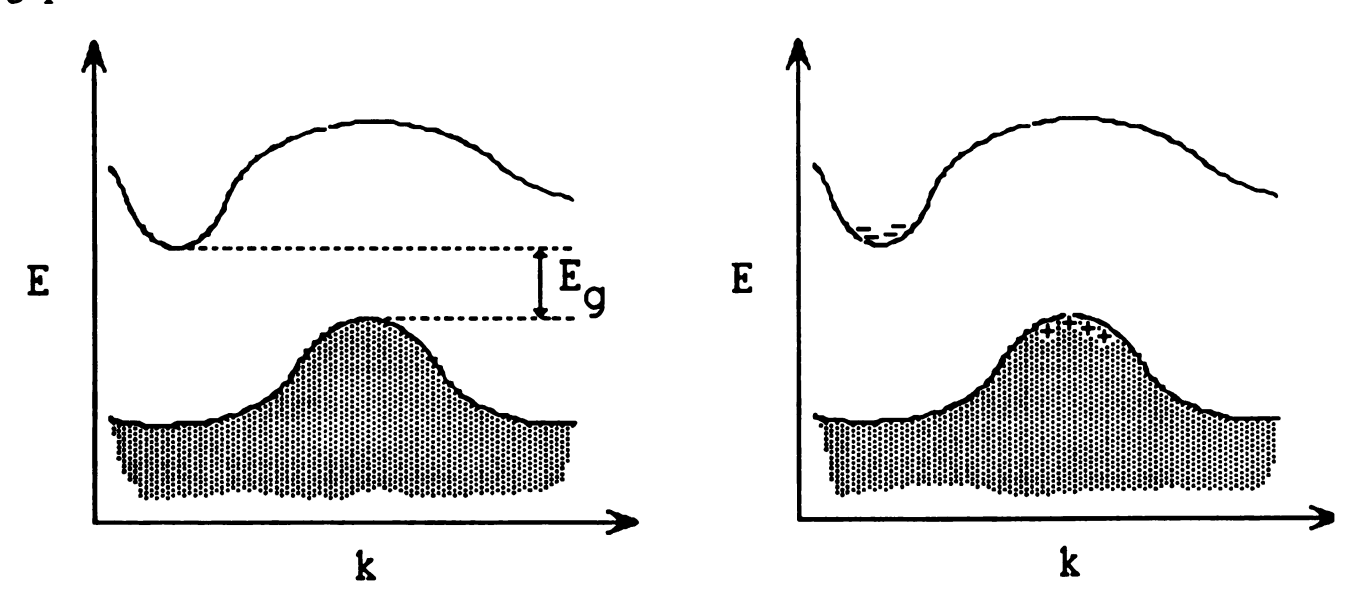


Figure 2: a) Band structure of a semiconductor at low temperature, E<sub>g</sub> is the band gap between the valence and conduction bands. b) Semiconductor at higher temperatures where some electrons have been excited into the conduction band creating two partially filled bands in which conduction may occur.

At 0 K, both semiconductors and insulators have infinite resistivity. Above 0 K, both semiconductors and insulators have a conductivity which increases exponentially with temperature. The difference between the two arises in the magnitude of the conductivity and hence upon their respective band gaps. Generally, semiconductors are considered to be those compounds whose band gaps are less than 3 eV which give rise to room temperature conductivities in the range of  $10^2$  to  $10^{-9}$  ohm<sup>-1</sup>cm<sup>-1</sup>.

The introduction of small amounts of impurities into a semiconductor can significantly alter its conductivity. The addition of impurities to a semiconductor is known as doping, while the impurities themselves are called dopants. Dopant atoms can fit either interstitially or substitutionally into the crystal lattice of a semiconductor. Doping at the parts per million level can increase the conductivity of a semiconductor by six or more orders of magnitude.

Dopant atoms have energy states that lie in the band gap of the pure semiconductor. Two types of dopants exist, depending on whether these impurity states are occupied or are empty. The two situations are shown in Figure 3. A dopant which places empty states in the band gap near the top of the valence band is called a p-type dopant. In this situation, electrons can be excited from the valence band into the empty (acceptor) states of the dopant with much less energy than is required to excite them into the conduction band. This creates positively charged holes in the valence band through which conduction can occur. Conduction does not occur through the acceptor states because there is not enough overlap

between these isolated states to allow electrons to move easily between them.

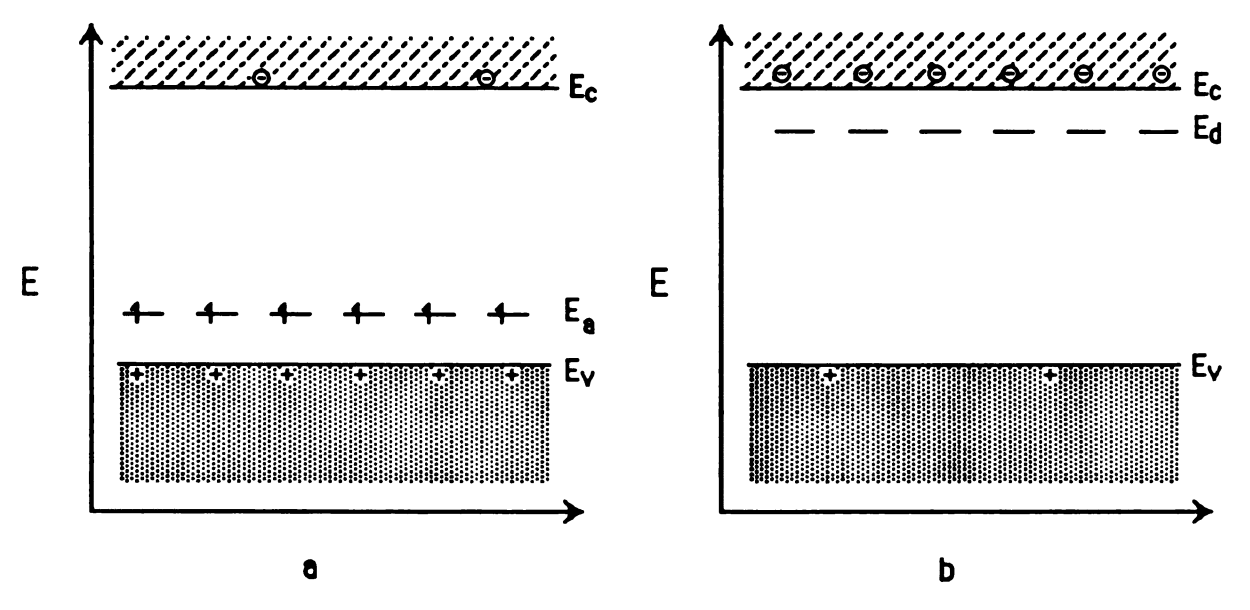


Figure 3: Simplified band structure showing the effects of a) p-type doping, and b) n-type doping at non-zero temperatures where excitation has occurred.

The second type of dopant has filled energy (donor) states which lie in the band gap near the bottom of the conduction band. Electrons from these states can be easily excited into the conduction band where conduction can occur. This type of doping is called n-type since it results in negative charge carriers (electrons) as opposed to the positive charge carriers (holes) donated by a p-type dopant.

For either type of dopant, it is much easier to excite electrons between dopant states and their nearby bands than it is to excite electrons across the band gap. A doped semiconductor, therefore,

has a different temperature profile to its conductivity than does a pure semiconductor. At low temperatures, the conductivity of a doped sample is due virtually entirely to contributions from the dopant species. Conductivity in this region is referred to as extrinsic conductivity. Due to the low concentration of dopant atoms there is virtually no overlap between their energy states. Since these dopant states are so widely separated, there is no movement of electrons between them to produce conductivity. The observed apparent band gap in this region, therefore, is twice the energy difference between the dopant state and the nearest electronic band since doping results in only one conductive site rather than the two sites created by the excitation of an electron from the valence band into the conduction band. At high temperatures, most of the dopant sites have been occupied or excited and the excitation of electrons across the band gap becomes the major conduction process. In this intrinsic conductivity region, the observed band gap is the actual band gap of the pure semiconductor since the change in the conductivity with temperature is due to the excitation of electrons between the valence and conduction bands.

### I.C.2 Conductivity of Alkalides and Electrides

The physical appearance of the first alkalide, Na<sup>+</sup>(C222)Na<sup>-</sup>, sparked immediate interest in the electrical conductivity of alkalides and, later, electrides. Na<sup>+</sup>(C222)Na<sup>-</sup> crystallizes as shiny gold colored crystals. From its metallic appearance it was thought that Na<sup>+</sup>(C222)Na<sup>-</sup> might be a metal. Although not entirely successful,

early conductivity experiments showed Na+(C222)Na-to be a semiconductor rather than a metal.<sup>39</sup>

Prior to the current work, the only alkalide or electride that had been well characterized electrically was Na+(C222)Na-. Many of the properties of this alkalide made it a good target for the first indepth electrical study of an alkalide or electride. The handling and manipulation of Na<sup>+</sup>(C222)Na<sup>-</sup> was made much easier by the fact that it is one of the most stable alkalides and can survive for several days at room temperature (under inert atmosphere or vacuum) without appreciable decomposition. In addition, single crystals up to several millimeters on a side can be grown which makes single crystal conductivity studies possible. These crystals can be grown with extremely low concentrations of the defect electron impurities which can plague other alkalides. This fact allows the measurement of the intrinsic band gap of the compound rather than an apparent band gap due to a doping effect by defect electrons as is seen in most alkalides.

Early conductivity studies of Na<sup>+</sup>(C222)Na<sup>-</sup> by Mei-Tak Lok and Michael R. Yemen showed semiconducting behavior with an apparent band gap of 2.4 eV.<sup>39,40</sup> Later studies confirmed this value and followed equation 5 very well. The value of  $\sigma_{\infty}$ , the conductivity extrapolated to infinite temperature, was large ( $10^6 - 10^{12} \Omega^{-1} \text{cm}^{-1}$ , run dependent) which suggests that Na<sup>+</sup>(C222)Na<sup>-</sup> is an intrinsic semiconductor.<sup>36</sup> These measurements were carried out both on pressed powders and single crystals. The high resistivity of the compound and instrumental limitations, however, limited single crystal measurements to a 2-probe method.

Evidence for ionic conductivity was also seen in Na+(C222)Naat temperatures above -24 °C. At voltages above 2 V, in this temperature range, highly non-linear Ohm's Law plots were observed for single crystal samples. With voltages greater than 2 V, the temperature dependence of the conductivity yields an activation of 1.6 eV compared to 1.2 eV for lower voltages and Also observed for these conditions was a current temperatures. which decayed with time while the voltage was applied. When the voltage was pulsed above 2 V with rectangular pulses of alternating polarity, however, Ohm's Law plots became linear and the observed activation energy for conduction was once again 1.2 eV. These results indicate the presence of ionic conductivity. When the applied potential is greater than 2 V, Na<sup>+</sup> can be reduced to Na<sup>o</sup> at the electrode surface and ionic conductivity is observed.

As further evidence of ionic conductivity in this system, experiments were carried out in which one electrode of the conductivity cell was covered with sodium metal. This arrangement resulted in non-zero current even in the absence of applied voltage across the sample. 2 V of potential were required to zero this background current with the sodium electrode being positive. With two different charged states of sodium present in Na+(C222)Na-, the possibility existed that Na- rather than Na+ was responsible for the observed ionic conductivity of this compound. To test for this possibility, the conductivity of a single crystal of Na+(C222)I- was studied. As expected, no evidence for electronic conductivity was observed in Na+(C222)I-. Non-linear Ohm's Law plots similar to those seen for Na+(C222)Na- were also observed for Na+(C222)I-. In

addition, the conductivity activation energy for Na<sup>+</sup>(C222)I<sup>-</sup> was found to be within experimental error of the 1.6 eV seen in Na<sup>+</sup>(C222)Na<sup>-</sup> at high temperatures and voltages. This is good evidence that Na<sup>+</sup> is the conducting species in both of these compounds.

The electrode reactions for the ionic conductivity of Na<sup>+</sup>(C222)Na<sup>-</sup> are postulated to be:

Cathode:

$$Na^{+}(C222) + e^{-}electrode ----> Na(s) + C222$$

Anode:

OI

$$Na^- + C222$$
 ----->  $Na^+(C222) + e^-_t + e^-_{electrode}$ 

If this hypothesis is correct, the previously mentioned behavior of Na+(C222)Na- can be explained. The observed non-ohmic behavior of Na+(C222)Na- at high temperatures and voltages is the result of ionic conductivity above 2 V in addition to the electronic conductivity of the system. The time dependence of the current under these conditions is the result of the formation of a depletion region at the electrode surface due to migration of Na+ in the applied field. When rectangular pulses of alternating polarity are used the non-ohmic behavior disappears because the electrode reactions are now reversible and a depletion layer formed on one half cycle is

replenished by the reverse reaction occurring on the following half cycle of opposite polarity.

The electrochemical reactions proposed for Na+(C222)Nasuggested that it may behave as an electrochemical cell if exposed to
a d.c. potential for a period of time. This behavior was seen for
Na+(C222)Na- after a single crystal had been exposed to a voltage of
5 V for 1 hr. The voltage dropped rapidly after charging to 2.6 V
and then decayed gradually to 2.2 V over a period of several hours.
When the charging potential was less than 2 V, the open circuit
voltage decayed quickly to zero at the capacitance discharge rate
presumably because the applied voltage was not large enough to
plate sodium.

As can be seen, the electrical characteristics of Na<sup>+</sup>(C222)Na<sup>-</sup> are complex. Ionic conductivity is present in addition to the expected electronic conductivity giving distinctly non-linear Ohm's Law plots. Somewhat surprisingly, Na<sup>+</sup> is responsible for the ionic conductivity rather than the uncomplexed Na<sup>-</sup>. It may be that the major contribution to the activation energy for ionic conductivity is the release of Na<sup>+</sup> from the cryptate complex. Under the proper conditions, Na<sup>+</sup>(C222)Na<sup>-</sup> can also act as an electrochemical cell.

From this single example, it would be expected that other alkalides and electrides would exhibit complex and interesting electrical behavior. Until recently, however, the greater instabilities of electrides and defect electron impurities of most alkalides prevented detailed studies of their electrical properties. Cursory studies of the electrical properties of many alkalides and electrides have been performed in the course of characterization of new

compounds. These studies usually included variable temperature measurements in the temperature range of 200 K to 280 K. These data were used to estimate the band gap and resistivity for the compound under study. In addition, some Ohm's Law data were collected to check for non-linearity and possible ionic conductivity in some of the compounds.

Compounds for which electrical data exist along with their apparent band gaps are listed in Table 1. It should be noted that in all cases except for Na<sup>+</sup>(C222)Na<sup>-</sup>, measurements were performed only on pressed powder samples due to difficulties in growing large single crystals.

In many of the compounds listed in Table 1, the conductivity was extrapolated to infinite temperature in order to obtain an estimate of  $\sigma_{\infty}$  from equation 5. The value of  $\sigma_{\infty}$  thus obtained was used to estimate whether the compound was an intrinsic or extrinsic semiconductor. In cases where this was done, all of the listed compounds were found to be extrinsic semiconductors with the exceptions of Na<sup>+</sup>(C222)Na<sup>-</sup>, Cs<sup>+</sup>(18C6)<sub>2</sub>e<sup>-</sup>, and Cs<sup>+</sup>(18C6)Na<sup>-</sup>. In most other semiconductors, when this extrapolation technique is employed, it is made from data obtained over a 200 K to 300 K The temperature range obtained for these temperature range. experiments was less than 80 K for all but Na+(C222)Na-. With such a narrow temperature range to work with, small errors and uncertainties in the data can change the value of  $\sigma_{\infty}$  by orders of magnitude. Because of this, even those compounds with large values of  $\sigma_{\infty}$  may be extrinsic rather than intrinsic semiconductors. Conversely, grain boundary and electrode resistances may couple

TABLE 1: Band gaps and references for alkalides and electrides for which conductivity measurements have been attempted.

Compound	Band gap	Reference
Cs+(18C6) <sub>2</sub> e-	0.9	11,21
K+(15C5) <sub>2</sub> e-	1.04	20
Rb+(15C5) <sub>2</sub> e-	1.20	20
K+(C222)e-	unsuccessful	41
Rb+(C222)e-	unsuccessful	41
K+(12C4) <sub>2</sub> Na-	2.17	42
Na+(C222)Na-	2.4	36, 39, 40
K+(C222)Na-	1.58	40
Rb+(C222)Na-	unsuccessful	40
K+(18C6) <sub>2</sub> Na-	0.93	43
Cs+(18C6)Na-	1.7	43
Cs+(18C6) <sub>2</sub> Cs-	0.80	43, 45
Cs+(18C6) <sub>2</sub> Rb-	0.8	44
K+(15C5) <sub>2</sub> Na-	1.36	20
K+(15C5) <sub>2</sub> K-	1.06	20
K+(15C5) <sub>2</sub> Rb-	0.87	20
Rb+(15C5) <sub>2</sub> Na-	1.03	20
Rb+(15C5) <sub>2</sub> Rb-	0.93	20
Cs+(15C5) <sub>2</sub> Na-	1.28	20
Cs+(15C5) <sub>2</sub> K-	0.85	20
Cs+(15C5) <sub>2</sub> Rb-	0.64	20

with these same data uncertainties to make a polycrystalline sample of an intrinsic semiconductor appear extrinsic in nature.

Magnetic susceptibility studies of several alkalides have shown that all, with the exception of Na<sup>+</sup>(C222)Na<sup>-</sup>, contain defect electrons in concentrations ranging from ~0.1% to greater than 10%.<sup>27,46</sup> The actual trapped electron concentration is both synthesis and compound dependent. Even at the lower end of this range, the electron concentration is great enough to show apparent band gaps due to doping effects which are smaller than the true band gap of an alkalide. From these results, it should be expected that few if any of the band gaps recorded in Table 1 are the intrinsic band gaps of these compounds.

Prior to the current work, electrical conductivity measurements had only been attempted on five electrides. For only three of these electrides, K+(15C5)<sub>2</sub>e-, Rb+(15C5)<sub>2</sub>e-, and Cs+(18C6)<sub>2</sub>e-, did these experiments yield any quantitative results. In these compounds apparent band gaps near 1 eV were measured. Small concentrations of defect electrons in addition to the electron anions are possible in electrides, so it is possible that even in these compounds the observed band gaps are not the true band gaps of the compounds.

Electrical measurements were unsuccessful for two electrides, Rb+(C222)e- and K+(C222)e-. Although measurements were unsuccessful, both of the compounds appeared to be highly conductive. Rb+(C222)e- was found to produce currents too high to measure with the then used instrumentation even at the lowest possible applied voltage. Large measurable currents could be obtained for K+(C222)e- but the current was not dependent upon the

applied voltage. These results indicated that both of these electrides are highly conductive. Also indicated was the need for better instrumentation and methods to deal with conductive compounds.

The past results of electrical conductivity measurements on alkalides and electrides have indicated the need for a more in-depth study of the electrical properties of these unique compounds. Also apparent was the need for better measurement techniques and instrumentation. This work will focus on the detailed study of several of these alkalides and electrides via improved measurement and handling techniques.

#### II. EXPERIMENTAL

# II.A. Synthesis of Doped Electrides

In addition to the normal syntheses of alkalides and electrides described briefly above, and in detail elsewhere, 20.21 it was necessary in the current work to synthesize several electrides that contain small amounts of alkalide impurities. In all cases, these impurities were either Na- or Cs-. Two methods were used in the synthesis of these doped electride samples which will be referred to as method A and method B.

Method A was used in only one case in which Cs<sup>+</sup>(18C6)<sub>2</sub>e<sup>-</sup> was doped with Cs<sup>-</sup>. In this method, the synthesis of the compound was performed as usual except that stoichiometric ratios of metal and complexant were used. In a normal synthesis of a "pure" electride, excess complexant is used to drive the reaction shown in equation 2 to completion and minimize alkalide impurity from equation 3. It was intended that stoichiometric ratios of metal and complexant would allow equation 3 to proceed to a great enough extent to produce significant (~1%) doping of Cs<sup>-</sup> in the electride sample.

The second doping method (B) was intended to allow more control over the amount of dopant present in a sample. Method B required the mixture of two compounds, the first being the pure electride which was to be doped. The second compound was a pure

alkalide with the same cation and complexant as the electride. Its anion was the alkali metal with which the electride was to be doped. To prepare the doped electride, the pure electride was combined with a small amount of the alkalide sample. This was done in a nitrogen filled glove bag and the samples were kept cold in a liquid nitrogen bath. The mixed sample was then placed in a crystallization cell<sup>47</sup> which was also cooled in liquid nitrogen. The cell was assembled and placed on a vacuum line where dimethylether was added to dissolve the mixture of compounds. Upon removal of solvent, the doped electride product remained.

Due to the handling problems of alkalides and electrides, it was not possible to combine weighed amounts of electride and alkalide samples for method B. Typically, the amount of alkalide used was ~10% of the amount of electride as discerned by eye. In most cases, attempts to use much more than this amount of alkalide resulted in phase separation of the product into its respective alkalide and electride components.

# II.B. Magnetic Susceptibility

Studies of the magnetic susceptibility of alkalides and electrides were performed on an S.H.E. 800 series S.Q.U.I.D. Magnetometer (SQUID). Magnetic fields from 0 to 7 kG and temperatures from 1.8 to 240 K were used. Powdered samples were loaded into Kel-F sample buckets in a nitrogen filled glove bag at liquid nitrogen temperature. The sample buckets were equipped

with tight fitting lids which could be tied to the bucket to prevent loss of sample during decomposition. The buckets and lids were washed in concentrated nitric acid before use to remove magnetic impurities. The airlock of the SQUID was enclosed in a helium filled glove bag to eliminate moisture and condensation on the cooled sample during loading. The sample was placed in the glove bag in a liquid nitrogen dewar and transferred to the airlock. The airlock was then evacuated to remove the final traces of moisture and air before the sample was loaded into the instrument. For very thermally unstable compounds, a copper block with a central hole was cooled in liquid nitrogen and placed in the airlock prior to introduction of the sample. This was done to keep the sample from decomposing during the short time it took to evacuate the airlock.

In order to determine the trapped electron contribution to the molar magnetic susceptibility, it was necessary to measure the apparent susceptibility of the sample and bucket, and also of the decomposed sample and bucket under the same conditions. The apparent susceptibility is given by:

$$\chi_{app} = \frac{M_{obs}}{H}$$

where H is the magnetic field and  $M_{0bs}$  is the observed magnetization of the sample and bucket. The electronic portion of the susceptibility ( $\chi_e$ ) can be calculated from the following equation:

$$\chi_e = \frac{\chi_{app liv} - \chi_{app decomp}}{moles of sample}$$

7

where  $\chi_{app\ live}$  and  $\chi_{app\ decomp}$  are the susceptibilities of the live sample and the decomposed sample respectively. This method successfully subtracts the diamagnetic background susceptibility from the susceptibility contribution of the trapped electrons of the sample.

### II.C. Differential Scanning Calorimetry

Differential scanning calorimetry (DSC) measurements were obtained by using an E.I. duPont de Nemours 9900 Thermal Analyzer with a 910 Differential Scanning Calorimeter. This system has a low temperature capability which allows samples to be handled and run at temperatures as low as -150 °C. Sample heating rates from 0.1 °C/min to 24 °C/min were used for the different studies in the current work. Calibration of the DSC cell was carried out by the measurement of the melting point and heat of fusion of a pure mercury sample. The calibration was carried out over the entire range of scanning rates and it was observed that cell parameters are essentially invariant with scanning rate.

For all DSC studies, samples were run in hermetically sealed aluminum sample pans. Alkalide and electride samples were loaded into preweighed sample pans in a nitrogen glove bag. The pans were then sealed with a sample press which was cooled in liquid nitrogen during use. The sealed samples were stored in liquid nitrogen until

being loaded into the DSC. The sample mass was obtained by weighing the pan and sample after the experiment and subtracting the mass of the empty pan. Sample masses ranged between 1 and 6 mg, and most samples were between 2 and 3 mg. Since samples of these unstable compounds have to be loaded while cold in most cases, the DSC module was enclosed in a nitrogen glove bag during use to prevent frost formation on the sample pans while they were being loaded.

## II.D. Conductivity Methods

## 1 Conductivity Cells

## 1.a 2-probe D.C. Cell

The 2-probe conductivity cell (d.c. cell) used for d.c. measurements was designed by Michael R. Yemen and Dr. James L. Dye.<sup>40</sup> The cell, with one modification, is shown in Figure 4. The sample chamber for this cell is a 4 mm glass tube which fits tightly over the bottom stainless steel electrode. The sample is placed in the quartz tube and compressed against the bottom electrode by the spring loaded top electrode. Sample requirements for this cell are typically 5 to 15 mg of powdered sample.

In its original design, the d.c. cell was unshielded. The entire cell, with the exception of the top electrode was in electrical contact with the bottom electrode. This setup resulted in background noise

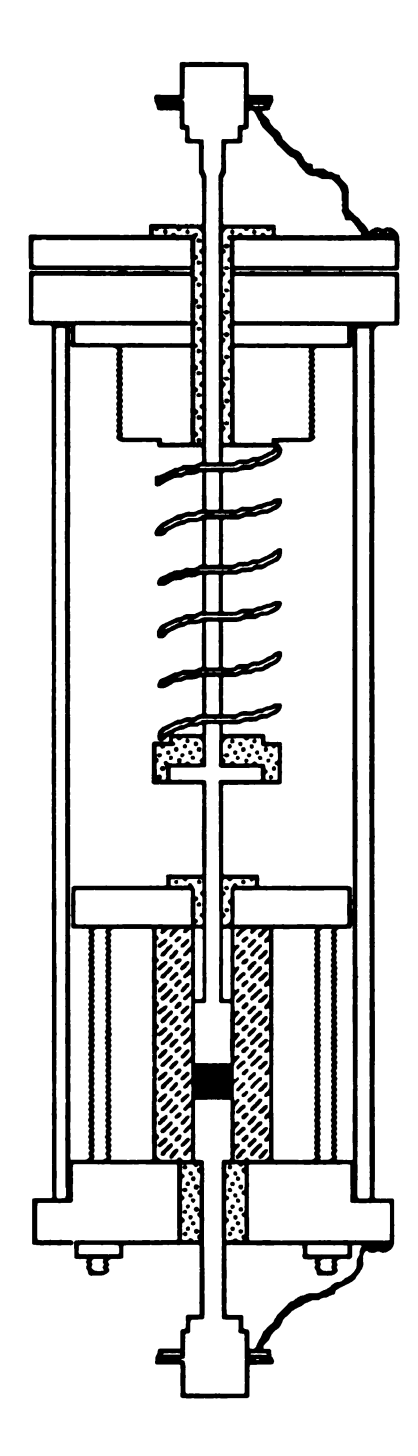


Figure 4: The 2-probe d.c. conductivity cell. Both electrodes are stainless steel, the sample chamber is a glass tube, and the body of the cell is brass. The top electrode is spring loaded to ensure that good pressure contacts between the sample and the electrodes are maintained.

currents that were often in excess of 100 pA and, therefore, limited the use of the d.c. cell to fairly conductive samples. In order to measure the conductivity of more resistive compounds an adaptation was made for the current work. The bottom electrode was electrically insulated from the body of the cell by a teflon spacer. The cell body was then connected to the shield of the coaxial leads used in conductivity measurements. This new arrangement kept background currents below 1 pA and allowed measurements to be made on compounds with resistances up to  $10^{13} \Omega$ .

## 1.b 4-probe Cell

A 4-probe conductivity cell was designed for both d.c. and a.c conductivity measurements of pressed pellet samples. The cell is shown in Figure 5. The sample chamber in the 4-probe cell is a Delrin cup built to hold a 3/16 inch sample pellet from the pellet die described below. Electrical connections to the pellet sample are made through four "pogo stick" type connections arranged in a square configuration to contact the sample pellet near its periphery. The "pogo" connections are set into a Delrin probe holder which can slide up and down in two slots cut into the cell body to make contact with the pellet sample. When the screw ring of the cell is turned down it forces the probe holder and probes against the pellet. The "pogo" connections are spring loaded so that they can be compressed against the pellet by the screw ring to make a point pressure contact. Resistance measurements are made by passing current through two

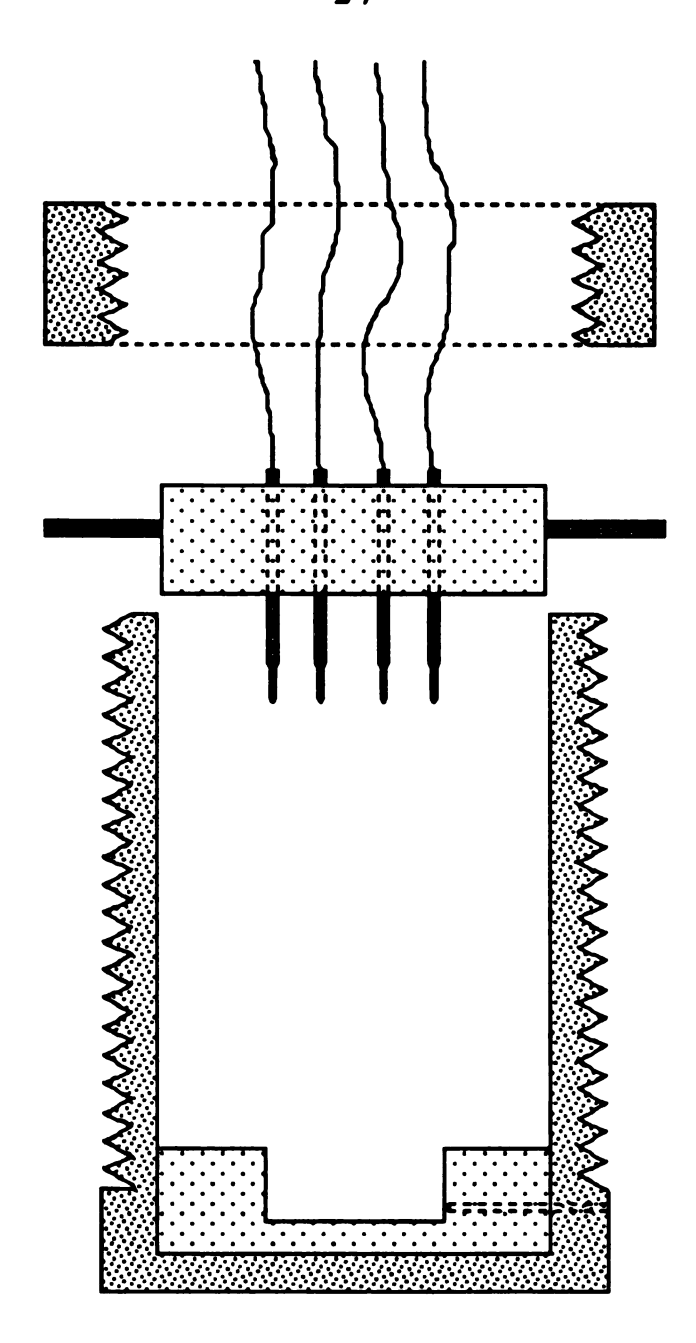


Figure 5: The 4-probe conductivity cell. The four pogo stick electrodes are arranged in a square configuration to contact the sample pellet near its perimeter.

adjacent probes and measuring the voltage drop across the remaining two probes. It was necessary in some cases to coat the tip of the pogo stick electrodes with alkali metal to ensure good electrical contact with the sample. Alkali metal was applied in a nitrogen glove bag under a cold nitrogen gas stream. The cold nitrogen gas was boiled off from a liquid nitrogen source and was used both to keep the sample cold and to prevent oxidation of the metal surface.

# 1.c Impedance Cell

For impedance spectroscopy experiments, a cell that was simpler and more compact than the d.c. cell was designed. The impedance cell (I.S. cell) was designed to involve as few parts as possible to make its assembly very rapid and straightforward. The design of the cell is shown in Figure 6. The top spring-loaded electrode applies pressure to the sample when the cell is assembled. The body of the cell is electrically connected to the bottom electrode of the cell. The sample chamber of the cell is a Delrin cylinder with a 3/16 inch hole in which pressed pellets or powdered samples may be used. The body of the cell is brass with the top electrode made of stainless steel. The bottom electrode is a stainless steel plate on which the sample chamber rests.

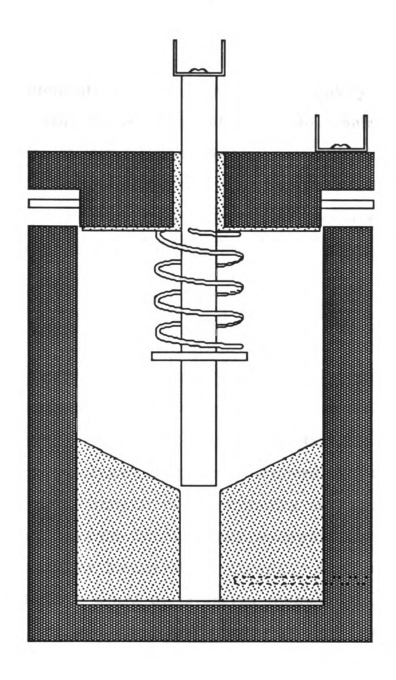


Figure 6: The I.S. cell. The top electrode and bottom plate are both stainless steel, the cell body is brass, and the sample chamber is Delrin. The top electrode is spring loaded to make pressure contacts between the sample and electrodes.

### 2. Temperature Control and Measurement

Measurements for the various conductivity methods were taken in the temperature range of 77 K to ambient temperature. Two methods of temperature control were employed in these measurements. The first method (A) was used only for variable temperature d.c. experiments to determine the conductivity activation energy or band gap. A "soft" 30 L liquid nitrogen dewar was used as the cryostat for this method. The dewar cryostat was precooled with liquid nitrogen. After the cryostat was cold the remaining liquid nitrogen was removed. The d.c. conductivity cell was then suspended in the center of the dewar by its electrical leads. Electrical measurements of the sample were then taken as the cryostat warmed. The cryostat takes up to 48 hours to warm from 77 K to room temperature and it was assumed that the conductivity cell warmed up uniformly at this slow heating rate. The speed of the warm-up process could be increased somewhat by flowing warm nitrogen gas into the bottom of the cryostat. Due to the possibility that large gas flows would cause uneven warming of the cryostat and conductivity cell, nitrogen gas flows were kept below 5 L/min. Temperature measurement for this method was accomplished through the use of a carbon-glass four probe thermometer. model CGR-1-100 thermometer was purchased from Lakeshore Cryotronics, Inc. calibrated over the temperature range of 1.4 K to In its working range, this thermometer can measure temperatures to an accuracy of +/-0.05 K. The thermometer was

attached to the exterior of the d.c. cell, approximately 1 cm from the sample. It was assumed that the cryostat warmed up evenly within this range. The thermometer was read by a Keithley Model 580 Micro-ohmmeter which is capable of true four probe measurements.

The second method of temperature control (B) was used chiefly for experiments in which a stable sample temperature was necessary. For this method, a 2 inch diameter glass tube closed on the bottom end was inserted into a 30 L liquid nitrogen dewar which was approximately half filled with liquid nitrogen. The tube extended from the top of the dewar approximately 8 inches. The top of the dewar and tube opening were covered with a nitrogen-filled plastic bag to prevent air and moisture condensation in the tube. The conductivity cell was suspended into the tube and its temperature was dependent on its height above the liquid level in With this method, it is possible to attain a temperature which is stable to within +/- 0.1 °C for over 24 hours. The temperature at various depths in the glass tube was roughly calibrated using a copper-constantan thermocouple suspended approximately 2 cm below a wooden meter stick into the tube. The temperature gradient in the tube varied with depth but had a maximum of about 12 °C/cm. This would yield a 1.2 °C temperature gradient within the typical 1 mm sample height used for conductivity measurements. The mass of the conductivity cell can be expected to mediate the temperature gradient to some extent. Temperature measurement for this control method is accomplished with a copper-constantan thermocouple. For the d.c. conductivity cell, the thermocouple was tied tightly to the side of the glass sample tube at the same height as the sample. For the I.S. and 4-probe cells, a small hole was drilled through the cell into the Delrin insulator to within ~2 mm of the sample chamber. A thermocouple was then inserted into this hole to measure the sample temperature.

# 3. General Handling

Conductivity samples are loaded into the various conductivity cells in a nitrogen glove bag. The conductivity cells are cooled in liquid nitrogen before loading and quickly assembled and cooled immediately after loading. The assembled cell with sample is then transferred to a cryostat where electrical connections are made.

## 4. Alkali Metal Electrodes

For several experiments it was necessary to coat one or more electrodes of a conductivity cell with an alkali metal. Attempts to do this in a nitrogen glove bag failed due to the fact that the bag atmosphere is not clean enough to prevent oxidation of the alkali metal surface in the time between application of the metal and sample loading. Successful coatings of alkali metal on the cell electrodes were applied in a helium filled dry box. The alkali metal was spread on the steel or gold plate electrodes of the cell with a knife and care was taken to cover the entire surface. The cell was then placed in a cold well which can be cooled to -80 °C from an

external source of boil-off nitrogen. In order to transport the alkalide or electride sample into the drybox, steps had to be taken to keep the sample cold during the evacuation of the drybox access To accomplish this, a large glove bag was placed over the port. mouth of the port and flooded with nitrogen gas. The sample was stored in a Cryotube and kept in liquid nitrogen prior to loading into A large copper block which had been cooled in liquid nitrogen was placed in the glove bag with the sample. The Cryotube holding the sample was placed into a hole in the copper block. The Cryotube lid was loosened to prevent it from rupturing during evacuation of the port. The block with sample was then placed into the port for evacuation. In the twenty or so minutes required to evacuate the port, the copper block never warmed above -100 °C, so that the sample was kept sufficiently cold to prevent decomposition. Once in the drybox, the sample was placed in the cooled conductivity cell which was quickly assembled and removed from the drybox. The cell was transported to the cryostat in liquid nitrogen.

### 5. Pressed Pellet Formation

Pellets of alkalide and electride samples are pressed on a 25 ton Model M Carver Laboratory Press. The sample die in which the pellets are formed is shown in Figure 7. This die has a carbide steel "piston" which transmits pressure to the powdered sample. The body of the die is made of hardened steel. The entire die can be cooled in liquid nitrogen prior to sample loading and keeps samples

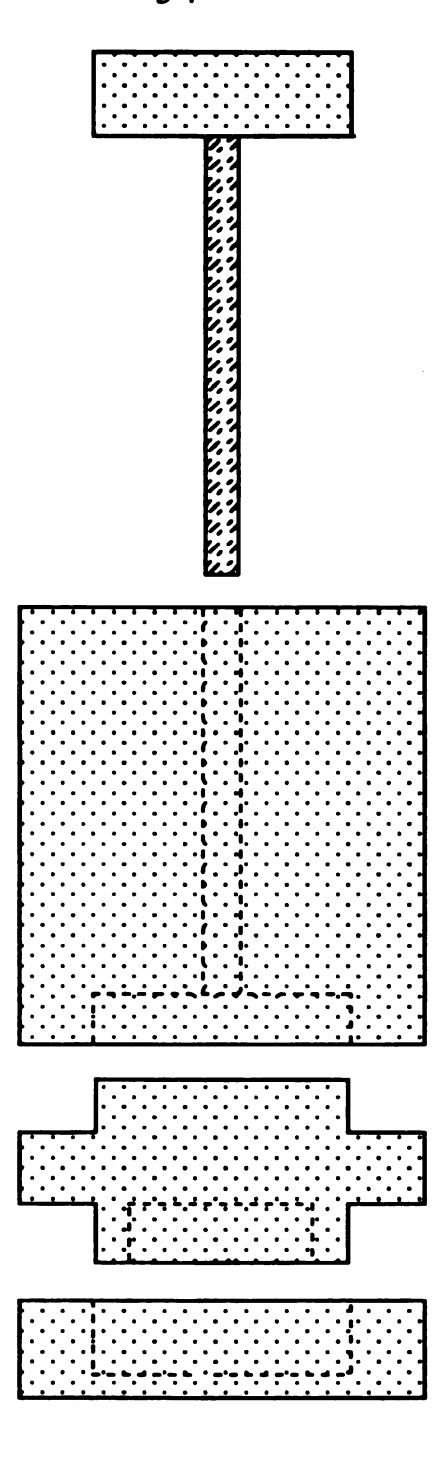


Figure 7: The pressed pellet die used to make pellet samples for conductivity measurements. The body of the die is hardened steel and the piston is carbide steel.

cold during the brief time required to press a pellet on the Carver press. This die was designed to create pellets 3/16 inch in diameter to fit into the impedance cells and 4-probe cell. A larger die of identical design which makes pellets 1/2 inch in diameter has also been built. Pellets of alkalide and electride powders were made by loading the cooled pellet die with sample in a nitrogen glove bag which also contained the Carver press. The pellet die was then assembled and placed the Carver press. The 3/16 inch pellets were pressed at 1000 to 1500 lbs which corresponds to 250 to 370 atm neglecting frictional losses.

# 6. D.C. Conductivity Methods

All d.c. conductivity experiments were performed with a Keithley 617 Programmable Electrometer. This instrument can act as a voltage source with an output range of -102 V to +102 V in 50 mV increments. The 617 can also serve as a sensitive ammeter, ohmmeter, and voltmeter. The instrument has an IEEE-488 interface for computer control of measurements and data acquisition.

In most d.c. conductivity experiments, the Keithley electrometer was used as both a voltage source and as an ammeter. Early experiments were all manually run and used temperature control method B exclusively. Experiments to determine the activation energy of conductivity for a sample required that the sample temperature be allowed to equilibrate in the cryostat before each measurement was made. Once the sample temperature was

stable, a unidirectional voltage was applied to the sample and the resultant current was measured. After a measurement, the sample temperature was again changed and allowed to equilibrate for the next data point. Typically, 45 to 75 minutes were required for the temperature to stabilize sufficiently so that the temperature did not drift during the period that measurements were being taken. In the same manner, Ohm's Law measurements were made by applying different voltages and measuring the current flow through the sample.

These early experiments made it apparent that a new method of measurement was needed. It was observed that in many cases the current flow through the sample at a fixed voltage is time dependent. Electrode polarization effects due to ionic conductivity could result in the observed behavior. The length of time required to stabilize the sample temperature for variable temperature experiments was also excessive. Often, only 10 to 15 data points could be collected in a normal work day. This meant that 2 to 3 days were required to obtain sufficient data to determine a sample's conductivity activation energy. Both of these problems were solved through the use of computer controlled data acquisition and an alternate method of temperature control (method A). An IBM PC/XT micro-computer equipped with an IE-48 General Interface I/O expansion board from MetraByte Corporation was used for all computer controlled conductivity experiments in this work. This configuration allows total instrument control through the use of the Basic programming language.

Variable temperature d.c. conductivity data were collected by using the Basic program DCRUN.bas listed in Appendix A. program controls a Keithley 617 electrometer for sample measurements, and a Keithley 580 micro-ohmmeter which reads resistance data from the four-probe carbon glass thermometer. Temperature method A was used in conjunction with this program. DCRUN.bas was written to allow rectangular voltage pulses of alternate polarity to be applied to the sample to eliminate polarization effects. Typically, pulses 10 s in length and 100 mV in amplitude were used. The program can take a measurement on each bias, or wait through a predefined number of cycles before taking data on two consecutive pulses. Each electrical measurement was performed at the end of a pulse. Temperature data were collected immediately following each electrical measurement. The length of an experiment using DCRUN.bas can be varied from 0 to 24 hours. Runs greater than 24 hours could not be performed because the computer clock will reset itself each day and destroy the timing sequence for For experiments of over 24 hours duration, the the program. program is simply restarted immediately after the end of the previous 24 hour run. As for all other instrument control programs in the current work, DCRUN.bas stores all data in ASCII format which can be imported directly into Lotus 123 for data reduction and graphing purposes. Resistance data from the carbon-glass thermometer are converted to Kelvin temperatures according to the equation for temperature calibration supplied with the thermometer. Sample resistances were calculated with the following equation:

$$R = \frac{(V^+ - V^-)}{(I^+ - I^-)}$$

where V+ and I+ are the positive voltage and its resulting current respectively, and V- and I- are the negative voltage and current. This difference method of calculating resistance is meant to compensate for any instrumental drift with time or improper zeroing of the background current in the measurement circuit.

Ohm's Law measurements were made at various temperatures using temperature control method B. The program OHMLAW.bas was written to perform these experiments. OHMLAW.bas allows the input of up to 100 voltages to be used in the experiment, in the order in which they will be applied. In addition, the length of time that each voltage pulse is to be applied can be controlled. The program is set up to collect current readings as fast as the electronics will allow for the entire period that each voltage is applied. This speed averages approximately three readings per second over the duration of the pulse. At the end of each pulse, the program immediately changes to the next bias and continues taking measurements. current measurement is stored along with its corresponding voltage and the length of the pulse at the time that the measurement is This program requires manual temperature recording for taken. each run. OHMLAW.bas is listed in the Appendix.

Experiments to determine the electrochemical cell behavior of ionically conducting samples utilized two separate control programs both of which are listed in the Appendix. In these experiments, it

was necessary to "charge" a sample by subjecting it to a d.c. voltage for a period of time. The program VOLTCHAR.bas applies a single voltage to the sample and periodically measures the current flow through the sample. This allows the current to be studied as a function of time to determine sample polarization effects. After charging of the system, the program DCVOLT.bas was used to measure the open circuit voltage of the system. This program requires that the Keithley 617 electrometer be connected to the sample circuit as a voltmeter. The program measures the voltage at programmed time delays for periods of up to 24 hours.

Two final d.c. measurement control programs are listed in Appendix A. These programs are both adaptations of DCRUN.bas. DCTIMDEP.bas was set up to measure the resistance of a sample as a function of time at a single temperature to check for possible electrochemical induced decomposition of the sample. Like DCRUN.bas, the program applies rectangular voltage pulses of alternate polarity to the sample. Instead of collecting temperature data, DCTIMDEP.bas records the time elapsed since the beginning of the experiment along with each current reading. This allows the study of sample resistance as a function of time. The second program adapted from DCRUN.bas is called INTERMIT.bas. Like DCTIMDEP.bas, this program records current through the sample as a function of time using rectangular voltage pulses of alternate polarity. INTERMIT.bas, however, only applies voltage pulses when it is ready to take a measurement. In the lag time between measurements, no voltage is applied to the sample.

## 7. Impedance Spectroscopy and A.C. Conductivity

All a.c. conductivity and impedance spectroscopy experiments in the current work utilized a Hewlett Packard 4192A Low Frequency Impedance Analyzer for measurements. The instrument is capable of true 4-probe measurements and has an output voltage range of 5 mV to 1100 mV in 5 mV increments. Frequencies from 5 Hz to 13 MHz can be attained. The measurement range for impedances is 0.1 m $\Omega$  to 1.3 M $\Omega$ . The instrument also has an IEEE-488 interface to allow computer control of measurements and experimental parameters.

2-probe and 4-probe impedance spectroscopy experiments were computer controlled through the program KIRP.bas listed in the Appendix. The program allows a voltage bias, starting frequency, and ending frequency to be chosen for each experiment. The program then performs a logarithmic sweep of the frequencies in the input range. The magnitude of the impedance vector and its phase shift are measured at each frequency in the sweep. The data are recorded together with respective frequencies for reduction to rectangular coordinates. The real, Re(Z), and imaginary, Im(Z), parts of the impedance are calculated from the following equations:

$$Re(Z) = |Z| \cos \phi$$
 9

$$Im(Z) = |Z| \sin \phi \qquad 10$$

where |Z| is the magnitude of the impedance vector in the complex impedance plane and  $\phi$  is the phase angle of the impedance vector relative to the real axis.

4-probe a.c. conductivity experiments on pressed pellet samples used the HP 4192A but were manually run. The measurement frequency for these experiments was set such that the phase shift of the impedance vector was zero or as small as was attainable. In most cases, any frequency less than 1 kHz will satisfy this condition. In the experiment, a known a.c. current is passed between two adjacent electrical contacts on the pellet, and the voltage drop across the other pair of probes was measured. This technique was first described by L.J. van der Pauw.<sup>48</sup> For a symmetric isotropic sample such as the disc shaped pellets used in the current work, the resistivity, ρ, of the sample can be calculated from the following equation:<sup>49</sup>

$$\rho = \frac{\pi d}{\ln 2} R$$

where d is the sample thickness and R is the measured resistance of the sample calculated from Ohm's Law.

#### III. DECOMPOSITION OF ELECTRIDES

### I.A. Introduction

As noted earlier, there are many handling problems associated with alkalide and electride research. These problems stem from the inherent instabilities of the compounds. Both the solid compounds and the metal-amine and metal-ether solutions from which they are made, appear to undergo autocatalytic decomposition below room temperature.<sup>2,50</sup> Although the cleavage of ethers by alkali metals in solution has been widely studied,<sup>51</sup> no detailed investigation of the decomposition of alkalides and electrides has yet been attempted. Most of what is known about the decomposition of alkalides and electrides has been assembled from scattered observations.

Preliminary studies of the stabilities of alkalides and electrides have utilized differential scanning calorimetry (DSC). Early DSC results were used to determine phase transitions, heats of reaction, and to compare the relative stabilities of several alkalides and electrides. 5,47 These studies were later extended to include new types of alkalides and electrides which utilize tertiary amines as complexing agents. 17,18 In addition, Mark Kuchenmeister of the Dye group studied the long term stability of these compounds at room temperature. By visually monitoring the color change of compounds

stored at room temperature in vacuo, he attempted to qualitatively compare their stabilities.

### III.B. <u>Differential Scanning Calorimetry</u>

Differential scanning calorimetry has been used by chemists and materials scientists since its invention in 1964. The technique has been widely used for the study of reaction kinetics, to determine the enthalpy of phase transitions and chemical reactions, sample purities and many other applications. The DSC technique is straightforward. Two identical pans, one an empty reference pan and the other containing the sample to be studied, are placed on separate holders which are each equipped with a thermometer and a heat source. Both pans are then heated at the same rate and the amount of extra energy required to keep the sample pan temperature equal to that of the reference pan is measured. In this manner, enthalpy changes due to phase transitions and chemical reactions are displayed as peaks in a plot of heat input versus temperature.

Although the peak shapes of phase transitions are affected by the heating rate of a DSC experiment, the onset of these transitions is constant once thermal lag has been accounted for. The situation is different for peaks due to chemical reactions such as decompositions. In the case of a chemical reaction the position and onset of a DSC peak are highly dependent on the heating rate of the experiment. It is this fact that makes the comparison of the stabilities of compounds from their DSC decomposition peaks difficult. The dependence of the

peak position on heating rate varies from reaction to reaction. In comparing two different compounds for stability, therefore, it is possible for one to appear more stable at a fast heating rate and for the other to appear more stable at a low heating rate.

Several methods which use the dependence of the position of a reaction peak upon the DSC heating rate to determine kinetic parameters have been proposed.<sup>52</sup> Two of the more commonly used methods were developed by H.E. Kissinger and T. Ozawa and are described below. These methods allow the determination of the activation energy of a chemical reaction from DSC data. Also described is a method to determine the long term stability of a compound at a given temperature.

## 1. Kissinger Method

The relationship between peak temperature and heating rate for a first order chemical reaction has been given by Murray and White<sup>53</sup>:

$$A \exp(\frac{-E}{RT_m}) = \frac{E}{RT_m^2} (\frac{dT}{dt})$$

where R is the gas constant, T is the absolute temperature,  $T_m$  is the peak temperature, A is the frequency factor, E is the activation energy, and dT/dt is the heating rate. This equation can be written in more usable form as:

$$\ln\left(\frac{\Phi}{T_{\rm m}^2}\right) = \ln\left(\frac{RA}{E}\right) - \frac{E}{RT_{\rm m}}$$
13

where  $\phi = dT/dt$ . Equation 13 shows that a plot of  $\ln(\phi/T_m^2)$  versus  $1/T_m$  should be a straight line with slope -E/R. Kissinger found this to be the case for a number of first-order decomposition reactions.<sup>54</sup> Once the value of E is found from this method, the frequency factor (A) can be determined from equation 12, or from the intercept of the plot made using equation 13.

It was later shown by Kissinger that for an nth order reaction, the relationship between the heating rate and peak temperature is given by the equation:<sup>55</sup>

$$\frac{E\phi}{RT_{m}^{2}} = An(1-x)_{m}^{n-1}exp(\frac{-E}{RT_{m}})$$
14

where  $(1-x)_m$  is the fraction of unreacted material at the peak temperature. Kissinger was also able to show that  $n(1-x)^{n-1}_m$  is independent of the heating rate and very nearly equal to unity. Equation 14, therefore, reduces to equation 13 and the Kissinger method is applicable regardless of reaction order.

### 2. Ozawa Method

A method which is slightly different from that of Kissinger has been developed by Ozawa.<sup>56</sup> This method was originally developed for use with thermogravimetric data but was adapted by Krien for

use in the analysis of DSC data.<sup>57</sup> The Ozawa method relates the heating rate to the peak temperature of a DSC trace by the equation:

$$\log(\phi) = C - 0.4567(\frac{E}{RT_m})$$

where C is a constant and all other terms are as previously defined. Thus, a plot of  $\log \phi$  versus  $1/T_m$  will give a straight line from which the activation energy of the reaction can be calculated.

It can be seen by comparison of equations 13 and 15 that the major difference between the Kissinger and Ozawa methods is the factor of 1/T<sup>2</sup><sub>m</sub> in the ordinate term of the Kissinger method. Initially, it would appear impossible that both of these methods could yield linear plots. The size of T<sub>m</sub> is typically 300 - 700 K, however, and the amount that it changes with scanning rate for a particular reaction is generally less than 50 K. The large size of T<sub>m</sub> and its small change make this term nearly constant on the log scale used for these methods. Consequently, both the Kissinger and the Ozawa methods yield linear plots. The two methods have been compared experimentally for a number of reactions and shown to yield values of E similar to each other and to those obtained by other experimental methods.<sup>58-60</sup> It has been shown, however, that values of the frequency factor found through use of the Kissinger method can differ from those found with other methods by orders of magnitude.59

### 3. Isothermal Stability and Kinetics Measurements

Although important reaction parameters can be obtained from the Kissinger and Ozawa methods, these techniques do not allow the reaction order or the rate of reaction at a single temperature to be calculated. In order to determine the stability of a compound, therefore, it is necessary to employ different methods. The method chosen for this work is a variation of one that has been widely used to study reaction kinetics not only from DSC data, but from a wide variety of experimental techniques.

The area under a reaction peak (the  $\Delta H$ ) is related to the amount of sample undergoing reaction. If a sample is allowed to partially react (or decompose) prior to a DSC experiment, therefore, the fraction of unreacted sample at the beginning of the experiment can be calculated from the observed  $\Delta H$  for a sample of known mass. This method requires that several samples of the compound under study be held at a stable temperature for varying periods of time to partially react before their decomposition in the DSC. From the observed  $\Delta H$ 's and knowing the amount of time that each sample was allowed to react prior to its DSC run, the reaction rate constant at that temperature and the reaction order can be determined by simple graphical methods. If this same procedure is carried out at several temperatures, the activation energy can be determined from the Arrhenius equation.

### III.C. Results and Discussion

The methods described above were applied to the electrides K+(C222)e- and Li+(PMPCY)e-. These two electrides were chosen for detailed studies because observations had previously indicated that Li+(PMPCY)e- is probably the most stable electride while K+(C222)e- is possibly the most unstable. Experimental results from these studies are presented and discussed below.

#### 1. Li+(PMPCY)e-

Li+(PMPCY)e- was the first electride synthesized from an aza complexant, and was shown to be rather thermally stable for an electride.<sup>17</sup> In particular, qualitative results indicated that this compound is stable at room temperature for periods of up to several days.<sup>17</sup> It was in an effort to quantify these observations that the current work was begun.

Samples of Li+(PMPCY)e- were run in the DSC at heating rates which varied from 1.0 °C/min to 11 °C/min. All runs were begun at -40 °C and heated through the decomposition peak. An example of a typical DSC trace for this compound is shown in Figure 8. The enthalpy of reaction for the decomposition measured from the DSC trace was independent of heating rate and averaged 170 +/- 20 J/g or 50 kJ/mole.

Plots from the Kissinger and Ozawa methods are shown in Figure 9a and 9b respectively. Some scatter in the data notwithstanding, the plots are both linear. Least squares fitting of

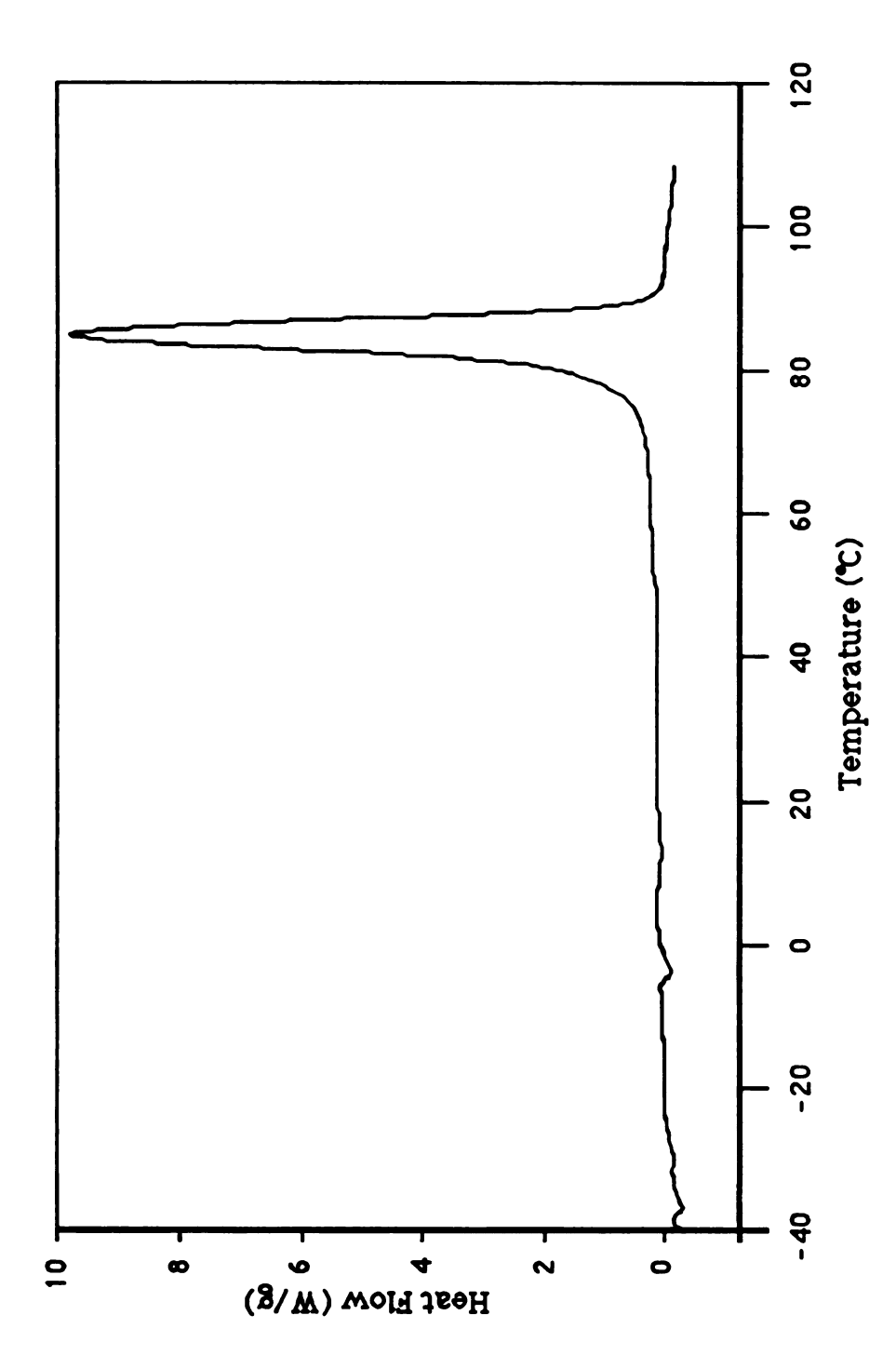


Figure 8: Li+(PMPCY)e- DSC trace from -40 °C through the decomposition.

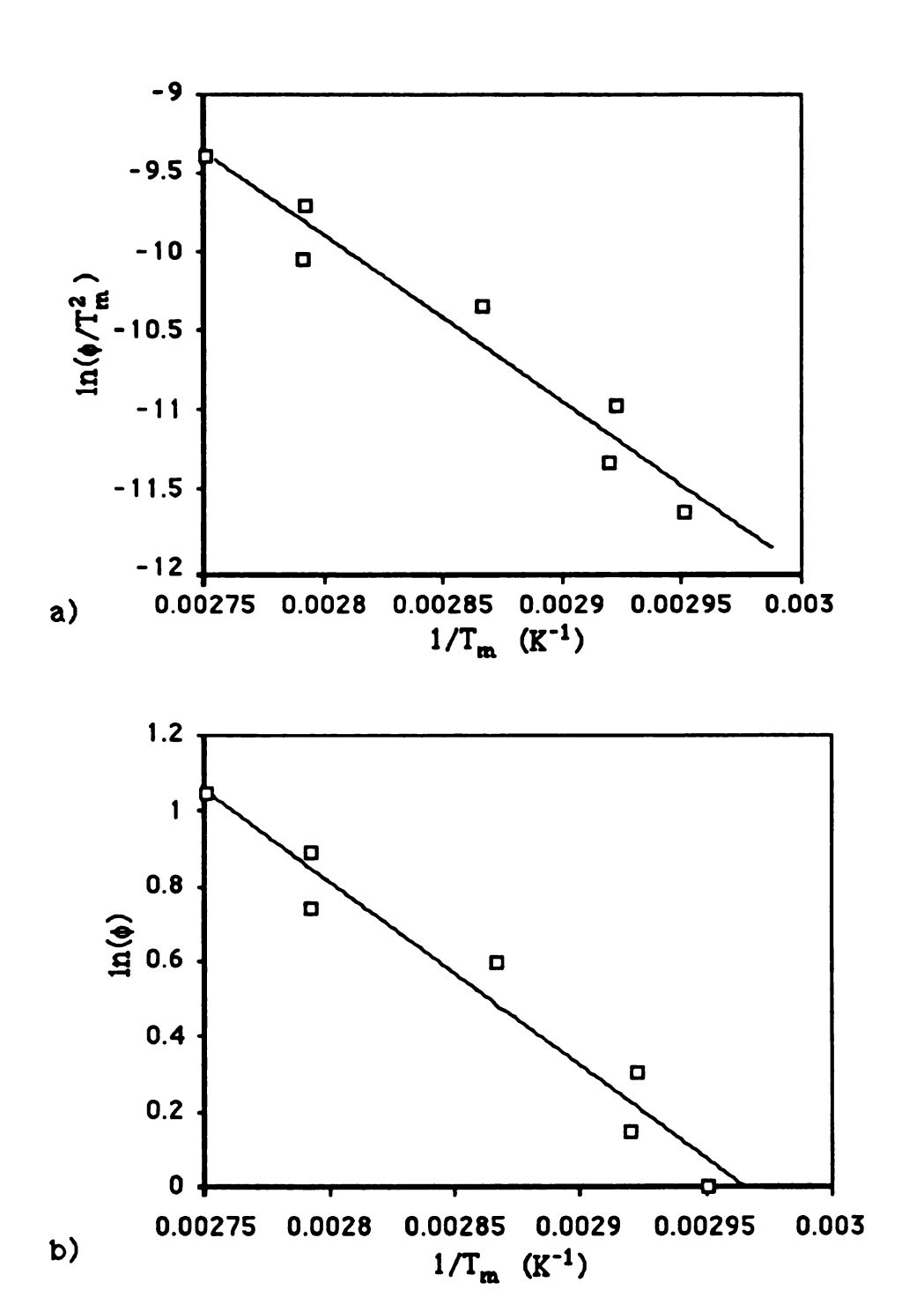


Figure 9: Activation energy analysis of Li<sup>+</sup>(PMPCY)e<sup>-</sup>, a) Kissinger method, b) Ozawa method.

the data results in a value of 87 +/- 9 kJ/mol for the activation energy from the Kissinger method, and a value of 88 +/- 9 kJ/mol from the Ozawa method.

It had been reported previously that Li+(PMPCY)e-decomplexed slowly at room temperature over a period of approximately 10 days.<sup>17</sup> The stability of this compound was checked at room temperature in the current work by following the change of the enthalpy of reaction as a function of time as has been described above.

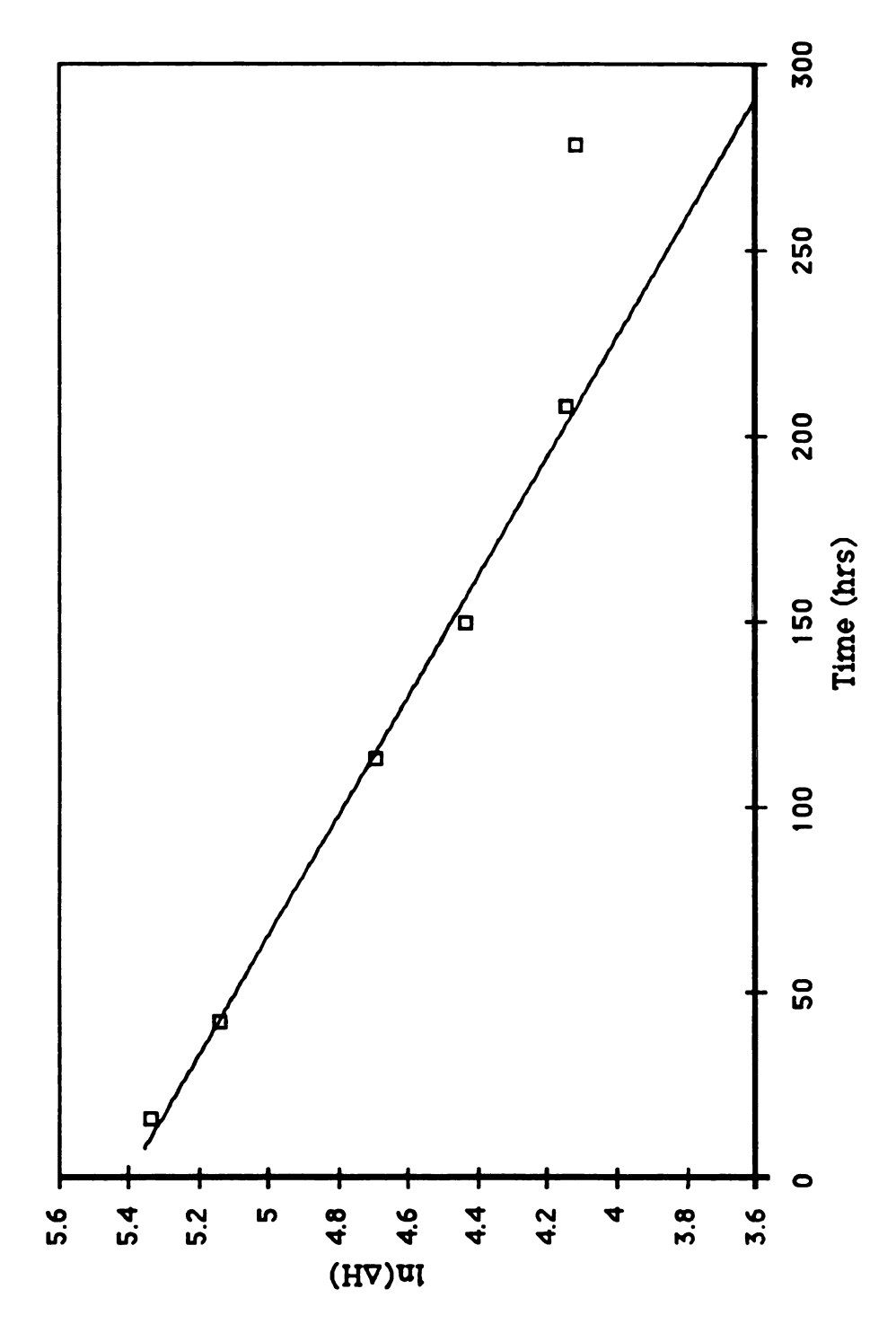
In the first attempt at this study, samples of Li<sup>+</sup>(PMPCY)e-were loaded into sample pans and stored at room temperature in a nitrogen-filled glove bag. The first sample was removed from the glove bag and run on the DSC after it had been warm for one week. No decomposition peak was observed. Apparently, the sample had reacted with either the aluminum pan or the nitrogen atmosphere inside the pan. The latter would be especially likely if the sample decomplexed prior to decomposition, since the free lithium metal which would result from decomplexation reacts quickly with nitrogen gas to form lithium nitride.

The second attempt at this study was more successful. A sample of Li<sup>+</sup>(PMPCY)e<sup>-</sup> was stored under vacuum in a Pyrex vessel at room temperature. Samples for DSC studies were removed periodically after the sample had been cooled in liquid nitrogen. The entire transfer and loading process was carried out at liquid nitrogen temperature in a nitrogen-filled glove bag. The cell which contained the remaining sample was evacuated before it was warmed back to room temperature. The loaded DSC sample pans were run on the DSC

from room temperature through the decomposition point at a heating rate of 2 °C/min.

The results of this experiment, once the data had been analyzed, were unexpected. As can be seen from a plot of the data in Figure 10, the reaction obeys first order kinetics very well. The slope of the least squares line through the data corresponds to a rate constant of  $6.2 \times 10^{-3}$  +/-  $2 \times 10^{-4}$  hrs<sup>-1</sup> at the experiment temperature of 23 °C. This corresponds to a half-life of ~110 hrs.

The major surprise of this experiment is that the decomposition reaction does not appear to be autocatalytic. As mentioned previously, many observations had indicated that the decomposition of alkalides and electrides is autocatalytic in nature. Secondly, no decomplexation of the compound was observed in this experiment. Li<sup>+</sup>(PMPCY)e<sup>-</sup> had been observed, by other workers, to decomplex, upon standing, to lithium metal and liquid complexant.<sup>17</sup> In this experiment, however, no evidence of decomplexation was observed. Visually, as the compound sat at room temperature, its color changed from the characteristic black of an electride to dark blue and, eventually, blue-gray. No liquid formation was observed. Even at the end of this experiment, the powdered sample was not sticky or oily as would be expected from decomplexation. Indeed, if decomplexation had occurred rather than decomposition, this experiment would not have succeeded since decomplexed metal and complexant will still react exothermically at high temperatures in the DSC.



Li+(PMPCY)e- first order kinetics, In(enthalpy) versus time at 23°C. Figure 10:

### 2. K+(C222)e-

K+(C222)e- was one of the first electrides to be synthesized, and much is now known about this unique compound.<sup>61</sup> The high instability of this compound makes it very difficult to synthesize, handle, and study. In order to determine exactly how unstable K+(C222)e- is, experiments similar to those run on Li+(PMPCY)e- were performed.

The high exothermicity of K+(C222)e- presented additional problems to the application of the Kissinger and Ozawa methods. The enthalpy of decomposition for K+(C222)e-, found from DSC data is 330 +/-10 J/g, or 140 kJ/mol. This is nearly double, gram for gram, the value found for Li<sup>+</sup>(PMPCY)e<sup>-</sup>. In addition, the decomposition reaction appears to be rapid once initiated. Together, these effects can cause a sample undergoing decomposition in the DSC to heat faster than the programmed heating rate. An example of a DSC trace of K<sup>+</sup>(C222)e<sup>-</sup> for which this occurs is shown in Figure 11. Also shown is the disruption of the ramping rate caused by this rapid Since both the Kissinger and Ozawa methods were reaction. developed assuming a constant heating rate, this temperature overshoot causes a problem in the reduction of DSC data. compensate for this experimental error, the base of the exotherm peak was divided in half and its midpoint was used as the peak temperature for both methods.

DSC data were collected at 10 heating rates for K<sup>+</sup>(C222)e<sup>-</sup>. Heating rates covered the range of 1°C/min through 30 °C/min. When the data were plotted, it was seen that they were linear with

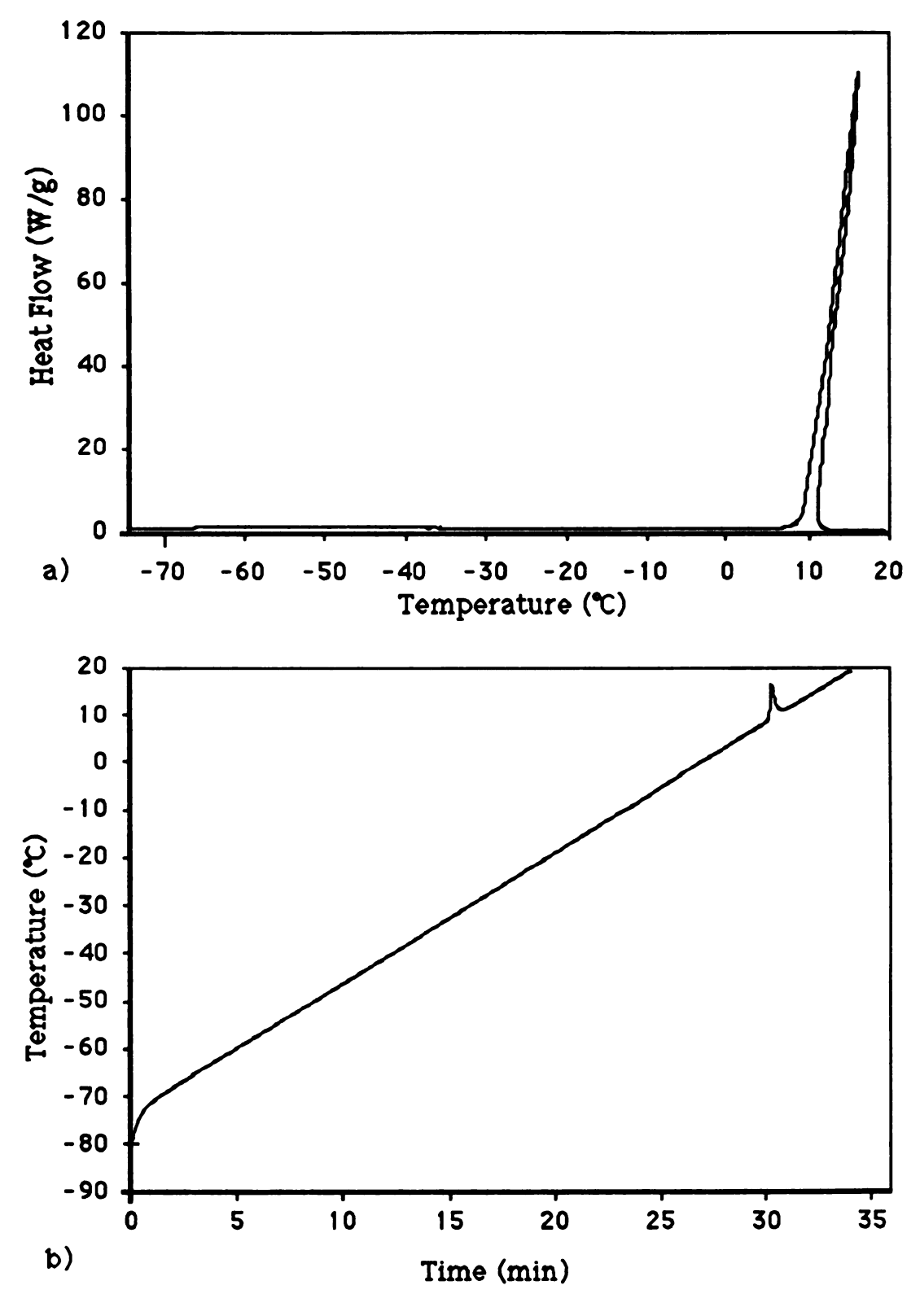


Figure 11: a) DSC trace of K<sup>+</sup>(C222)e<sup>-</sup> showing the large temperature overshoot, and b) disruption of the heating rate.

the exception of the two highest scanning rates. It is possible that these points strayed due to instrumental limitations since they were run at much higher rates than are normally used in DSC experiments on this instrument. As such, they were excluded when the data were fit. The results of the data analysis yielded an activation energy of 66 +/- 6 kJ/mol for the Kissinger method, and 67 +/- 6 kJ/mol for the Ozawa method. This is substantially lower than that seen for Li+(PMPCY)e-, and is reflected in the much lower stability of K+(C222)e-. Plots of the data are shown in Figure 12.

The experiment to study the long term stability of K+(C222)e<sup>-</sup> was set up slightly differently from the Li+(PMPCY)e<sup>-</sup> study. Samples of K+(C222)e<sup>-</sup> were sealed in Pyrex tubes under vacuum at liquid nitrogen temperatures. For the experiment, these tubes were placed in a refrigerated bath at -57 °C. Individual tubes were removed periodically and their contents were loaded into DSC pans in a nitrogen-filled glove bag at liquid nitrogen temperature. The loaded pans were also stored at liquid nitrogen temperatures until they could be run on the DSC.

The data for K+(C222)e- proved to be impossible to fit to any reaction order. After the first day at -57 °C, the DSC peak was virtually identical to that found for the pure sample. After the second day, the peak had decreased by two thirds, while the sample for the third day actually gave a larger peak than had the sample from the previous day. Beyond three days, decomposition peaks whose sizes were less than 2% of the pure sample were observed. By the sixth day, no decomposition peak was observed indicating that

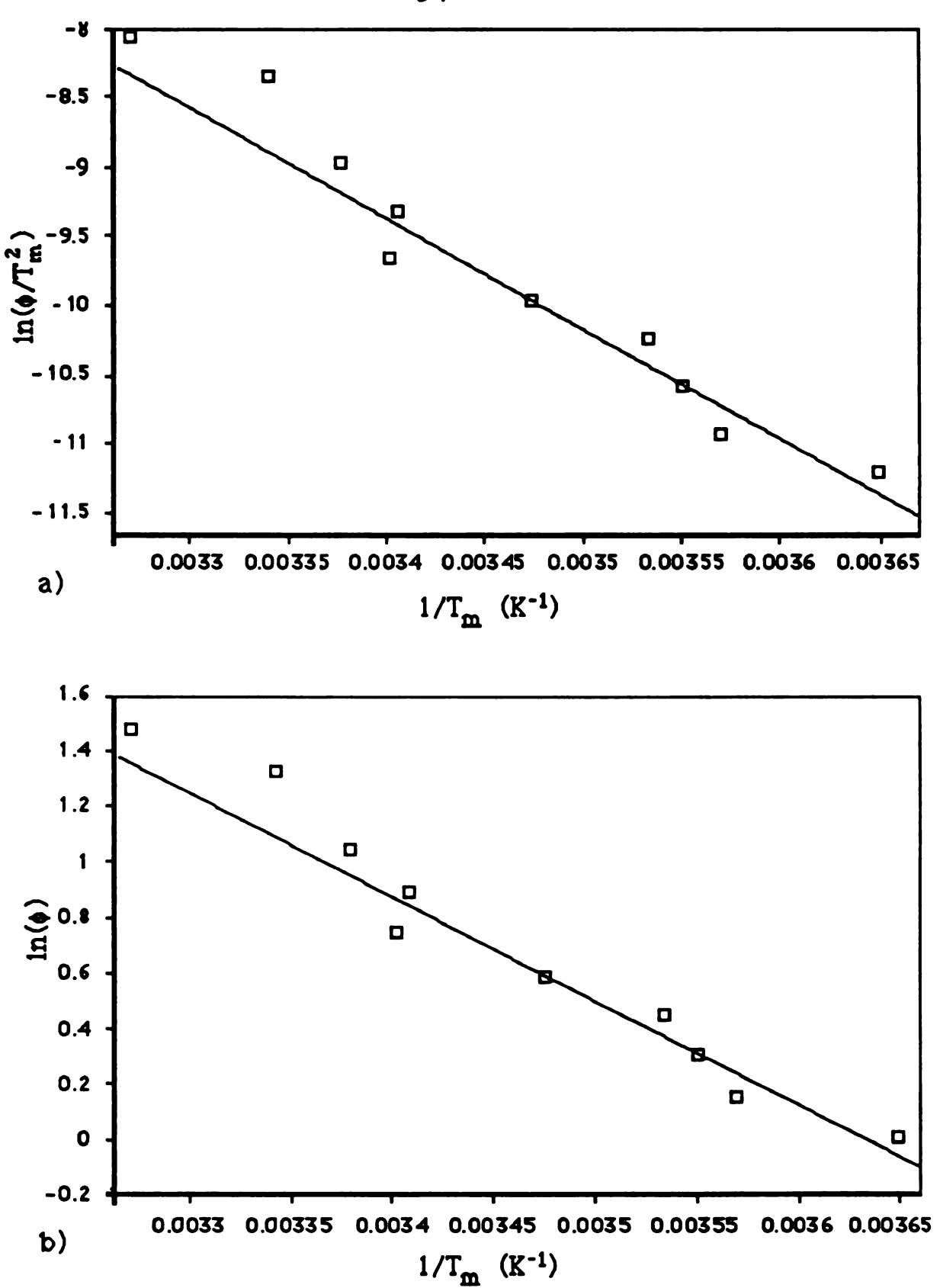


Figure 12: Activation energy analysis of K<sup>+</sup>(C222)e<sup>-</sup>, a) Kissinger method, and b) Ozawa method.

the sample had already completely decomposed. A plot of the data is shown in Figure 13.

The results listed above are consistent with an autocatalytic reaction. Presumably, the initiation step of this reaction is the slow step and the activation energy found from the Kissinger and Ozawa methods relates to it. At low temperatures, decomposition may affect mostly individual crystallites at first, but spread to other crystallites as the reaction progresses. At higher temperatures, such as those encountered in the DSC, the reaction may be initiated in large portions of the sample nearly simultaneously. This would cause the very rapid temperature increase observed in many DSC experiments for K+(C222)e<sup>-</sup>.

Also observed in this experiment was the color change undergone by the sample during time it was in the isothermal bath at -57 °C. The samples began as a dark black material, and gradually changed to dark blue and finally gray-blue. In some cases, small isolated specks of white material were observed in the otherwise dark material, further indication of a nonhomogeneous reaction. It should be noted that even samples which appeared to be totally decomposed based on DSC data retained much of their blue color and turned white over a period of several minutes when warmed to room temperature. This indicates that color has little to do with the purity of an electride.

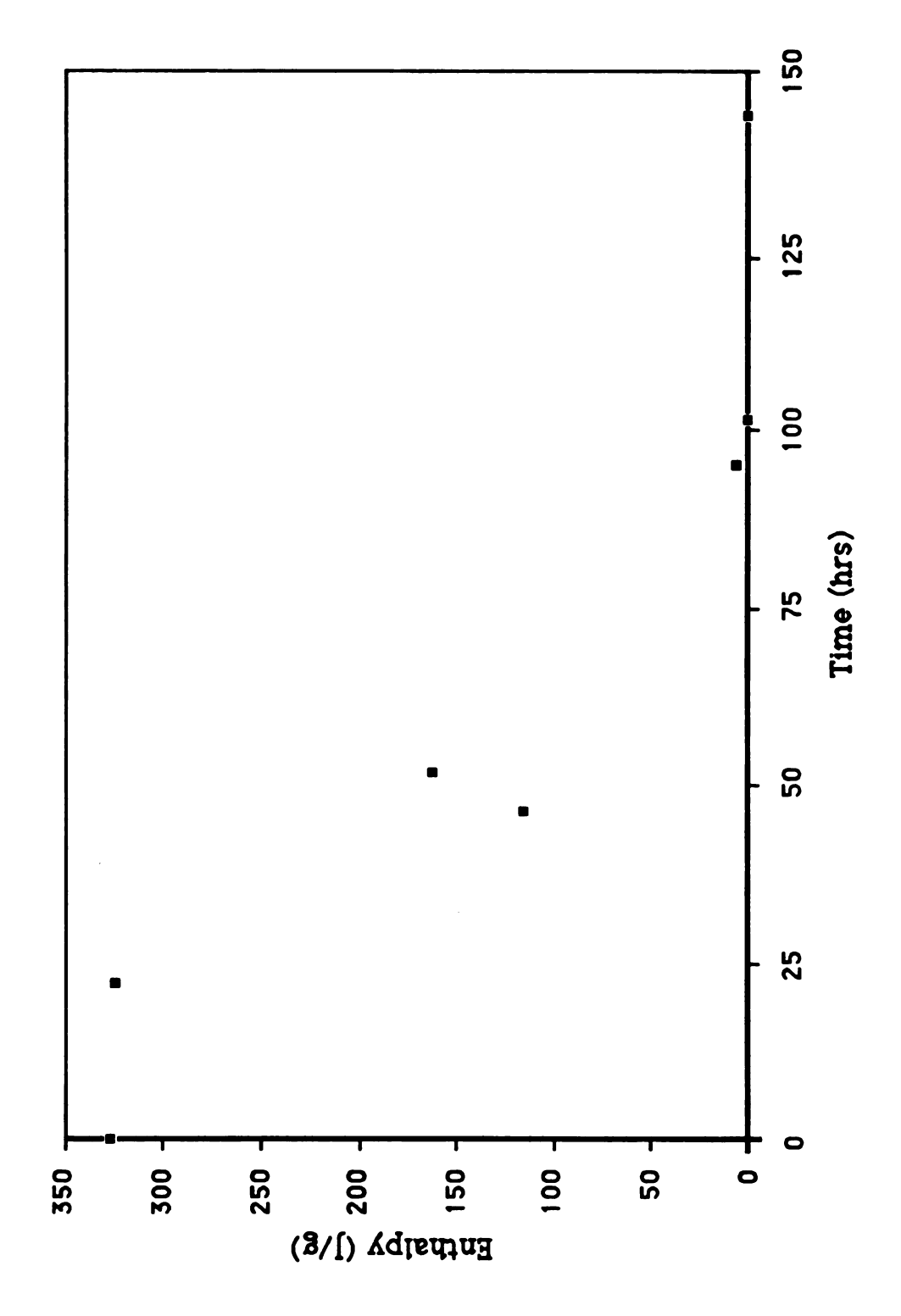


Figure 13: K+(C222)e- long term kinetics at -57 °C, enthalpy of reaction versus time at -57 °C.

### III.D. Conclusions

These experiments have clearly shown two different types of behavior associated with the decomposition of electrides. K+(C222)edecomposes autocatalytically with the liberation of much heat, while Li+(PMPCY)e- undergoes a first order decomposition which is much less exothermic. Although two examples make a limited data base, there are possible explanations for the differences noted above. Until recently, oxa- crown ethers and cryptands were utilized exclusively as complexants in alkalides and electrides. Anecdotal observations have indicated that the decomposition of such compounds is autocatalytic<sup>46</sup> as has been found in this work for K+(C222)e-. It may be, however, that electrides formed from amine complexants such as PMPCY decompose through a different Clearly, more work must be done before it can be determined whether the behavior of Li+(PMPCY)e- is characteristic of all electrides which contain amine based complexants. In particular, recent results indicate the presence of methylamine in at least some syntheses of this compound.<sup>46</sup> Further work to determine whether methylamine is a part of the compound, and its possible effect on the decomposition of Li+(PMPCY)e- is required. Also seen in this study was the higher activation energy for decomposition observed in the more stable Li+(PMPCY)e-. Once again, it is too soon to say with certainty whether or not this effect is characteristic of amine complexants or is only due to the large difference in the stabilities of these two electrides.

One conclusion that can be drawn with certainty concerns the relationship between the color of an electride and its purity. Both of these compounds retained much of their characteristic color even when DSC results indicated that they were well over 50% decomposed. In the case of K+(C222)e-, blue-gray color persisted even when the DSC indicated that no compound remained undecomposed. These results imply that color is a very poor indicator of purity in an electride. In retrospect, this was to be expected. Trapped electrons have such a strong absorbtion in the optical region of the spectrum that it takes only a very small concentration to produce color in a sample. The purity of electride, then, is better tested through different experimental techniques such as EPR or magnetic susceptibility which can be used to determine the amount of trapped electrons present in a sample.

#### IV. ELECTRICAL PROPERTIES OF ELECTRIDES

### IV.A. Theory

As noted earlier, studies of the electrical properties of alkalides and electrides have been severely hindered by the inability to grow large single crystals of these reactive compounds. As a result, most past studies have consisted of d.c. resistivity measurements performed on pressed powder samples. It was initially hoped that single crystal methods could be utilized in the current work. As this did not prove possible, methods to eliminate the many problems associated with polycrystalline conductivity measurements were pursued. This section will describe many of the problems involved in pressed powder studies and experimental techniques to overcome them.

# 1. Polycrystalline Conductivity Problems

In an ideal case, the data obtained from d.c. conductivity measurements on a polycrystalline sample should approach that of a single crystal. Unfortunately, few examples of this exist. In practice, incomplete sample packing and orientational, grain boundary, and electrode contact effects combine to limit the amount of information that can be obtained from this type of measurement. In many cases,

the limitation is extreme enough that conductivity values measured on such samples are many orders of magnitude different from those measured on single crystal samples. The natures of these obstacles are discussed below.

### 1.a. Orientational and Packing Effects

Many crystalline compounds exhibit some amount of anisotropy in their conductivity characteristics. Several techniques have been developed to measure this anisotropy in single crystal samples. Anisotropy information is lost in polycrystalline samples since the crystallites in a packed powder are usually orientated randomly. As a result, the conductivity of such samples tends to be isotropic and the measured conductivity is a combination of the conductivity tensors of the individual crystallites in the sample.

A second limitation of polycrystalline conductivity measurements also has to do with the packing of the crystallites in a sample. Crystallites in a powder do not pack to fill space completely. The empty spaces left between grains lower the apparent conductivity of such samples. This effect can be partially corrected by pressing powdered samples into pellets under high pressure, which tends to minimize the size of the empty spaces in a sample. If the crystal structure of the compound is known, the size and mass of the pellet can be used to determine the fraction of free space in the pressed pellet sample. From this, the measured value of the conductivity can be adjusted to compensate for the empty space.

### 1.b. Grain Boundary Effects

The properties of many polycrystalline materials are greatly influenced by grain boundaries. In most cases, the resistance across the grain boundaries of polycrystalline materials is higher than that of the grains and may be many orders of magnitude larger. The effects of grain boundaries on the conductivities of polycrystalline systems can arise from impurities, point defects, and second phases such as oxide layers at the crystallite surface. These tend to form a barrier to charge transfer between adjacent crystallites. These effects make determination of the bulk properties of such compounds nearly impossible by d.c. methods. In fact, the study of grain boundaries and their properties by various other methods has been an active area of research in physics, chemistry, and engineering. Devices such as thermistors, varistors, and capacitors which utilize the properties of grain boundaries have been made from a variety of polycrystalline ceramics. 62,63

A general energy-band diagram for two n-type semiconductor grains with a grain boundary region, which has a lower chemical potential (a lower Fermi level) than that of the bulk, is shown in Figure 14.64 Band theory dictates that the Fermi levels of two materials in contact must be coincident at thermal equilibrium. Since this is not generally the case for dissimilar materials, current flows between the materials until their Fermi levels are at equal energy. In this example, charge must flow from the grains into the boundary to bring its Fermi level up to that of the grains. This results in a negative space charge at the boundary and a corresponding positive

charge in the grains. Because of the relatively low carrier concentration in a semiconductor, this positive charge is distributed over a depletion region near the grain surface. This causes band bending in the grains over the depletion region forming a barrier to current flow. Also shown in Figure 14 is the variation of the barrier height with applied voltage. The height of the barrier and the depletion width both decrease in the negative grain with applied voltage. This effect leads to increased current flow at high voltages and non-ohmic behavior in polycrystalline samples. It should be noted that even in the absence of a second phase in the boundary, impurities and defects at the grain surfaces cause band bending and barrier formation at the boundary.

In the above case, the flow of charge between grains is impeded and depends upon the height of the boundary. The height of a grain boundary barrier is difficult to calculate since it is heavily dependent upon the amount and nature of impurities and defects at the grain surface. Regardless, the characteristics of the boundary resemble those of oxide layers and Schottky barriers at electrode surfaces which are described in somewhat more detail below.

## 1.c. Electrode Effects

Contact resistance effects between a sample and the measuring electrodes pose a further problem to polycrystalline conductivity measurements. There are two main types of electrode contact effects; oxide layers and Schottky barriers. Both of these effects

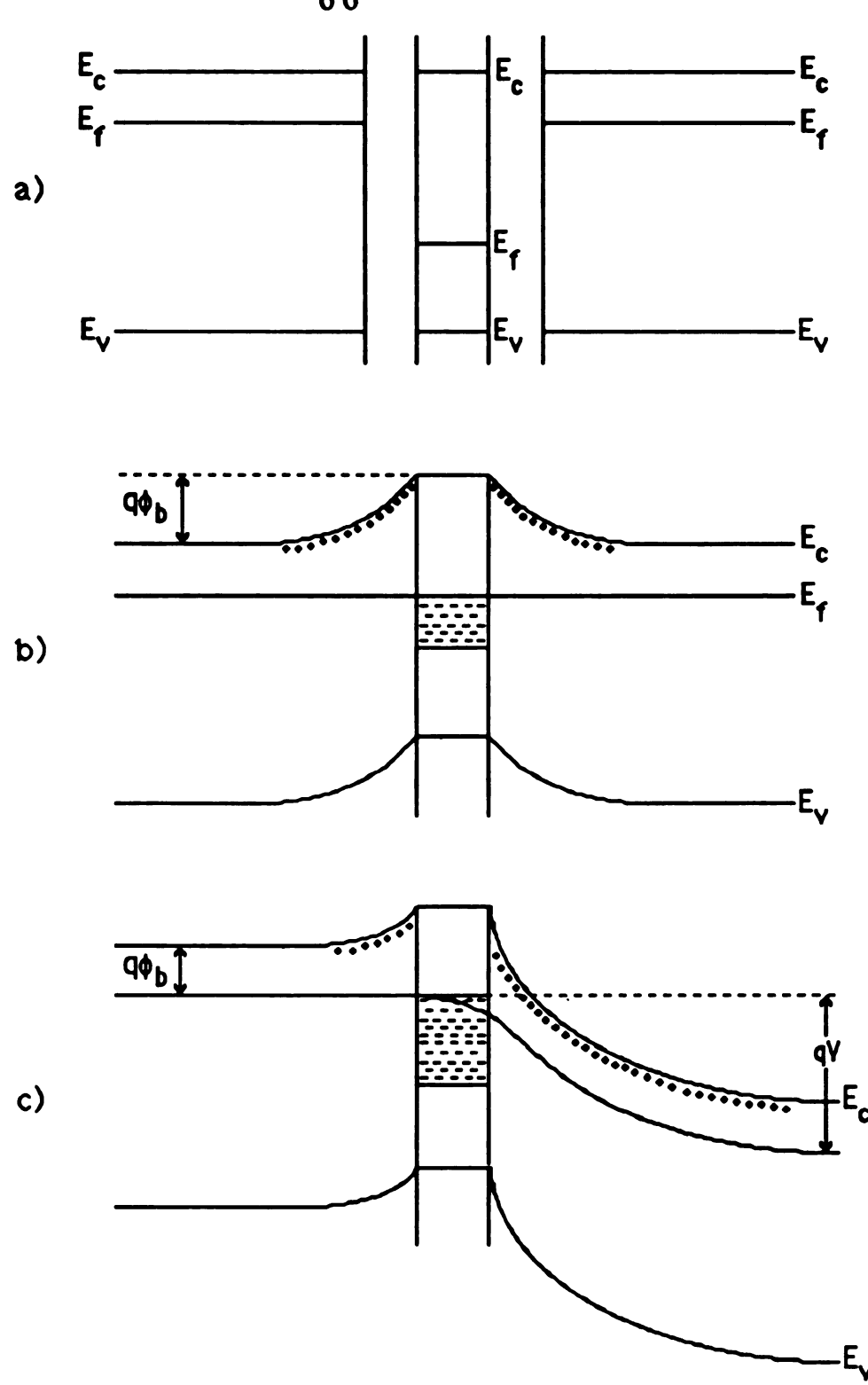


Figure 14: Band diagram for two semiconductor grains and their contact region. a) The grains and their boundary as three isolated materials. b) The contact at thermal equilibrium. c) boundary region under an applied voltage V.

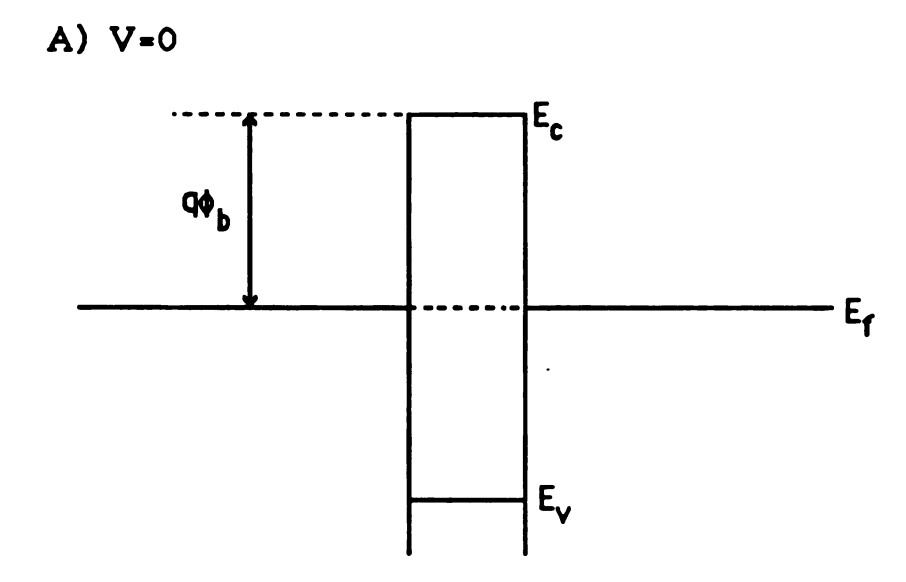
have similarities to grain boundary barriers and lead to non-ohmic behavior in 2-probe conductivity measurements.

Oxide layer formation is a common problem when an oxidizable metal is being used as an electrode material. Also, when the sample being measured is itself an oxidizable metal, the formation of oxide layers can be the major cause of resistance in the sample. A diagram of an oxide layer between two metals is shown in figure 15. Note that there is no depletion layer formation in the metal since the number of charge carriers is large and depletion layers, therefore, are immediately erased by current flow. The height of the oxide barrier  $(q\phi_b)$  in such a contact is given by:

$$q\phi_b = q(\phi_m - \chi)$$
 16

where  $\phi_m$  is the work function of the metal,  $\chi$  is the electron affinity of the oxide measured from the bottom of the conduction band, and q is the electronic charge.

Current flow across the oxide barrier is limited by the height of the barrier. Since metals are good conductors, when a bias is applied across the sample virtually all of the voltage drop occurs across the oxide barrier. Most oxide layers are relatively narrow and tunnelling is responsible for a portion of the current flow even at low applied voltages. As the voltage drop across the oxide layer approaches the barrier height, however, tunnelling becomes more important. As seen in Figure 15b, a large voltage bias decreases the barrier width relative to the more negative metal leading to increased tunnelling and highly non-ohmic behavior.



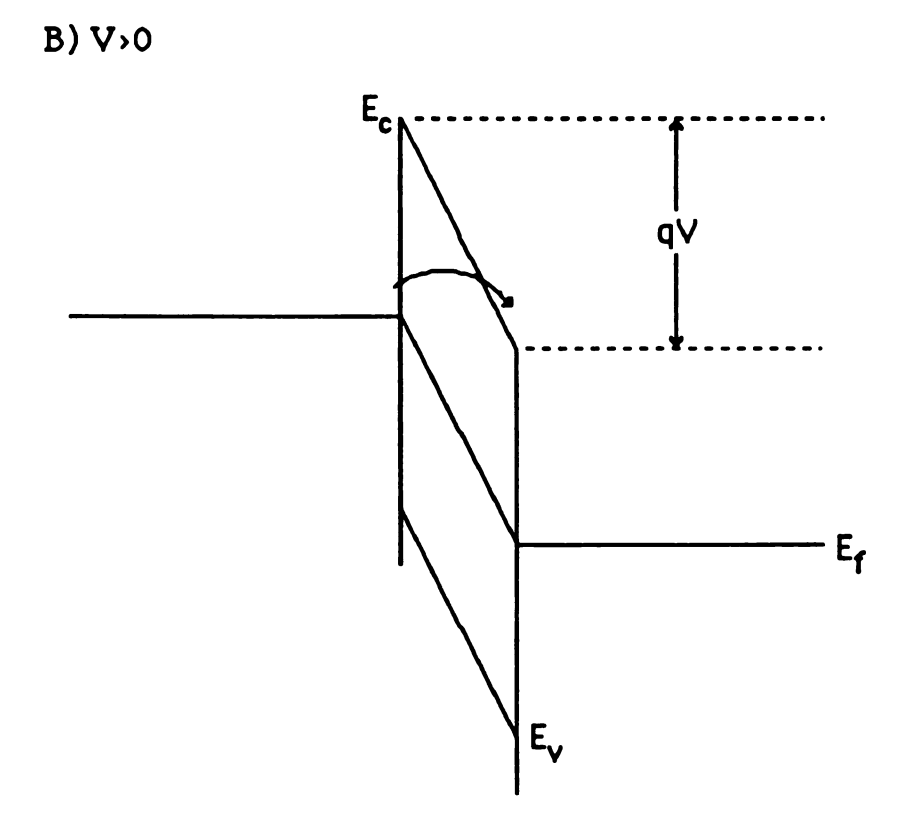


Figure 15: A) Oxide barrier at thermal equilibrium between two metals. B) Oxide layer under an applied voltage V.

Unlike grain boundary barriers and oxide layer barriers, Schottky barriers are directly related to the properties of the electrode and sample which are in contact, rather than any defects or impurities present. Figure 16 shows the band diagram for an n-doped semiconductor in contact with a metal.<sup>65</sup> Note that prior to contact the Fermi levels of the two substances lie at different energies. The difference in potential between the Fermi levels is called the contact potential  $(E_{CD})$  and is given by the equation:

$$E_{cp} = q\phi_m - q(\chi + V_n)$$
 17

where  $qV_n$  is the energy difference between the Fermi level and the conduction band of the semiconductor. As the materials are brought into contact, current flows from the semiconductor into the metal forming a depletion region and barrier in the semiconductor. It can be seen from the diagram that the barrier height is given by equation 16. The barrier height relative to the conduction band of the semiconductor varies with voltage in the same manner as we have previously seen in grain boundary contact barriers.

It can be easily shown that for a p-type semiconductor in contact with a metal, the barrier height is given by:

$$q\phi_b = E_g - q(\phi_m - \chi)$$
 18

where all terms are as previously defined. The case of an intrinsic semiconductor in contact with a metal is difficult to describe since the Fermi level of such a material can lie either above or below that

of the metal. The barrier height then can be described by equation 16 or 18 depending on whether the Fermi level of the semiconductor is above or below that of the metal respectively.

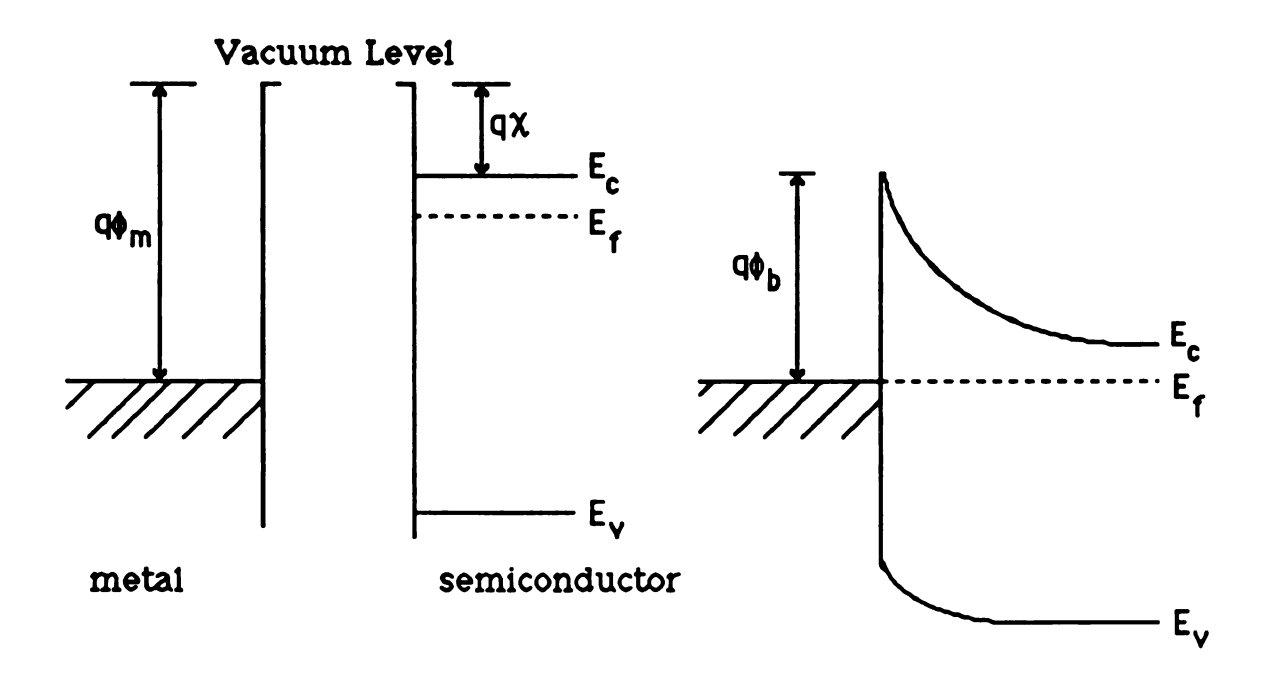


Figure 16: Energy band diagrams of a metal-semiconductor contact.

Left: Energy levels before contact, Right: Energy levels

and Schottky barrier at thermal equilibrium after contact.

Current transport from a semiconductor across a Schottky barrier to a metal can occur via four processes. These processes are 1) transport of electrons over the barrier, 2) tunneling of electrons through the barrier, 3) recombination in the depletion region, and 4) hole injection from the metal into the semiconductor. In high mobility (i.e. low band gap) semiconductors, the first of these is dominant 65 and will be described here.

Transport of electrons over a Schottky barrier can be described by thermionic emission theory. The theory assumes that 1) the barrier height  $q\phi_b$  is much larger than  $k_bT$ , 2) thermal equilibrium is established at the emission plane, and 3) current flow does not affect this equilibrium. If these are true, then the net current flow can be represented as the sum of two current fluxes, one from the semiconductor into the metal, and the other from the metal into the semiconductor. With these assumptions, the shape of the Schottky barrier becomes immaterial and current flow depends only on barrier height. Only electrons whose kinetic energy exceeds the barrier energy will be able to traverse the barrier.

For electrons crossing from the semiconductor into the metal, the current density is given by:

$$J_{sm} = AT^{2} exp \left( \frac{-q\phi_{b}}{k_{b}T} \right) exp \left( \frac{qV}{k_{b}T} \right)$$

where V is the voltage drop across the barrier region and

$$A = \frac{4\pi q m k_b^2}{h^3}$$

is the effective Richardson constant for thermionic emission with m the effective mass of an electron in the conduction band of the semiconductor. The barrier height for electrons moving from the metal into the semiconductor is unchanged by applied voltage, so the current flowing into the semiconductor is unaffected by applied voltage. At thermal equilibrium (i.e. when V=0), this current from metal to semiconductor must be equal to the current from the semiconductor into the metal. The metal to semiconductor current density, therefore, can be obtained by setting V=0 in equation 19 which results in:

$$J_{ms} = -AT^{2} exp \left( \frac{-q\phi_{b}}{k_{b}T} \right).$$
 21

By adding equations 19 and 21 the total current density can be obtained:

$$J_{n} = \left\{ AT^{2} exp \left( \frac{-q\phi_{b}}{k_{b}T} \right) \right\} \left\{ exp \left( \frac{qV}{k_{b}T} \right) - 1 \right\}.$$
 22

Equation 22 is often written as

$$J_{n} = J_{s} \left\{ exp \left( \frac{qV}{k_{b}T} \right) - 1 \right\}$$
23

where

$$J_{s} = AT^{2} exp\left(\frac{-q\phi_{\beta}}{k_{b}T}\right).$$

As can be seen from equation 23, when the forward bias voltage V is in excess of  $k_bT/q$  the exponential term is much larger than 1. In

this case, a plot of ln(I) versus V will yield a straight line whose intercept is  $J_8$ . From the intercept of such a plot, the barrier height can be obtained if A is known.

Although Schottky barriers have been studied since they were first proposed by Schottky in 1938,67 experimental limitations hampered research in the area for much of the intervening time. In particular, impurities at the metal and semiconductor surfaces caused by limitations in vacuum technology prevented ideal behavior of the barrier regions. It is only with high purity samples and clean surfaces that ideal behavior can be approached. Presently, the properties of Schottky barriers are widely utilized in Schottky diodes and other applications.65,66,68

### 2. The van der Pauw Method

One of the easiest methods for measuring the conductivity of a polycrystalline sample is via a two probe technique. Typically, in this method, the sample is held between two electrodes while a voltage is applied to it and the current through the sample is measured. The sample resistance is then calculated from Ohm's Law. This method suffers from the fact that the resistance thus calculated includes the lead resistances of the measuring circuit and the electrode contact resistance. As discussed above, the contact resistance can sometimes be larger than that of the sample which makes the two probe method inadequate for the study of many compounds.

To counter the problems associated with two probe measurements, four probe techniques can be employed. These techniques require a polycrystalline sample to be pressed into a solid pellet or grown as a thin film. The principle advantage of four probe methods is their ability to measure only the sample resistance and exclude contact and lead resistances. The general technique involves mounting four electrical probes on a sample in a certain configuration. The probe arrangement and sample shape vary between specific methods. Through two of the probes a known current is passed while the resultant voltage drop across the remaining two probes is measured. Since the measured voltage drop is due only to the current flow through the sample, the measured resistance does not include lead and electrode effects.

Many four probe techniques require samples to be cut into specific shapes prior to measurement. One technique that does not was developed by van der Pauw.  $^{48,49}$  This method allows thin samples of random shape to be used provided the following conditions are fulfilled: a) The contacts are at the circumference of the sample. b) The contacts are small. c) The sample is homogeneous in thickness. d) The sample does not contain isolated holes. When the above conditions are met, van der Pauw showed that it is possible to calculate the resistivity ( $\rho$ ) of a sample regardless of sample shape or probe spacing.

If four electrical contacts A, B, C, and D are placed on the circumference of a sample as in Figure 17a, we can define R<sub>AB,CD</sub> as the potential drop V<sub>D</sub> - V<sub>C</sub> between contacts D and C per unit current

through contacts A and B. Similarly, R<sub>BC,DA</sub> can be defined. When this is the case, van der Pauw showed the following relation to hold:

$$\exp\left(\frac{-\pi dR_{AB,CD}}{\rho}\right) + \exp\left(\frac{-\pi dR_{BC,DA}}{\rho}\right) = 1$$

where d is the sample thickness. From equation 25, there are several methods available to calculate  $\rho$ , of which the easiest is simple regression analysis.

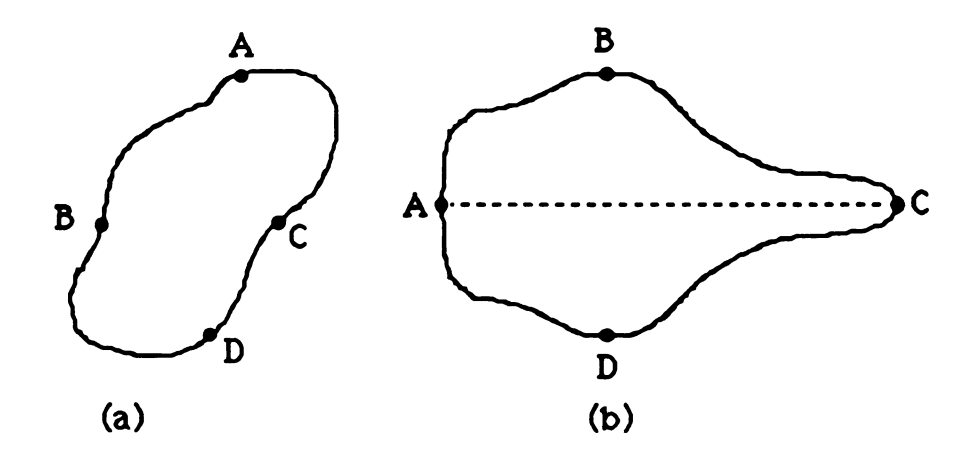


Figure 17: a) Placement of electrical contacts in the van der Pauw method. b) Placement of electrical contacts to simplify data reduction in a symmetric sample.

If the sample used contains a line of symmetry, analysis is further simplified provided the contacts are place in specified positions on the sample. In this case, contacts A and C are placed on the line of symmetry with B and D aligned perpendicular to it as shown in Figure 17b. When this is the case, R<sub>AB,CD</sub> is equal to R<sub>BC,DA</sub>. This reduces equation 25 to:

$$\rho = \frac{\pi d}{\ln 2} R_{AB,CD}.$$
 26

The method outlined above was originally intended for use with samples whose conductivity is isotropic. The method was later adapted by van der Pauw<sup>69</sup> and others<sup>70-72</sup> for use in determining the resistivity tensor of anisotropic samples such as single crystals. The technique is especially useful for this purpose in that it is more sensitive than other four probe techniques to anisotropy effects.

# 3. Impedance Spectroscopy

Impedance Spectroscopy (IS) is an a.c. conductivity technique which has been widely used in the study of polycrystalline samples since 1969 when it was first applied to solid systems by Bauerle.<sup>73</sup> The technique is not limited to solid systems and has been used since 1925 in the study of ion transport across biological membranes. In addition, IS has been used in the study of corrosion, coatings, and the reaction of solids in liquid electrolytes. In the study of polycrystalline conductivities, IS can often separate the bulk electrical properties of a sample from grain boundary and electrode effects.

Like its d.c. analog, resistance, impedance is a measure of opposition to current flow through a material. Impedance is a more general term, however, because it takes into account phase

differences between an applied sinusoidal voltage v(t) and a response current i(t) where:

$$v(t) = V_{m} \sin(\omega t)$$
 27

and

$$i(t) = I_{m} \sin(\omega t + \phi).$$
 28

In these equations,  $\omega$  is the angular frequency of the voltage signal, t is the time and  $\phi$  is the phase shift of the current relative to the voltage. Impedance,  $Z(\omega)$ , is defined by the relation:

$$Z(\omega) = v(t)/i(t)$$
 29

in direct correlation to Ohm's Law. Impedance is actually a vector quantity whose magnitude  $|Z(\omega)| = V_m/I_m(\omega)$  and phase angle  $\phi(\omega)$  are both frequency dependent. The impedance can be represented in the complex plane as shown in Figure 18. The conversion of the impedance vector into rectangular coordinates has been given previously in equations 9 and 10 as:

$$Re(Z) = Z' = |Z|cos(\phi)$$
 9

$$Im(Z) = Z'' = |Z|sin(\phi).$$

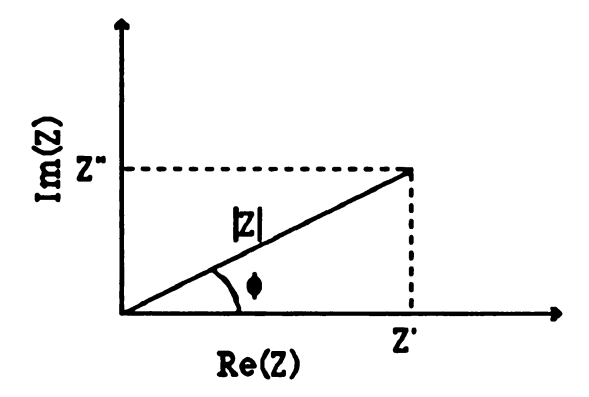


Figure 18: Representation of the impedance vector Z in the complex plane showing the phase angle φ, magnitude |Z|, and the real and imaginary components Z' and Z", respectively.

As seen above, impedance is a complex quantity and is only real when  $\phi = 0$ . This is only true at all frequencies for purely resistive behavior in which case  $Z(\omega) = Z' = R$  independent of frequency. For a real sample or resistor, one which is necessarily distributed in space, this is never the case. For such systems, it is usually the case that  $\phi$  is approximately zero at low frequencies, but that both  $\phi$  and  $Z(\omega)$  become frequency dependent at higher frequencies. The reason for this becomes clear when we look at the difference between a perfect point resistor and a real material. For a point resistor, impedance is due to the scattering of charge carriers from a single point. As such, response is instantaneous and no phase difference between voltage and current is seen for any frequency. A real system, on the other hand, has a finite size and responds to an applied voltage by the movement of charge carriers in the system. This response is not instantaneous and, therefore, results in the phase difference  $\phi$  between the applied voltage and the response current that is observed in real systems. At low frequencies, this

delay causes negligible phase shift and the impedance is nearly constant (and real) with frequency.

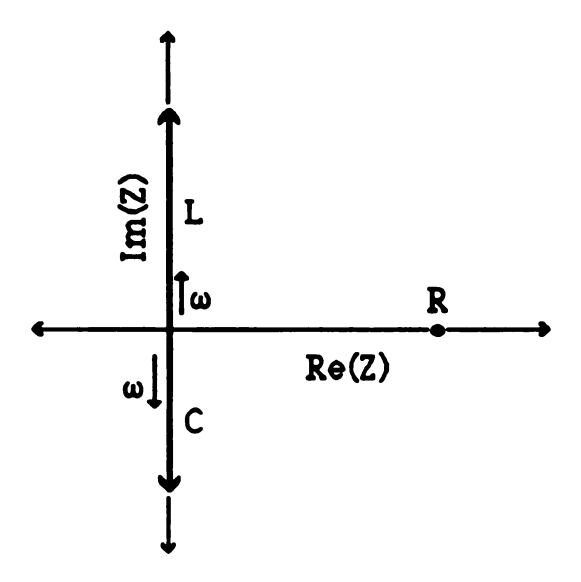


Figure 19: Representations of a perfect inductor (L), capacitor (C), and resistor (R), in the complex plane.

The result of the above is that many real systems respond to an applied voltage like an electrical circuit composed of perfect resistors, capacitors, and occasionally, inductors. The response of each of these ideal circuit elements to a sinusoidal voltage is shown in Figure 19. It can be seen that a pure resistance yields a single point in the complex plane, as described earlier. The impedance of a capacitor corresponds to a phase shift of -90° (current precedes voltage) and the impedance vector increases with decreasing frequency. An inductor introduces a phase shift of +90° and also has an impedance which increases with decreasing frequency. Since few real systems contain substantial inductive components, observed

phase shifts are usually negative. It has become customary, therefore, to plot impedance data as -Im(Z) versus Re(Z) in order to represent the data in the first quadrant of the complex plane.

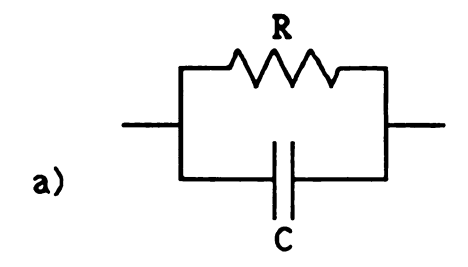
The impedance response of an ideal, single phase, real material can be represented by the parallel RC circuit of Figure 20a. For such a circuit, the impedance can be shown to be:

$$Z = \left(\frac{R}{1 + i\omega RC}\right)$$

The response of this circuit in the complex plane over a range of frequencies is shown in Figure 20b. It can be seen that such a system yields a semicircular arc whose center lies on the real axis of the complex plane. The low frequency intercept of this arc yields the resistive component of the circuit and is equivalent to the d.c. resistance of the real material. At its high frequency limit, the circuit impedance approaches zero and the impedance arc intersects the origin of the complex plane. The capacitance of the circuit can be obtained from the frequency at the peak of the arc,  $\omega_p$ , which is equivalent to:

$$\omega_{\rm p} = \frac{1}{\tau_{\rm D}} = \frac{1}{\rm RC}$$

where  $\tau_D$  is the time constant of the RC circuit or the dielectric relaxation time of the real material.<sup>74</sup>



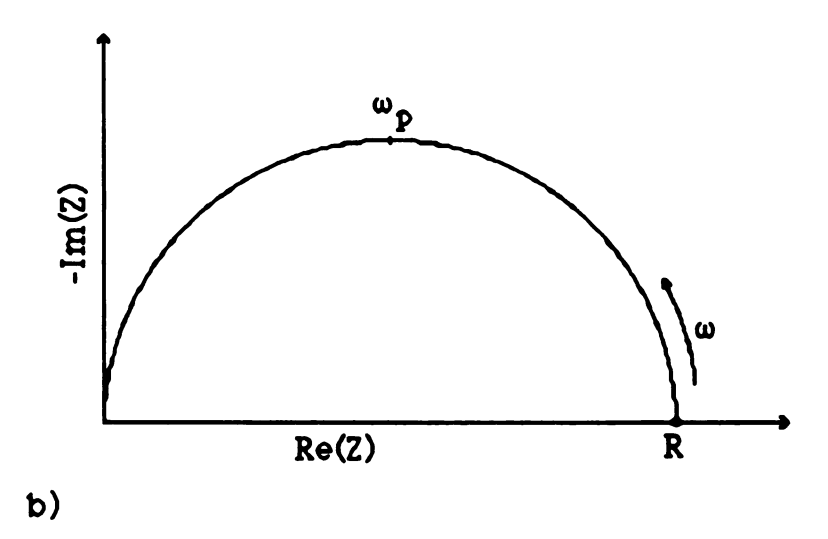
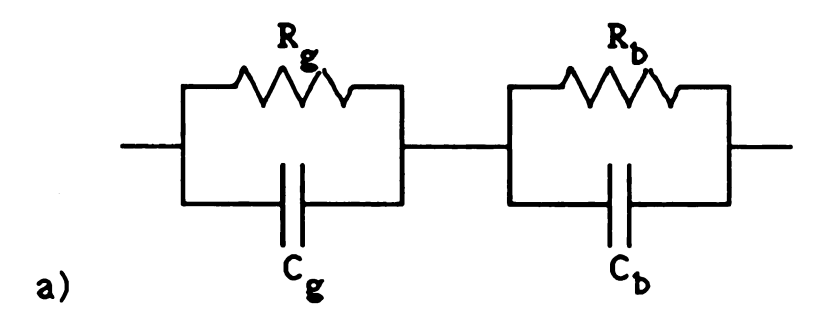


Figure 20: a) RC circuit representing an ideal single phase material b) The impedance spectrum of that circuit.

In an ideal multiphase system, such as a polycrystalline sample where grain boundary effects are important, IS can be more useful. In such a case, the sample can be represented by a pair of RC circuits connected in series. The equivalent circuit is shown in Figure 21a. If the time constant for the grain boundary portion of the circuit differs from that of the bulk by two orders of magnitude or more, the corresponding spectrum is that shown in Figure 21b. In this case, as is usually true for such systems, the grain boundary region has a longer relaxation time than the bulk and appears at lower frequencies. It is here that the real use of IS can be seen. As shown in the figure, the d.c. resistance of the system would include resistances due to both the bulk and the grain boundaries. With IS, however, the bulk sample arc and its properties have been separated from the properties of the grain boundaries. This is especially important in the case where an oxide layer covers the surface of the grains. Not only is the resistance of such a grain boundary usually much larger than that of the bulk, it usually also has a temperature dependence different from that of the bulk. Because of this, a variable temperature d.c. conductivity experiment would yield incorrect values for both the resistance and the band gap of the bulk By the use of variable temperature IS, it is possible to material. follow the behavior of only the bulk compound and obtain a true band gap for the material.

The above example can be further extended to include electrode effects which often yield a third IS arc or low frequency spike (blocking electrode behavior). The situation is often not as



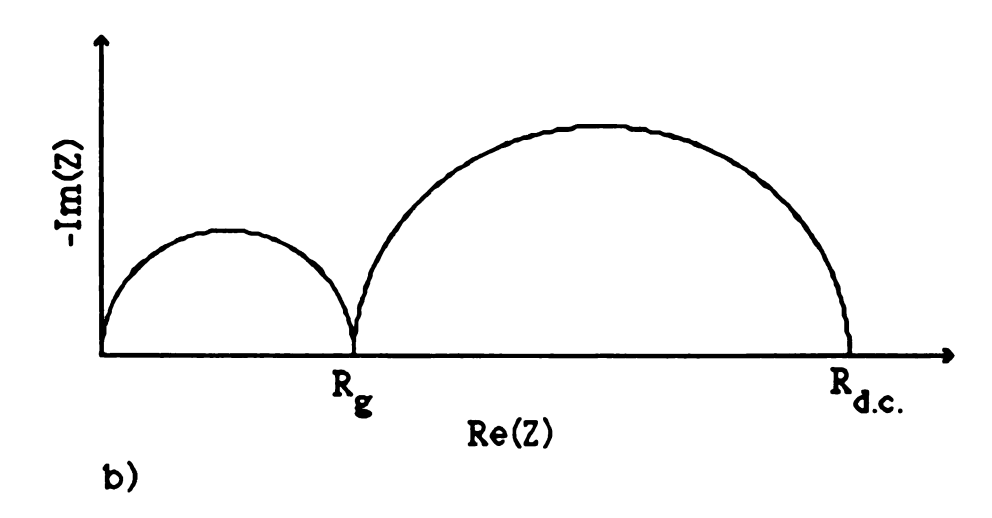


Figure 21: a) The equivalent circuit for an ideal two phase system and b) the impedance spectrum of that circuit.

straightforward as that outlined above, however. Several factors can combine to make the analysis of IS data more difficult. The most common of these factors are described below.

Two closely related problems commonly encountered in IS are that the observed impedance arc does not pass through the origin of the complex plane or that only a partial arc is observed. Experimental limitations are responsible for both of these problems. An arc that does not pass through the origin is observed when one or more arcs exist at higher frequencies than can be obtained The relaxation time of many bulk materials is so experimentally. small (<10<sup>-7</sup> s) that instrumental frequency restraints do not allow a bulk arc to be observed.<sup>74</sup> This is also the reason that only a partial IS arc is sometimes observed. In order for most or all of an IS arc to be seen, the maximum experimental frequency  $(\omega_{max})$  must satisfy the condition  $\omega_{max} >> 1/\tau_D$  or only a portion (low frequency part) of the arc will be observed. If  $\omega_{max} \ll 1/\tau_D$ , none of the arc is seen. For non-metallic materials, lowering the temperature will often increase the relaxation time of the material sufficiently that the bulk arc can be resolved.

An impedance arc whose center lies on the real axis of the complex impedance plane is the result of a material or process which has a single relaxation time. When the relaxation time is is not single valued but is distributed either discretely or continuously around a mean value  $\tau_m$ , an impedance arc whose center is depressed below the real axis is observed. Although this is most common in grain boundary and electrode arcs, it can also be observed in the bulk arc of some materials. When a depressed arc is observed, the relaxation

time obtained from equation 31 is the mean relaxation time  $\tau_m$ . There are several causes of depressed arcs. Firstly, the purity of materials at grain boundaries and electrode interfaces is usually less than in the bulk and is seldom homogeneous causing multiple relaxation times in these regions. Roughness and porosity of the electrodes themselves can also lead to depression of the electrode arc. In the bulk material, relaxation time distribution is usually less although some sample impurity and inhomogeneity can exist. Anisotropy in the conductivity of the bulk compound also causes depressed arcs since the relaxation time is often different for each of the crystal directions and the crystallites are randomly ordered in the polycrystalline sample.

Lastly, distorted or overlapping arcs can result from relaxations whose time constants are within two orders of magnitude of each other. In this case, the impedance spectrum must be deconvoluted to reveal the individual component arcs. Since such arcs seldom have the same temperature dependence, they can sometimes be separated experimentally by changing the sample temperature.

Combinations of the above problems can make it difficult to model real systems electrically since simple RC circuits do not fit these systems well. The use of distributed circuit elements such as Warburg impedances and constant phase elements have been employed in the modelling of such systems.<sup>74</sup> In addition, the use of complex non-linear least squares fitting is sometimes necessary to completely reduce an impedance spectrum into individual electrical components.<sup>74-76</sup> Associated with such complex equivalent circuits is the problem that more than one equivalent circuit can often be used

to represent the same IS spectrum and, thus, the physical meaning of such modelling is not easily understood.

#### IV.B. Results and Discussion

## 1. $K^{+}(C222)e^{-}$

Early interest in the electrical conductivity of K+(C222)e- was sparked by the optical spectra of solvent free films of the compound. These films showed broad plasma absorptions throughout the visible region similar to those observed in metallic solutions of alkali metals in ammonia.<sup>30</sup> EPR and microwave conductivity experiments also suggested metallic character.<sup>30</sup> The structure of this compound shows the presence of large vacancies (4x6x12 Å) connected in two dimensions by wide channels, but blocked in the third direction.<sup>61</sup> The structure and magnetic susceptibility results indicate that the anions of this electride exist as weakly bound pairs probably centered at the large vacancies of the crystal structure.<sup>61</sup> The susceptibility increase with temperature indicates that these electron pairs can be either thermally dissociated or excited into triplet states.

The earliest attempts at measuring the electrical conductivity of K+(C222)e- indicated a high conductivity, but were unable to yield quantitative results due to experimental problems.<sup>41</sup> In order to obtain quantitative estimates of the band gap and resistivity of K+(C222)e-, pressed powder conductivity measurements were performed. Early measurements used the 2-probe d.c. cell in its unshielded form. The large noise and background currents of this

arrangement made voltage-current measurements nearly impossible. To overcome this problem, an ohmmeter was used to measure the sample resistance. Variable temperature measurements on several samples indicated semiconductor behavior for K+(C222)e- with a band gap of 0.02 to 0.06 eV. The data from one such experiment are plotted in Figure 22 and indicate a band gap of 0.03 eV. The resistance of the sample, however, was much higher than would be expected for such a low band gap conductor. No hysteresis was observed in this or later experiments when the temperature was scanned up or down.

After adaptation of the d.c. cell, it became possible to perform Ohm's Law measurements on the compound and a typical result is shown in Figure 23. The data show highly non-linear behavior for the sample with a marked increase in apparent conductivity with increasing voltage. The apparent conductivity for samples increased by nearly two orders of magnitude in scanning the voltage from 0 to 3 V. Despite this, no significant time dependence of the current was observed.

Although bulk non-ohmic behavior is sometimes observed, these effects are usually small. Extreme behavior such as that seen in K<sup>+</sup>(C222)e<sup>-</sup> is usually due to grain boundary or electrode effects. Impedance spectroscopy was employed in an effort to separate these effects from the bulk sample effects. The earliest IS experiments on K<sup>+</sup>(C222)e<sup>-</sup> were performed by John Papaioannou in the frequency range of 200 Hz to 100 kHz and 500 kHz to 15 MHz.<sup>77</sup> The experiments employed an EG&G Model 5207 Lock-in Amplifier and a Wavetek Model 116 Multi-purpose VCG for the low frequency range,

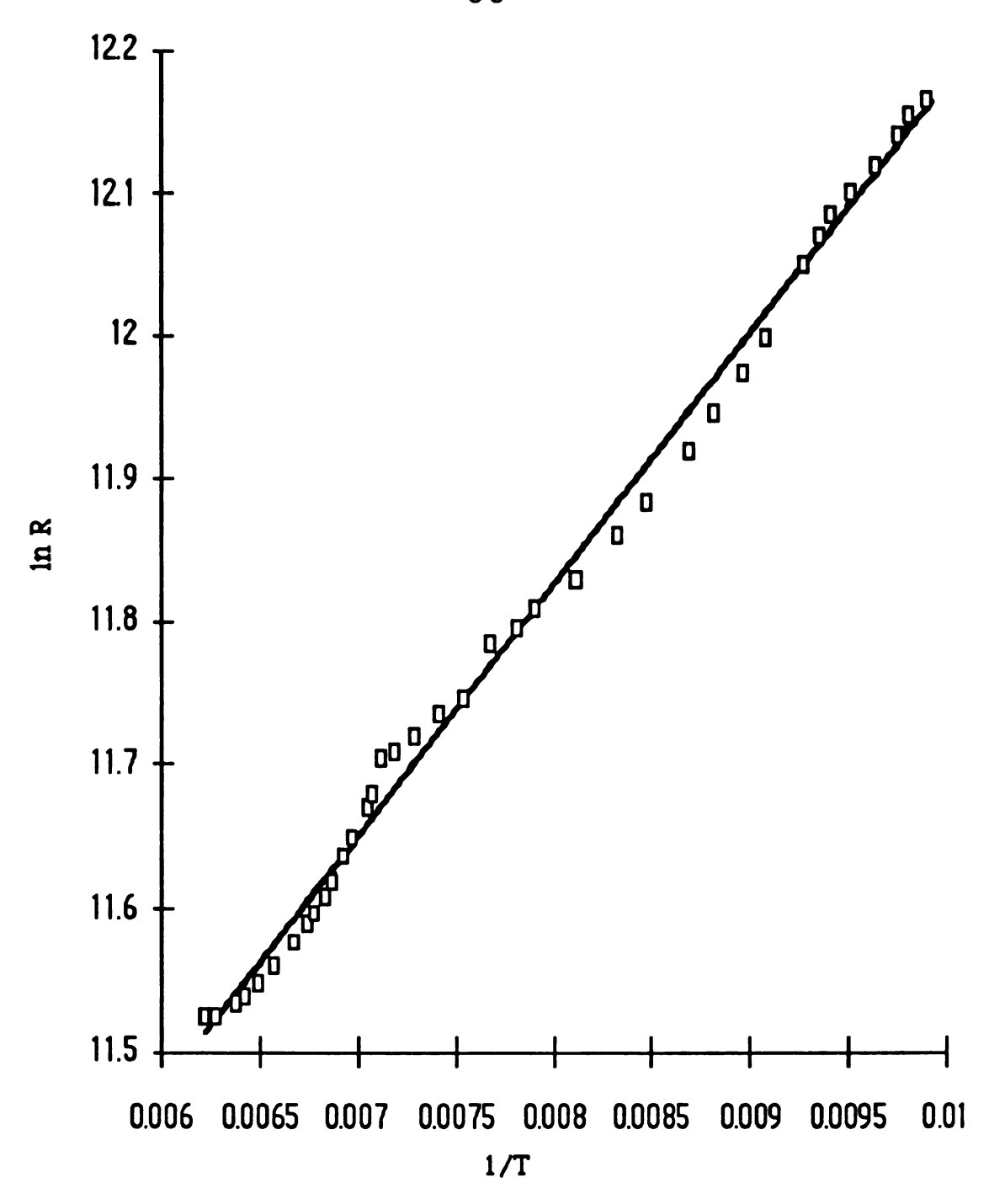


Figure 22: The temperature dependence of the resistance of K+(C222)e<sup>-</sup> plotted as ln R versus 1/T.

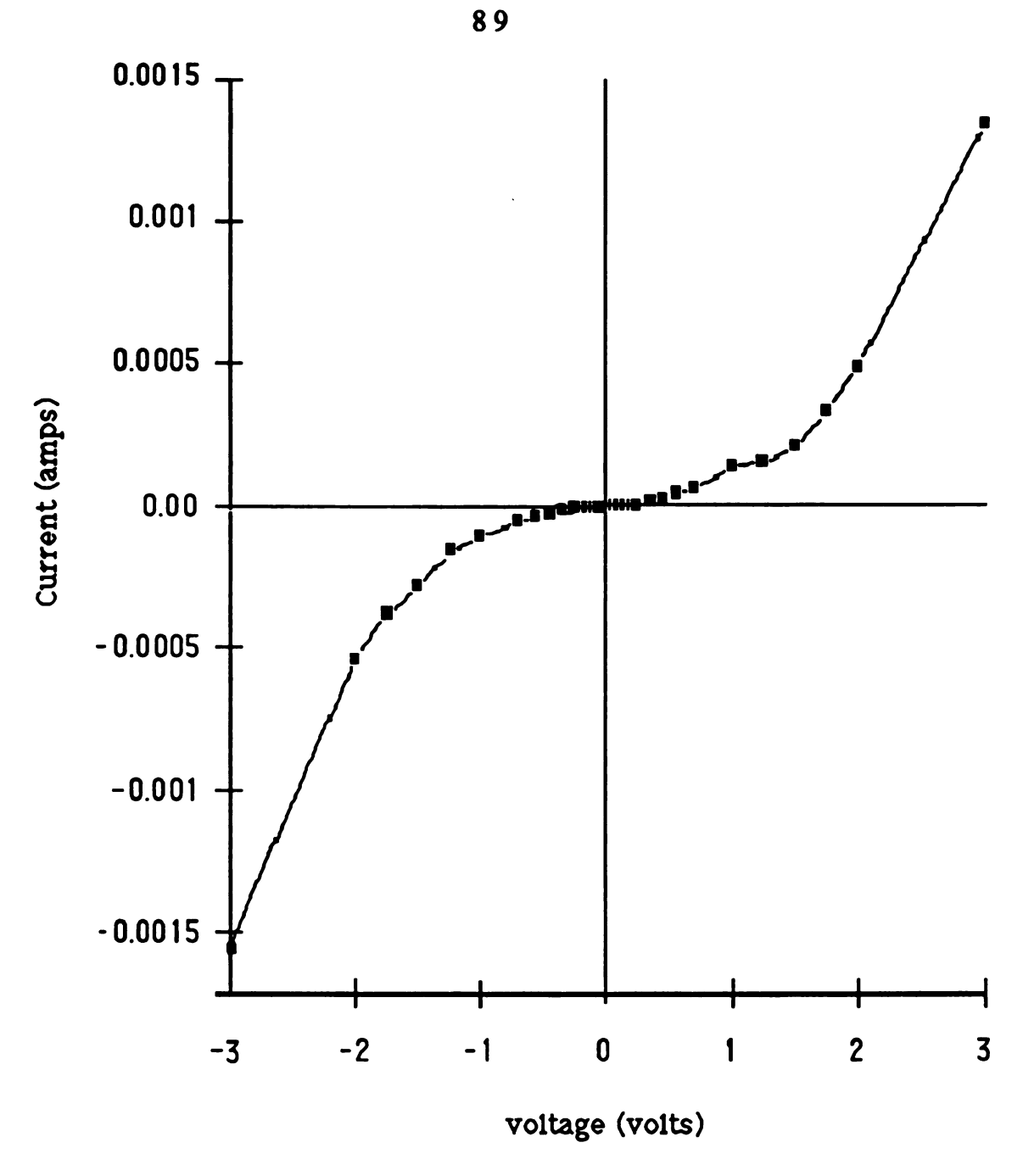


Figure 23: Ohm's Law plot for K+(C222)e- showing the extreme nonlinearity observed in d.c. conductivity data.

and a Hewlett Packard 4815A Vector Impedance Meter for the high frequency range. Although there was no overlap of the measurement ranges, these experiments indicated the presence of two impedance arcs in the complex plane.

Later IS studies of K+(C222)e- performed with the Hewlett Packard 4192A Low Frequency Impedance Analyzer, yielded only a single impedance arc in the complex plane. Although the reason for the two apparent arcs observed with the older arrangement is not known, incompatibilities and inaccuracies of the instrumentation may have been responsible. For example, there appeared to be considerable mismatch between the results from the two types of instrumentation in those cases where interpolation between the two measurement regions was possible.

An example of an impedance arc of  $K^+(C222)e^-$  as obtained from the 4192A system is shown in Figure 24. This result was a disappointment in that no separation of bulk, grain boundary, and electrode effects seemed to have occurred. Closer examination of the arc, however, reveals that its high frequency intercept does not pass through the origin even after cell impedances have been subtracted out. The amount of the offset is small, typically 2-20  $\Omega$ , and appears to be dependent on the sample thickness. This indicates that the bulk sample arc may lie at frequencies beyond our measurement range. The observed arc, then, must be due to electrode and/or grain Further indication of this came from IS boundary effects. experiments run at different voltages. As seen in Figure 25, the magnitude of the impedance arc changes dramatically with voltage in the same manner as the Ohm's Law data.

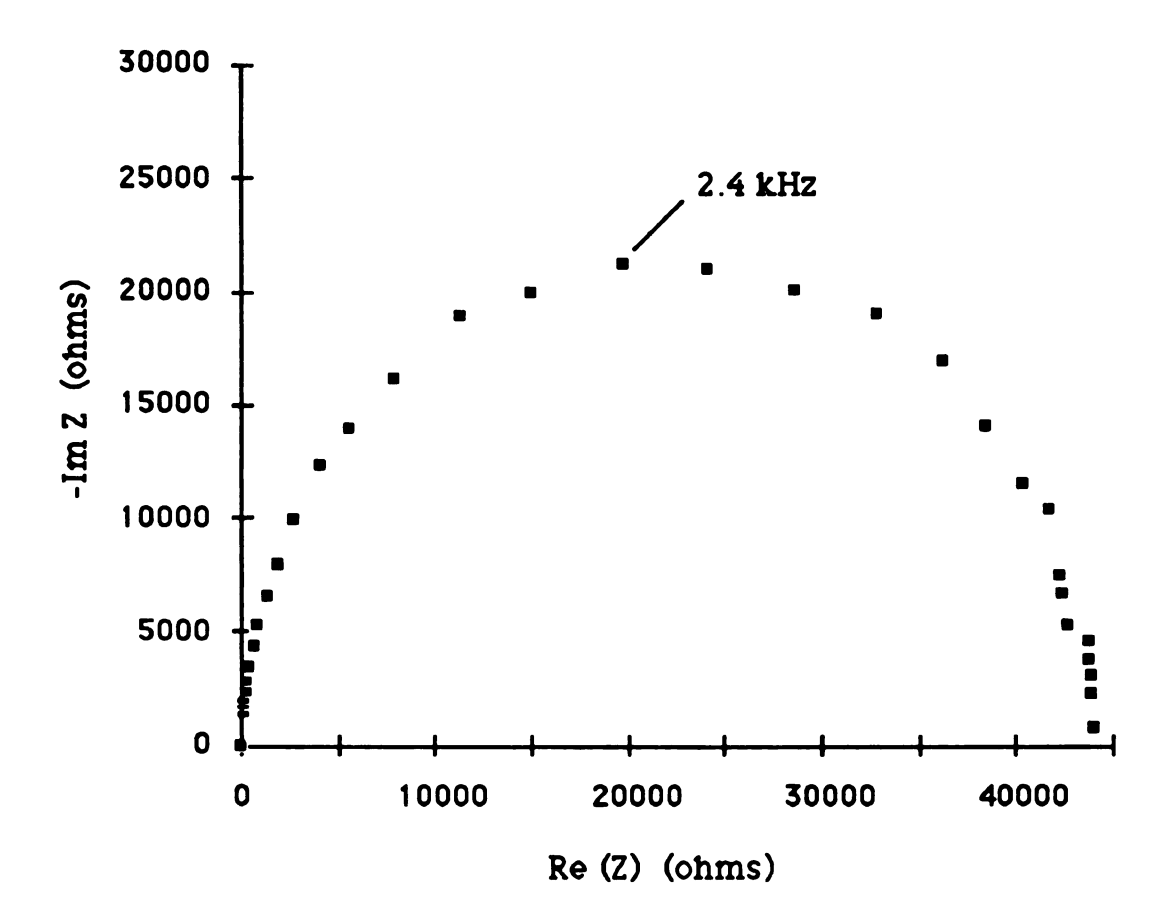


Figure 24: Impedance arc for K+(C222)e- at -147.5 °C and 20 mV.

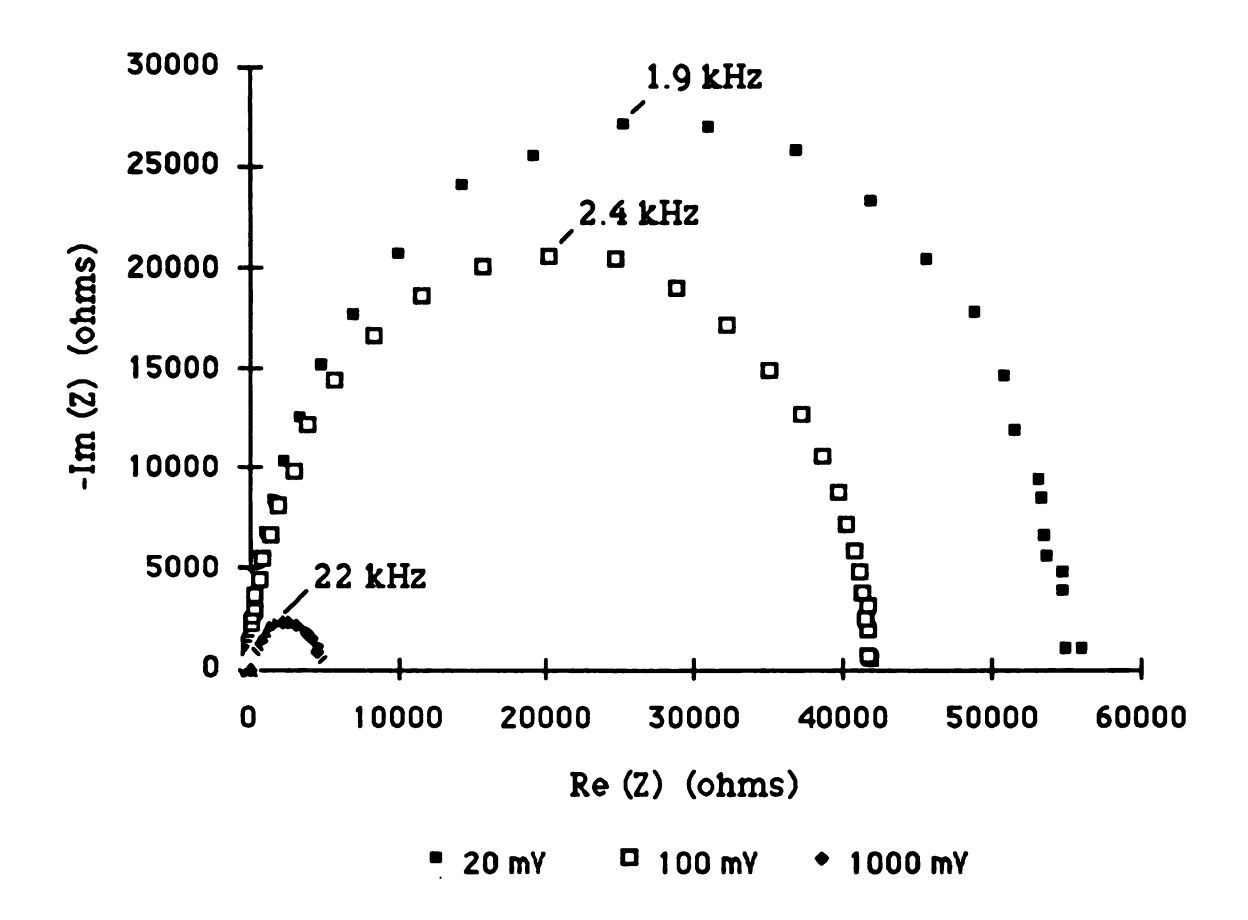


Figure 25: Impedance arc of K<sup>+</sup>(C222)e<sup>-</sup> at three voltages showing the large dependence of the impedance on applied voltage.

If the observed arc is not due to the sample bulk, it could be due to one of three things, grain boundary impedances, an electrode oxide layer, or a Schottky barrier. The use of gold plates over the stainless steel electrodes proved that the observed arc is due predominantly to an electrode effect rather than grain boundaries. As shown in Figure 26, gold electrodes decreased the size of the impedance arc by nearly two orders of magnitude but retained the voltage dependence of steel electrode experiments. This indicates that the arc is due mainly to an electrode effect since grain boundary impedance would be independent of the nature of the electrode material.

Several experiments were necessary to distinguish between an oxide layer and a Schottky barrier. Although there should have been no oxide layer between the sample and the gold electrodes, it was possible that such a layer existed between the gold plate and the stainless steel electrodes of the cell. The variable temperature data for this arc, however, yield a small apparent band gap (<0.06 eV), much lower than what would be expected for an oxide (>2 eV). This, then, points to a Schottky barrier as the source of the observed arc.

Potassium metal was placed over the cell electrodes to check for the presence of a Schottky barrier. The impedance arc which was obtained from the potassium electrode experiment is shown in Figure 27. It can be seen that this arc is four orders of magnitude smaller than was observed with steel electrodes. Also, the arc does not intersect the origin of the complex plane, and most of the voltage dependence of the arc has been eliminated. This result can be explained in terms of a Schottky barrier. Since potassium has a

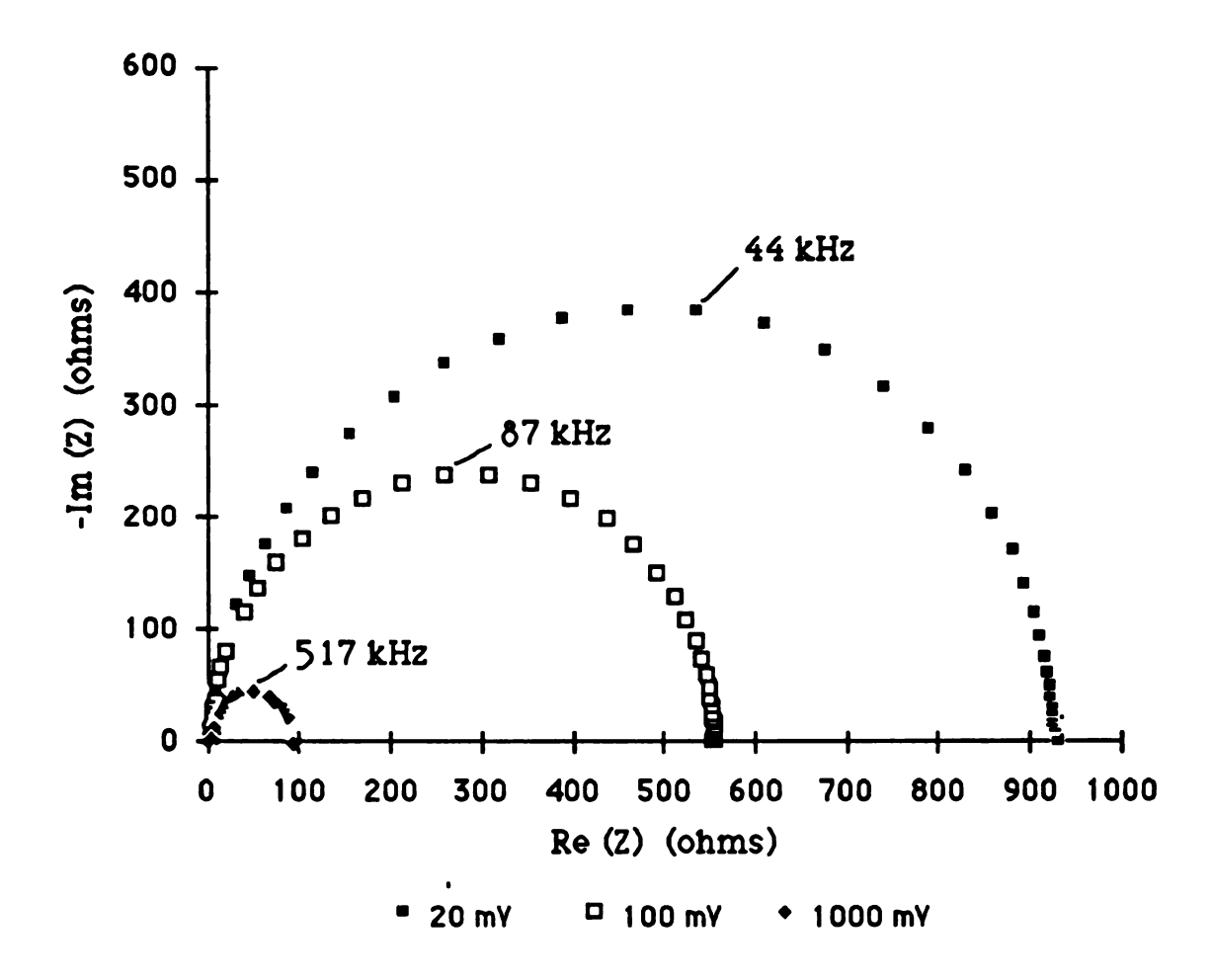


Figure 26: Voltage dependence of the impedance arc of K<sup>+</sup>(C222)e<sup>-</sup> with gold electrodes at -184.4 °C.

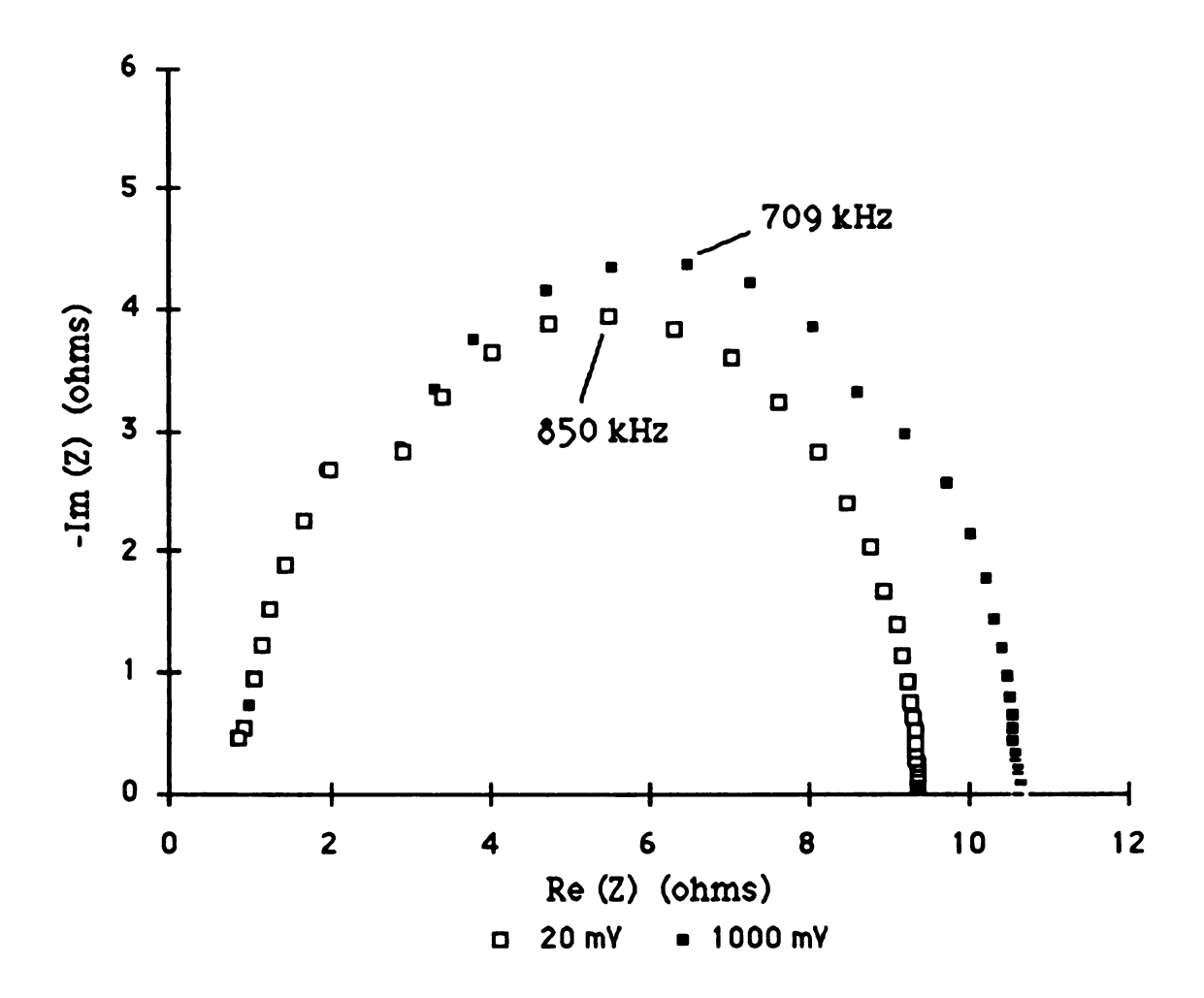
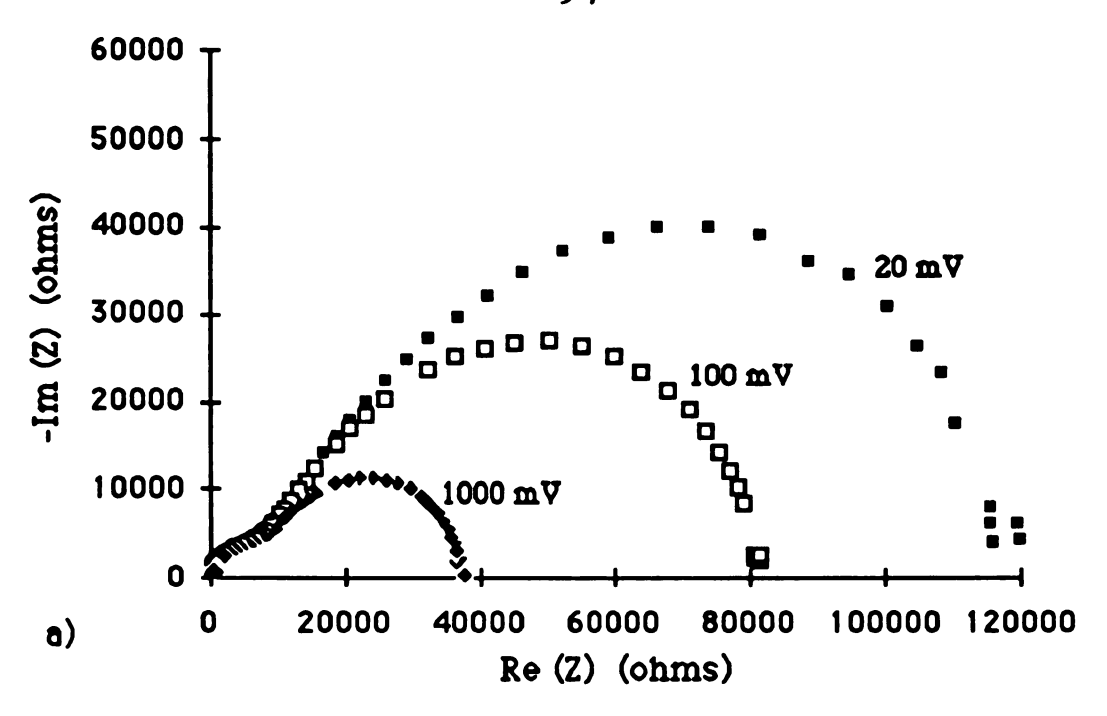


Figure 27: K+(C222)e- impedance arc for a sample in contact with potassium electrodes at -183 °C.

much lower work function than gold (2.3 eV as opposed to 5.3 eV) or stainless steel, the size of the barrier and, hence, the impedance arc should vary with the change in electrode material. Potassium metal should have a Fermi level much closer to that of the electride than that of either gold or steel, so the Schottky barrier height and voltage dependence of the impedance arc are both decreased. It is also possible that part of this arc is due to grain boundary impedance.

There were alternate explanations for the behavior of the impedance arc in the presence of potassium metal that needed Since the compound K+(C222)K- is known, the investigation. possibility existed that potassium metal from the electrodes had reacted with the  $K^+(C222)e^-$  sample to form  $K^+(C222)K^-$ . It was also possible that the potassium metal had dispersed into the electride sample to form a conductive path and, therefore, a lower impedance. Proof that significant amounts of  $K^+(C222)K^-$  had not been formed was obtained from IS experiments with samples of  $K^+(C222)K^-$ . Figure 28a shows the impedance spectrum of K<sup>+</sup>(C222)K<sup>-</sup> obtained with steel electrodes. It can be seen that the spectrum consists of two partially overlapped arcs. The low frequency arc exhibits a marked voltage dependence similar to that due to the proposed Schottky barrier of K<sup>+</sup>(C222)e<sup>-</sup>. The high frequency arc does not appear to be voltage dependent and is probably the bulk arc of the system. When potassium metal is used as an electrode material, a single depressed arc is seen (Figure 28b). The impedance of this arc is much larger than was observed for samples of K<sup>+</sup>(C222)e<sup>-</sup> between potassium electrodes. The apparent band gap of this compound,



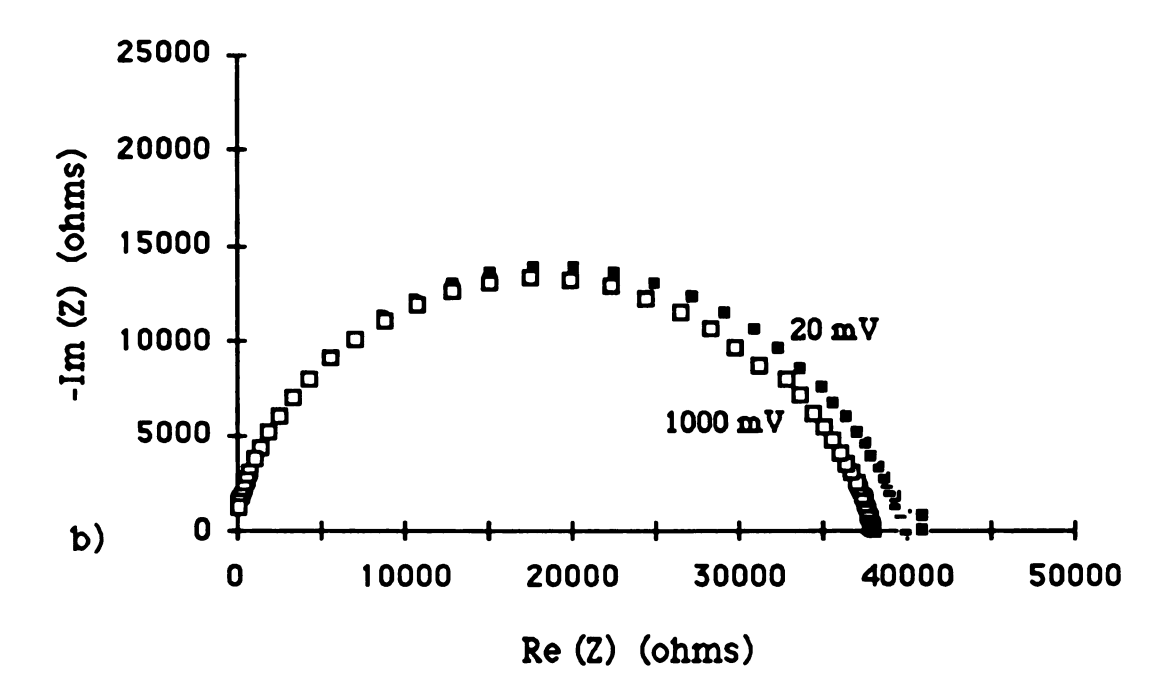


Figure 28: a) Impedance spectrum of K<sup>+</sup>(C222)K<sup>-</sup> with steel electrodes at -143 °C. b) Impedance spectrum for K<sup>+</sup>(C222)K<sup>-</sup> between potassium electrodes at -169 °C.

obtained from IS and d.c. conductivity measurements, is 0.25 eV, much larger than that seen in  $K^+(C222)e^-$ .

The absence of dispersed potassium metal in the electride samples was also demonstrated. A sample of K+(C222)e- was pressed between two potassium metal electrodes for over 24 hours and then separated from the electrodes. An IS run of the sample between stainless steel electrodes was then performed. The sample exhibited the same impedance arc and voltage dependence as had all previous K+(C222)e- samples.

It should be possible to form a Schottky diode from K<sup>+</sup>(C222)e<sup>-</sup> and a steel or gold electrode if a suitable ohmic contact could be made to the other electrode of the conductivity cell. Although such a contact was not possible, it was possible to set up an asymmetric system which used potassium metal as one electrode contact to K+(C222)e- and stainless steel as the other. It was known from the impedance data that the Schottky barriers should be of different sizes at the two electrode contacts. When two such experiments were performed, however, no significant asymmetry (diodic behavior) was observed in the I-V data. A plot of the data from one of these experiments is shown in Figure 29. Clearly, in a system containing Schottky barriers at both contacts, ideal diodic behavior would not be expected. It was expected, however, that some asymmetry would be observed. Lipsetter and Sze have shown that ideal behavior of a Schottky diode requires a diffuse guard ring geometry 78 which was not used in the current experiment. The reason for non-ideal behavior in systems without the guard ring is attributable to surface leakage and premature breakdown of the

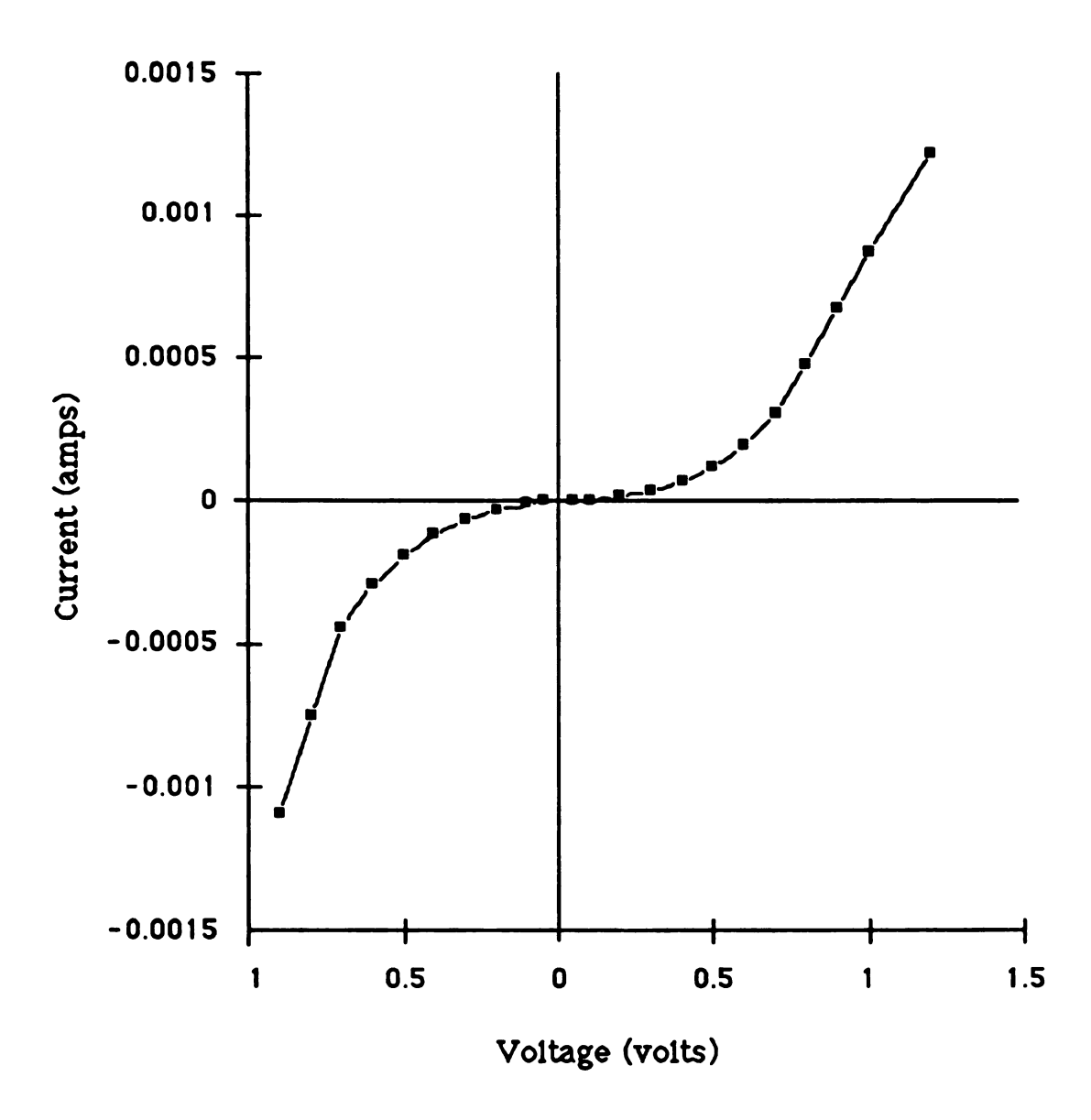


Figure 29: Ohm's Law data from a sample of K<sup>+</sup>(C222)e<sup>-</sup> between one potassium and one stainless steel electrode.

diode under reverse bias.  $^{65}$  Other workers have shown that these leakage currents are proportional to the area of the device.  $^{79}$  Since the attempt at diode formation had three faults, non-ideal electrodes, absence of a guard ring, and a large 4 mm diameter size (typical Schottky diodes are <100  $\mu$ m in diameter), the diode could not be expected to behave ideally. Nevertheless, the absence of an asymmetric response is puzzling and suggests that other effects than a Schottky barrier may be involved.

The voltage dependence of current flow across a Schottky barrier has been given in equation 23. When data from Ohm's Law experiments on K+(C222)e- were plotted as ln (I) versus V according to equation 23, the results were mixed. An initial experiment did not yield the expected linear behavior while a later experiment did, as shown in Figure 30. The plot is reasonably linear up to 5 V. Nonlinear behavior beyond 5 V was also observed. The reasons for the high voltage behavior may be the same as those responsible for the lack of diodic behavior above. Most barrier heights are determined on samples which have an ohmic contact to one electrode and a Schottky barrier to the other so that only the effects of a single barrier are studied.

Four-probe conductivity methods were employed in order to obtain resistivity estimates free of electrode effects. The van der Pauw arrangement in the four-probe cell was used for this purpose. The point contacts were tipped with potassium metal to ensure good electrical contact. The contacts were placed ~0.7 mm in from the perimeter of a 4.76 mm diameter pellet to prevent crumbling of the pellet edge. A.C. conductivity measurements yielded a resistivity of

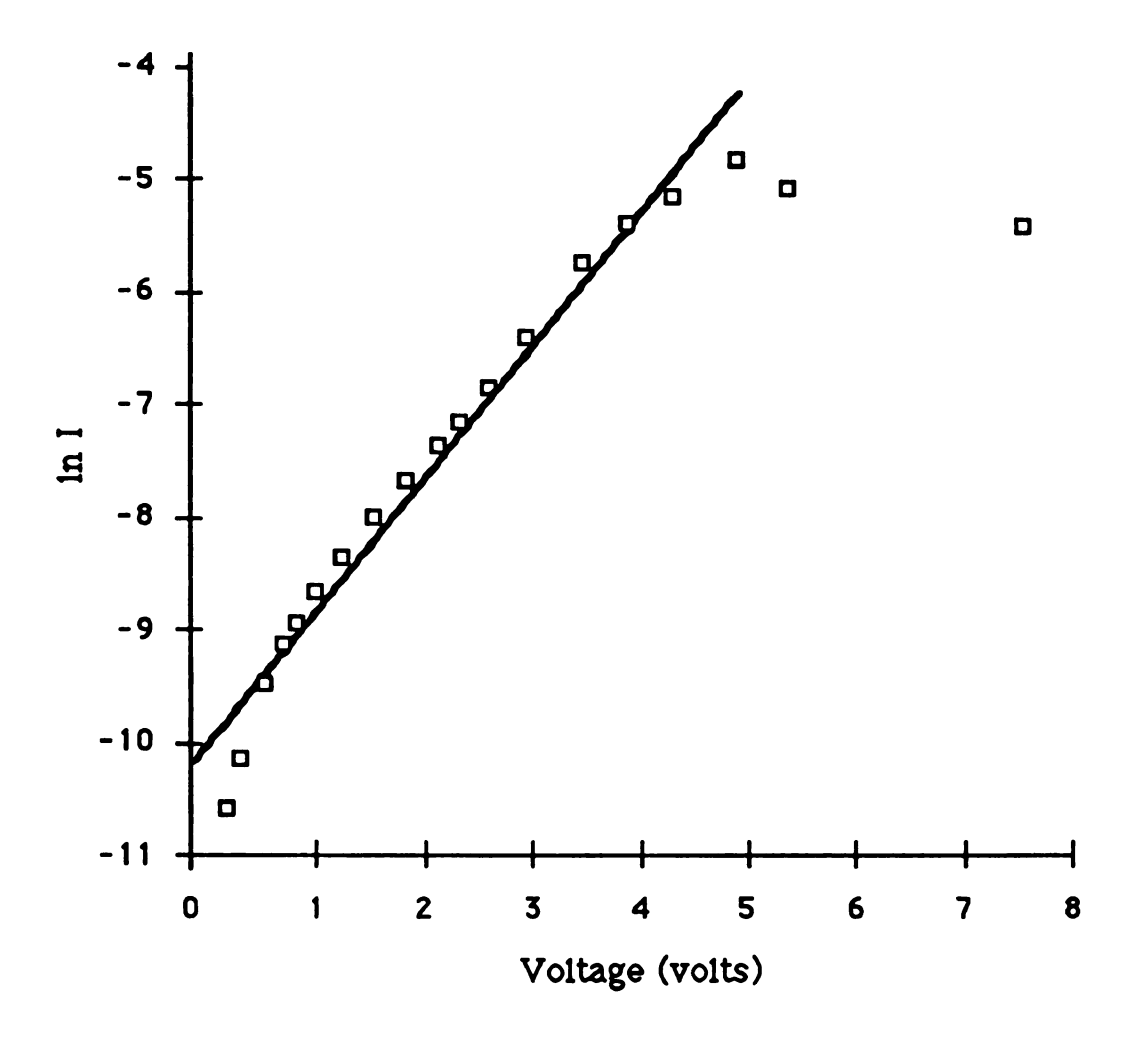


Figure 30: Plot of ln (I) versus applied voltage from Ohm's Law data of K<sup>+</sup>(C222)e<sup>-</sup>.

0.87 Ωcm at 85 K for the pellet. Temperatures below 135 K yielded an apparent band gap of 0.055 eV. The ln R versus 1/T plot of the data shown in Figure 31 contains an apparent break in the slope of the data at ~135K. Above this temperature a band gap of 0.086 eV was observed. Evidence of this break had been seen in two-probe measurements previously, but experiments had not been run at high enough temperatures for the complete break to be seen. Although the reason for the break is not known, it could be due to a switch from doped (extrinsic) conductivity at low temperatures to intrinsic conductivity at high temperatures. Alkalides and electrides are known to contain defect electrons which could be responsible for this doping and evidence for their presence in K+(C222)e- has been seen as a Curie law "tail" in magnetic susceptibility data.61

The results of experiments on K+(C222)e- indicate that it is a highly conductive, nearly metallic compound in contrast to other electrides which show semiconductor behavior with band gaps in excess of 0.9 eV.11,20.21 The high apparent resistivity of K+(C222)e-observed in d.c. measurements has been shown to be due to a Schottky barrier at the sample-electrode interface. The behavior of this Schottky barrier is less than ideal. The presence of impurities and small oxide layers at the sample-electrode interface are probably responsible for the non-ideal behavior of the barrier. Techniques have been developed which allow reactive alkali metals to be applied to the electrodes of conductivity cells at low temperatures and under inert atmosphere. It has been shown that the use of potassium metal as an electrode material for K+(C222)e-

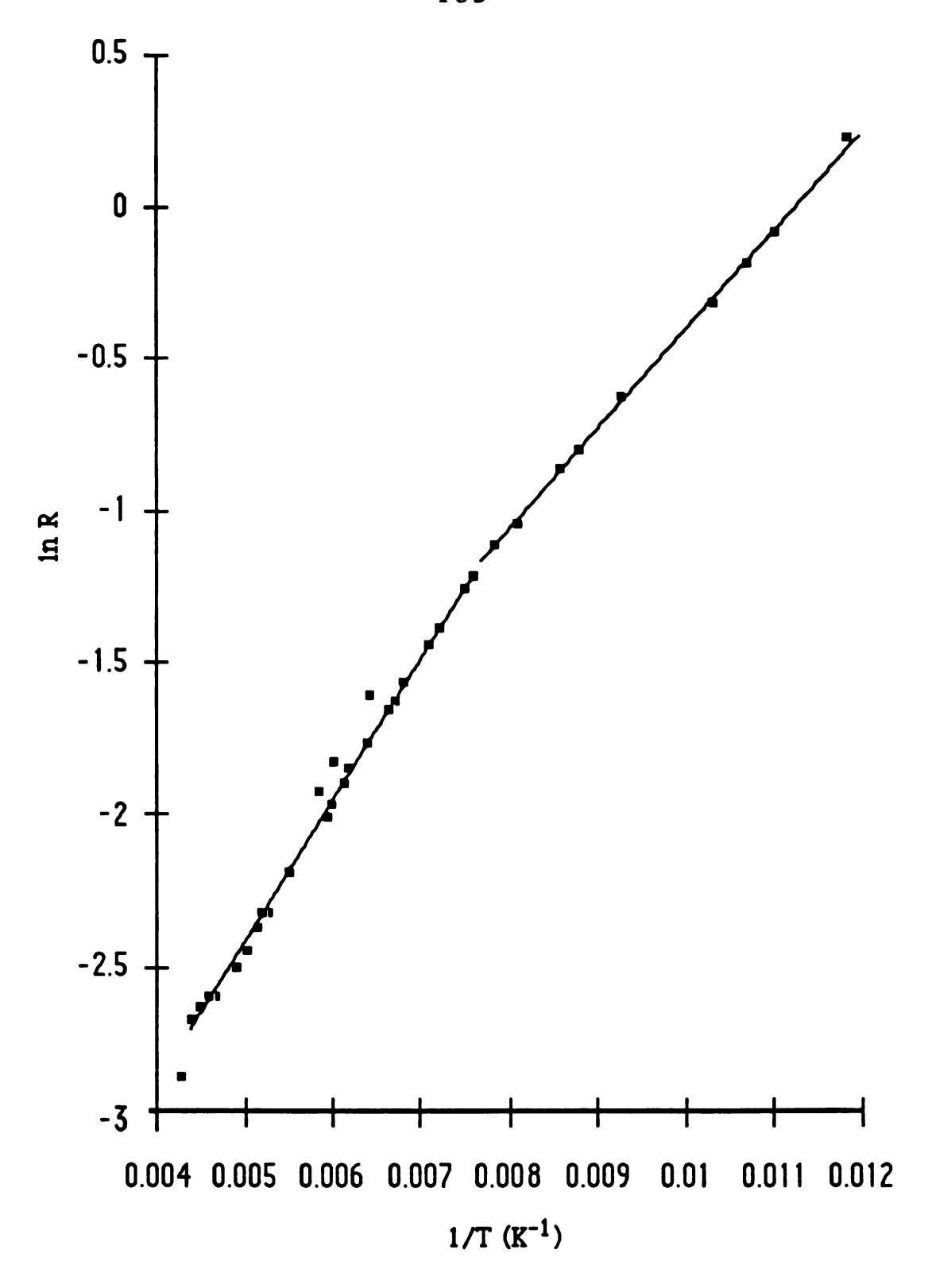


Figure 31: Four-probe conductivity of K+(C222)e-.

can decrease the electrode impedance due to Schottky barriers by nearly four orders of magnitude.

IS studies of K<sup>+</sup>(C222)K<sup>-</sup> have shown that potassium metal does not react with K<sup>+</sup>(C222)e<sup>-</sup> to form a more conductive alkalide. impedance spectrum of  $K^+(C222)K^-$  is composed of two partially overlapped arcs with a combined impedance more than four orders of magnitude larger than was observed for samples of K+(C222)ebetween potassium electrodes. The use of potassium metal as an electrode material for K<sup>+</sup>(C222)K<sup>-</sup> eliminated the lower frequency arc of the spectrum which indicated that it was probably due to a Schottky barrier. The high frequency arc which remained was seen to have its center depressed below the real axis of the complex impedance plane. This fact indicates that the arc is partially due to grain boundary impedances which tend to exhibit multiple relaxation times which lead to depressed arcs. Conversely, anisotropic conductivity of the sample would also cause a depressed impedance arc.

IS and four probe a.c. conductivity experiments have placed upper limits on the band gap and resistivity of  $K^+(C222)e^-$ . The measured band gap was 0.086 eV in the "intrinsic" temperature region while the resistivity was  $\sim 10$  cm near liquid nitrogen temperatures. Grain boundary resistances may be responsible for much of the observed resistivity. Since both the grain boundary and bulk impedances of the sample require frequencies beyond the range of our instrumentation, however, the role of grain boundaries could not be determined experimentally.

Optical absorption, EPR, and microwave conductivity data all indicate metallic behavior for K+(C222)e-.30 The crystal structure also suggests that the electron anions in this system may be able to interact in two directions. These suggest that K+(C222)e- may be a two dimensional metal. It may be, therefore, that the observed band gap of K+(C222)e- is a result of activated transport of electrons between crystal grains which are not oriented the same in pressed pellet or powder samples. Conversely, the band gap may be a real characteristic of the compound and may be related to the dissociation of the electron pairs in the system, or to the population of a metallic triplet state. Single crystal conductivity data are required to determine whether K+(C222)e- is, in fact, a metal or a very low band gap semiconductor.

## 2. $Cs+(15C5)_2e^{-}$

In contrast to the delocalized, near metallic behavior of K+(C222)e-, many data show Cs+(15C5)2e- to be a localized electride. Magnetic susceptibility measurements show that Cs+(15C5)2e- obeys the Curie-Weiss law above about 15 K.81 The susceptibility data indicate the presence of localized trapped electrons in the system which are at least 95% unpaired.<sup>47,81</sup> The crystal structure contains anionic cavities with a mean diameter of 4.7 Å in which the electrons are presumably centered.<sup>82</sup> The anionic sites are connected in one direction by restricted channels.

Impedance spectroscopy experiments on Cs<sup>+</sup>(15C5)<sub>2</sub>e<sup>-</sup> had to be run at relatively high temperatures in order for the impedance

spectrum to be resolved. At temperatures below about -30 °C, the impedance of the compound was too large to be measured with the current instrumentation. Above -30 °C, the spectrum consists of a high frequency arc and a low frequency spike. An example of the spectrum is shown in Figure 32. The high frequency arc has a capacitive component in the nanofarad range. Such a large capacitance indicates that the arc is at least partially due to grain boundary effects which tend to have large capacitive components.83 The observed low frequency spike is similar to that due to blocking electrodes in ionic conductors.<sup>74</sup> In such systems, the conductive species cannot penetrate or exchange charge with the electrode which results in a capacitive layer at the electrode surface. In the ideal case this would result in a vertical spike in the impedance plane. Roughness of the electrode surface, however, usually leads to a spike which lies an an angle of <90° to the real axis.

The presence of a possible blocking electrode effect was unexpected since steel electrodes should not be blocking to electronic conductivity. The presence of blocking electrodes implies ionic conductivity which had been observed previously in an alkalide<sup>3 6</sup> but never in an electride. Further indication of ionic conductivity was given by the temperature dependence of the impedance arc in "live" and decomposed samples of Cs+(15C5)<sub>2</sub>e<sup>-</sup>. In the live sample, a value of 0.68 eV for the conductivity activation energy was obtained. The decomposed sample yielded a value of 0.63 eV, which is within experimental error of the live sample value. In addition, the observed impedance of the decomposed sample was approximately equal to that of the live sample.

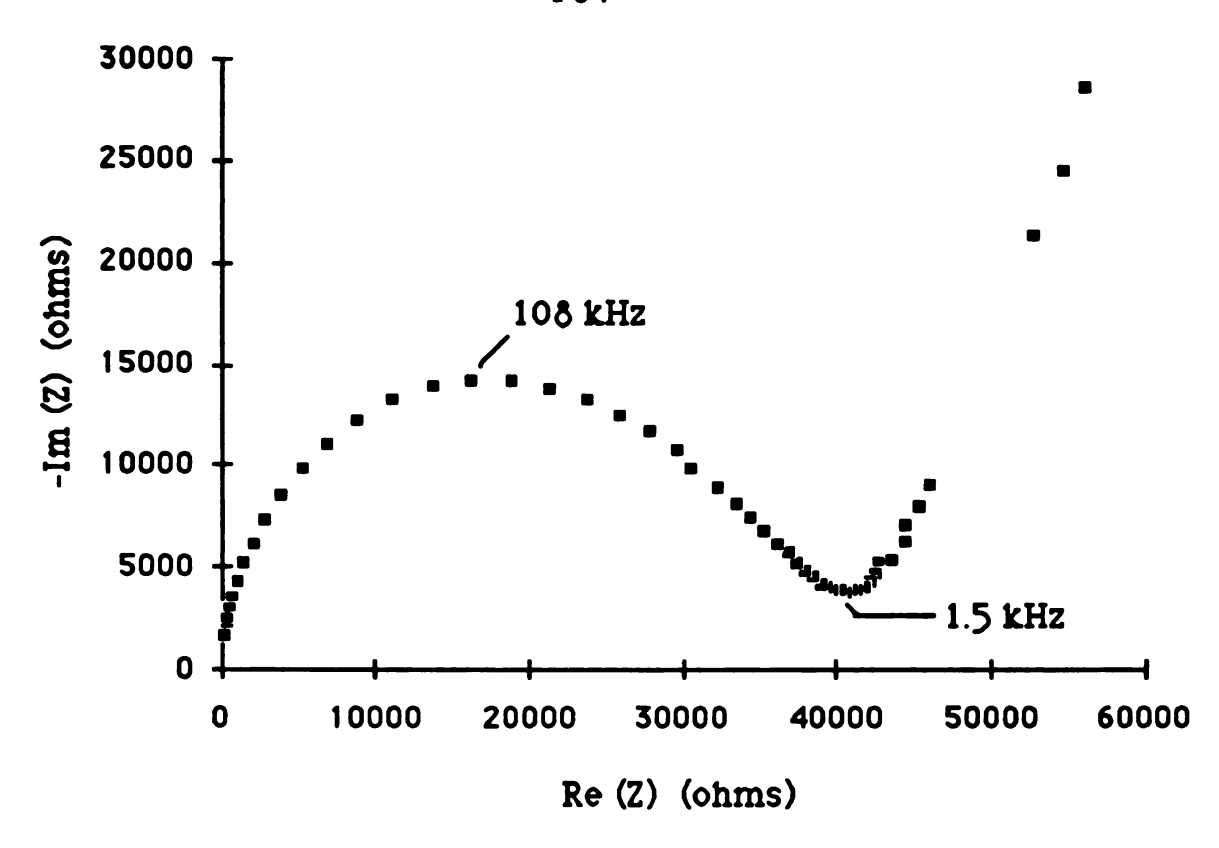
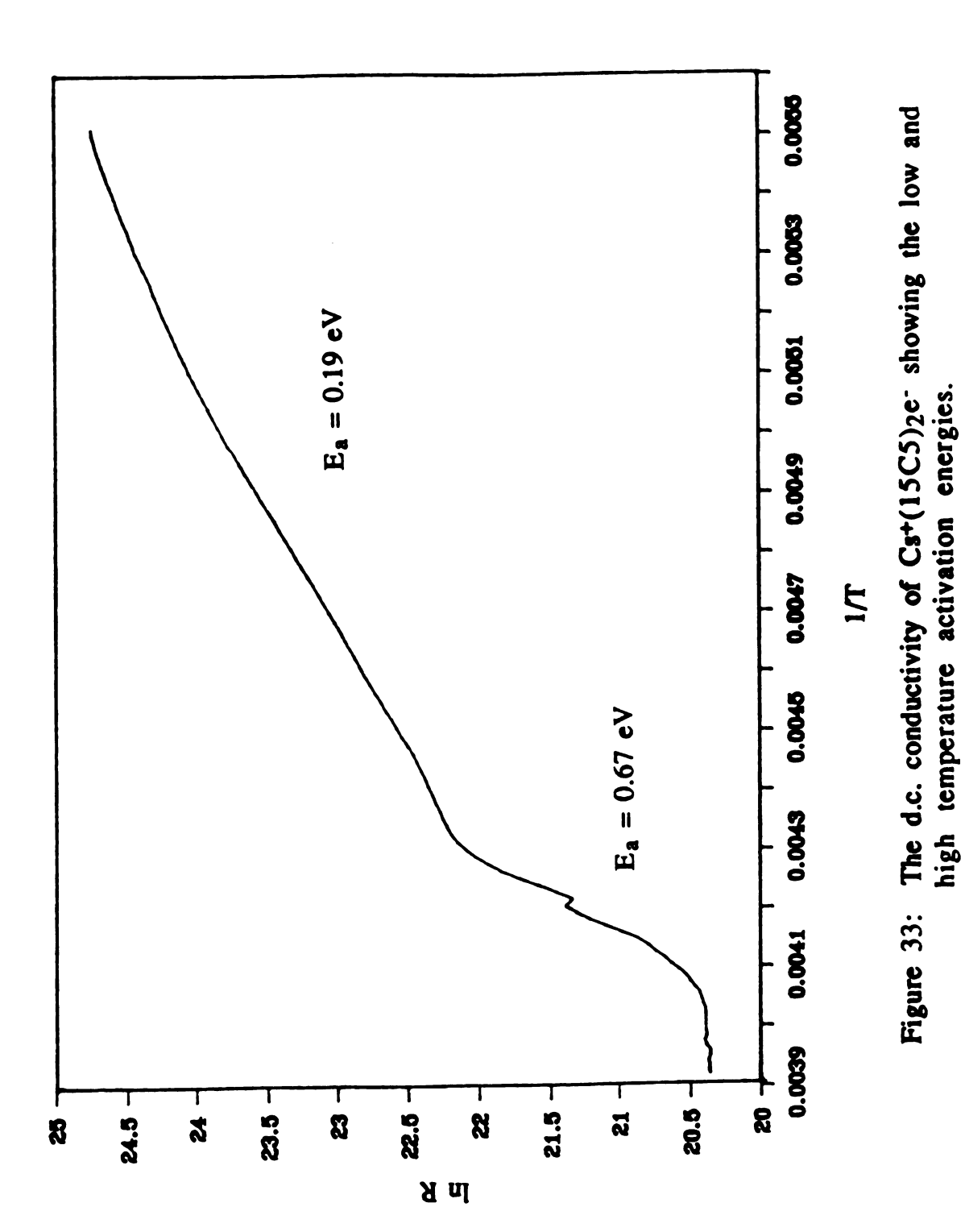


Figure 32: The impedance spectrum of Cs+(15C5)<sub>2</sub>e<sup>-</sup> at -17.2 °C and 20 mV.

D.C. conductivity measurements were employed to verify the possible ionic conductivity of Cs+(15C5)<sub>2</sub>e<sup>-</sup>. The results of one variable temperature d.c. experiment are shown in Figure 33. From the figure, it can be seen that Cs+(15C5)<sub>2</sub>e<sup>-</sup> has a large resistivity coupled with a low activation energy at low temperatures. At a point which corresponds to a temperature of about -40 °C, there is break in the plot. Above this temperature, the conductivity has an activation energy of 0.67 eV, the same as was seen in IS experiments. The activation energy of the low temperature region and the crossover point between the two activation regimes are both synthesis dependent. This indicates that defect electrons are responsible for



the low temperature conductivity of Cs+(15C5)<sub>2</sub>e<sup>-</sup>. Although these defects are in shallow traps as indicated by the low activation energy in this region (0.19 eV for the experiment of Figure 33), the number of defects is small which makes the resistance high. The measured resistance from this d.c. experiment was much larger than the value of the impedance minimum seen in IS experiments. The reasons for this are twofold. Firstly, the d.c. conductivity technique includes the blocking electrode impedance in the measured sample resistance. Secondly, sample thickness and packing affect the measured resistance. D.C. conductivity measurements used packed powder samples in contrast to the pressed pellets used for IS experiments. Combined, these effects caused the d.c. resistance of different d.c. experiments to vary by several orders of magnitude.

Minor synthesis dependence of the high temperature activation energy was also observed. In various d.c. conductivity experiments, the measured activation energy ranged between 0.57 and 0.71 eV. Coupled with IS experiments which show a large capacitive component of the impedance arc, this implies that part of the activation energy may be due to grain boundaries. Since the properties of grain boundaries are both synthesis and history dependent, it is not unexpected that at least a small range of activation energies was observed.

The crossover point of the conductivity from low to high activation is not associated with any phase transition which can be detected from magnetic susceptibility, NMR, or DSC data.<sup>80</sup> This fact indicates that the crossover is either due to a change from extrinsic (doped) to intrinsic conductivity, or from electronic to ionic

conductivity. Most other processes which yield a change in the activation energy of conductivity would be associated with an observable phase transition. Coupled with the blocking electrode behavior observed in IS experiments, this is further evidence of ionic conductivity in the compound.

A typical Ohm's law plot taken in the high activation temperature region is shown in Figure 34. The data were taken with a program which recorded the current flow through a sample as a function of time at each specific voltage. For this particular experiment, 10 second voltage pulses were used. The figure shows the decay of the current through the sample during the 10 s pulse length. Also shown is the curvature of the plot. These effects can be explained as polarization effects at the electrodes due to ionic motion. As the ions move in the applied field, a depletion layer is formed in the sample near the electrode surface which causes decreased current flow. It was initially thought that this behavior could be due to the charging of a capacitive double layer at the sample electrode The effect became more pronounced as the temperature was increased, however, indicating that it was probably due to depletion effects since double layer capacitive effects should decrease as temperature is increased.

When a sample of Cs+(15C5)<sub>2</sub>e- was placed between a steel electrode and a cesium metal electrode a much different behavior was observed. In this case an electrochemical cell with a potential of ~100 mV was formed and the system produced current flow in the absence of an applied voltage. I-V data for this cell (Figure 35) show a non-zero current in the absence of an applied voltage. Under a

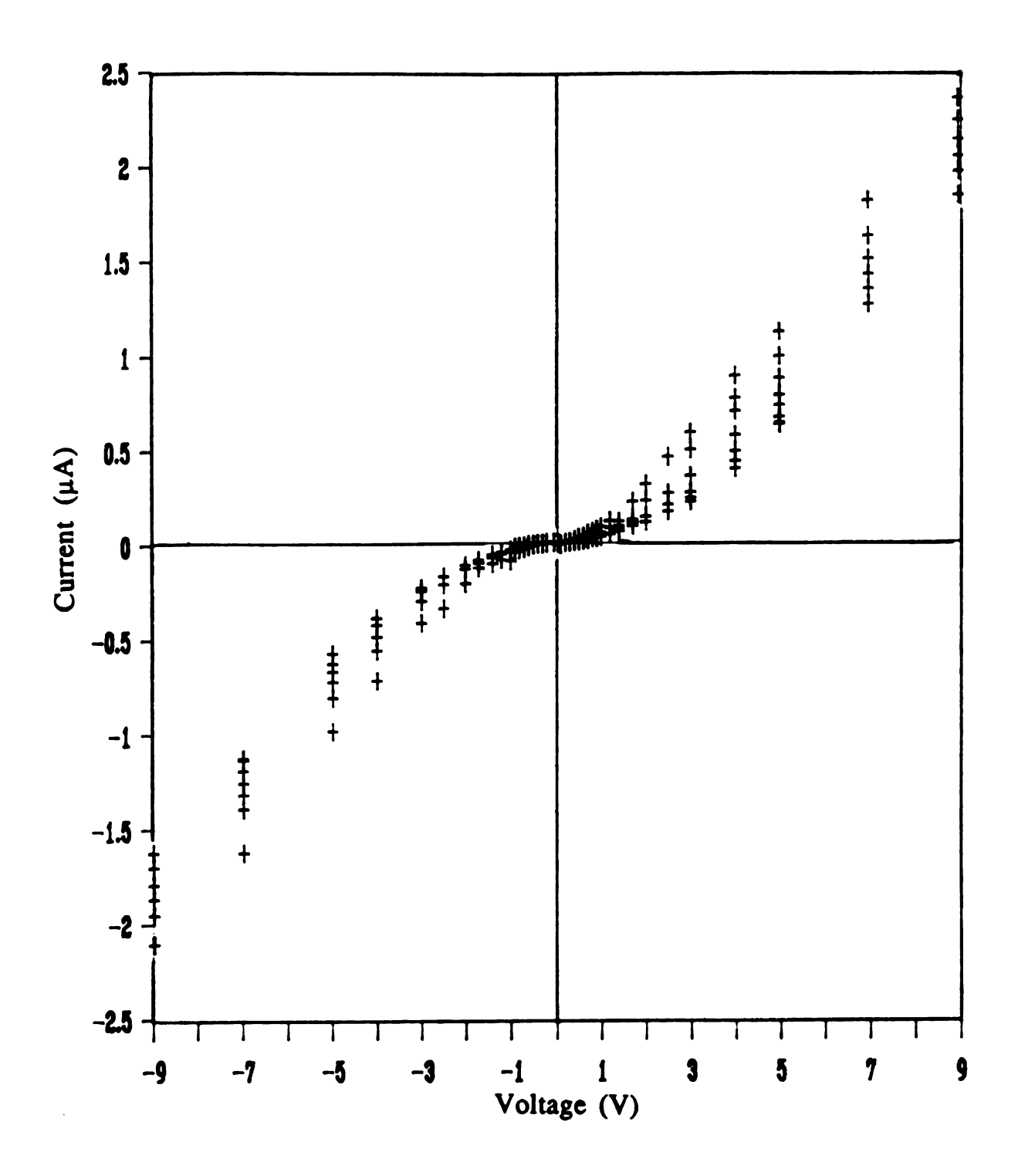


Figure 34: Ohm's law plot from the high temperature conductivity region of Cs+(15C5)<sub>2</sub>e<sup>-</sup>.

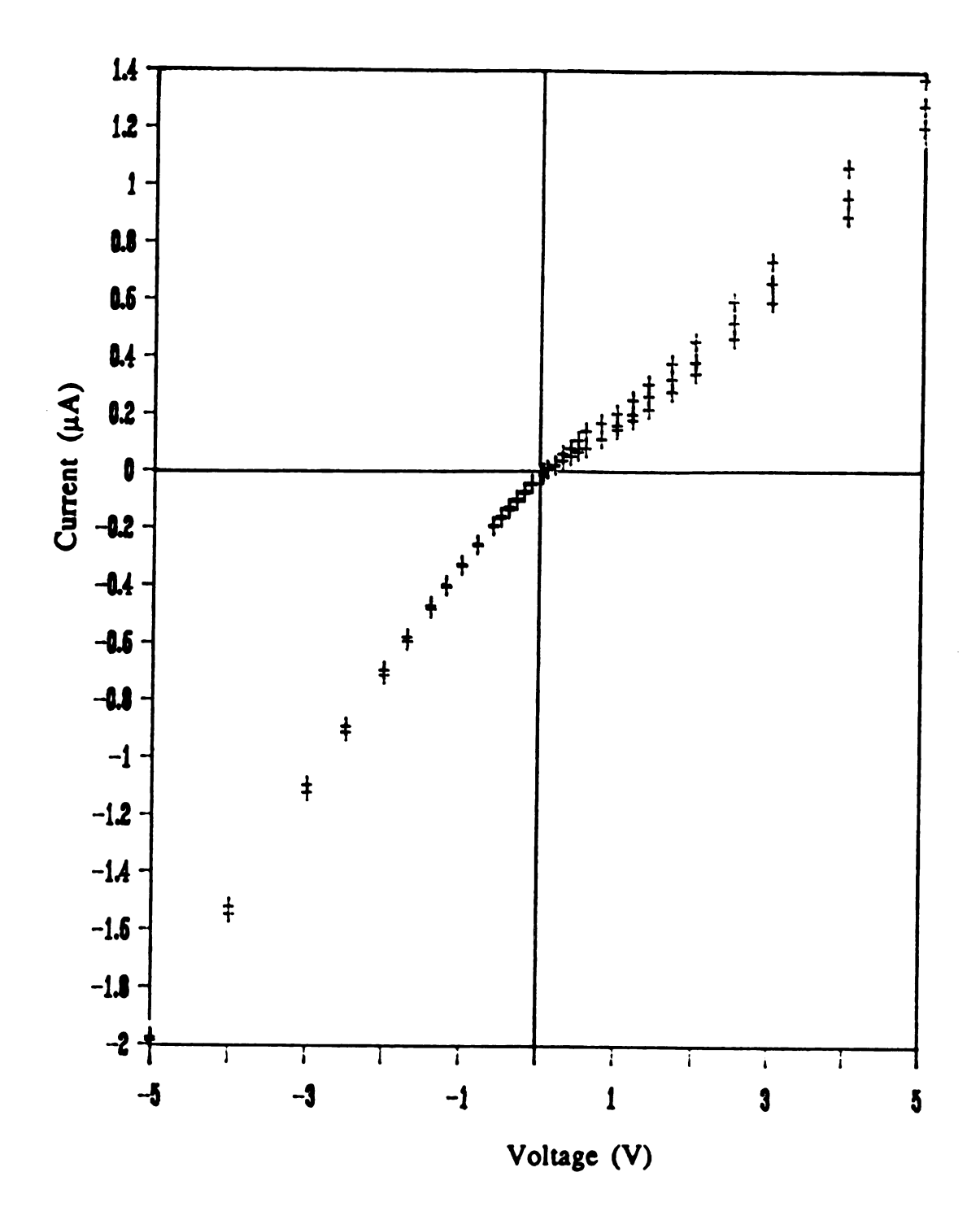


Figure 35: Ohm's law plot of data from the electrochemical cell formed by placing Cs<sup>+</sup>(15C5)<sub>2</sub>e<sup>-</sup> between one cesium and one steel electrode.

forward voltage bias, the current flow is time dependent. Presumably, this is due to the movement of Cs<sup>+</sup> away from the steel electrode, forming a depletion layer and a time dependent current. When the bias is reversed and Cs<sup>+</sup> migrates away from the cesium metal electrode, virtually no time dependence of the current is seen. In this case, the cesium electrode acts as a source of cesium cations and no depletion layer is formed. A possible set of spontaneous electrode reactions that would explain this behavior is:

Anode: 
$$Cs_m ----> Cs^+ + e^-_{electrode}$$
 32

and

Cathode: 
$$Cs^+ + e^-_{electrode} ---- > Cs_m$$
 33

The net process described by the above equations is the transport of cesium metal from one electrode to the other. This process should proceed until both electrodes are coated with cesium. When a sample of Cs<sup>+</sup>(15C5)<sub>2</sub>e<sup>-</sup> was placed between two cesium electrodes, I-V data were as predicted by Ohm's law. The data, shown in Figure 36, show no curvature of the I-V plot or time dependence of the current since both electrodes are now reversible.

Attempts to form an electrochemical cell by charging samples of Cs<sup>+</sup>(15C5)<sub>2</sub>e<sup>-</sup> at a 5 V potential for periods of up to 2 hours failed. In all cases, the open circuit voltage decayed quickly to zero once the charging voltage had been removed. Ohm's law experiments performed on samples which had been charged yielded data that was

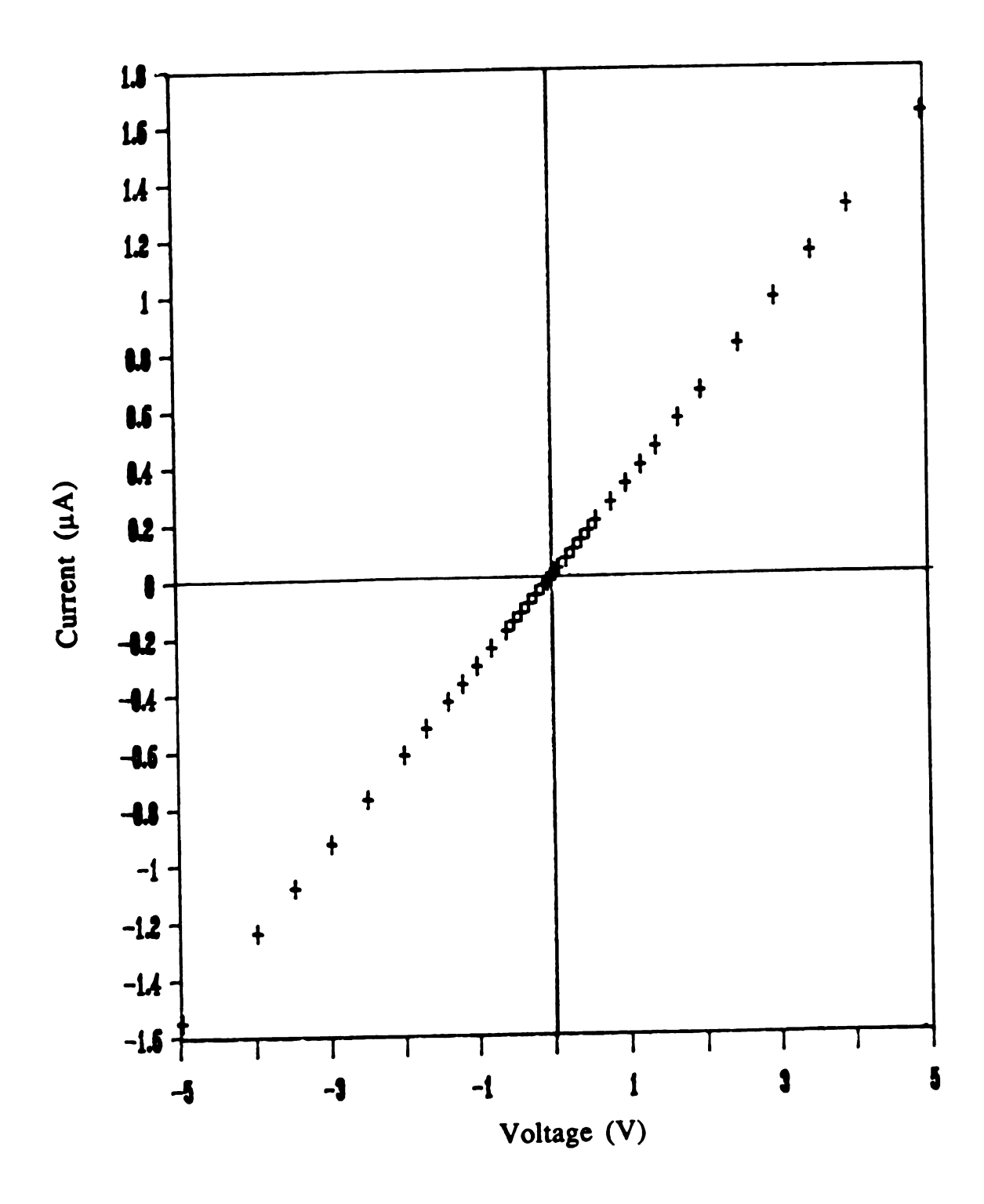


Figure 36: Ohm's law plot for a sample of Cs+(15C5)<sub>2</sub>e<sup>-</sup> between two cesium metal electrodes.

virtually identical to similar experiments performed on uncharged samples.

The possibility that the observed conductivity of Cs<sup>+</sup>(15C5)<sub>2</sub>e<sup>-</sup> was due to partial decomposition of the sample in the high temperature region was also investigated. It was thought such decomposition could be electrochemically induced. To test this, the resistance of a sample of Cs<sup>+</sup>(15C5)<sub>2</sub>e<sup>-</sup> was measured as a function of time at a single temperature, by two different methods. method pulsed the sample with a 100 mV voltage for a period of 10 seconds every 300 seconds. The voltage pulses were of alternate polarity. The resistance of the sample increased by less than 6 % over a period of 60 minutes. In the second method, 100 mV pulses of alternate polarity were applied to the sample with no down time between the pulses. In the same 60 minute period, the sample resistance increased by less than 10 %. In addition, d.c conductivity experiments which were run on samples of Cs<sup>+</sup>(15C5)<sub>2</sub>e<sup>-</sup> which had been used previously for other conductivity measurements gave results similar to experiments run on fresh samples. experiments indicate that significant decomposition was not induced electrochemically in the course of conductivity experiments.

A sample of the model salt Cs<sup>+</sup>(15C5)<sub>2</sub>I<sup>-</sup> proved to be too resistive to be studied by IS. D.C. conductivity of the salt indicated an activation energy of 2.8 eV for conduction. D.C. conductivity of the decomposed electride failed. At low temperatures, the resistivity of the sample was too large (>10<sup>13</sup> ohms) to be measured with the instrumentation. As the sample temperature increased, the sample resistance quickly dropped to near zero. It is believed that this was

caused by melting of the sample which was then squeezed out from between the cell electrodes. This seems likely since the decomposed sample is a syrup-like liquid at warmer temperatures.

The d.c. conductivity of the related alkalide Cs+(15C5)<sub>2</sub>Cs-, showed no evidence of ionic conductivity. Figure 37 shows that the conductivity behaved normally for a semiconductor with an activation energy of 0.20 eV up to the decomposition of the sample. I-V data for Cs+(15C5)<sub>2</sub>Cs- lacked the time dependence of similar experiments on Cs+(15C5)<sub>2</sub>e-, although some slight curvature of the data was seen. Likewise, the low frequency spike seen in the impedance spectrum of Cs+(15C5)<sub>2</sub>e- was not observed for Cs+(15C5)<sub>2</sub>Cs- which yielded only a single impedance arc. Attempts to dope samples of Cs+(15C5)<sub>2</sub>e- with cesium to create a partial ceside also failed. In all cases, attempted synthesis of the doped electride resulted in phase separation of the product.

IS and d.c. conductivity experiments have shown that Cs+(15C5)<sub>2</sub>e- undergoes ionic conductivity in which the cesium cation participates. This is the first evidence for ionic conductivity ever observed in an electride and indicates that the electron anions in this system are trapped more deeply than was previously believed. Similar behavior was not observed in Cs+(15C5)<sub>2</sub>Cs-. Data for the ceside gave an apparent band gap of 0.40 eV. This is very low for an alkalide and probably reflects extrinsic conductivity due to doping by defect electrons. The mechanism of ionic conductivity in Cs+(15C5)<sub>2</sub>e- is unknown but probably involves the initial release of Cs+ from its crown ether cage. The direct transport of Cs+ from cage to cage seems unlikely since the cation would probably be reduced to

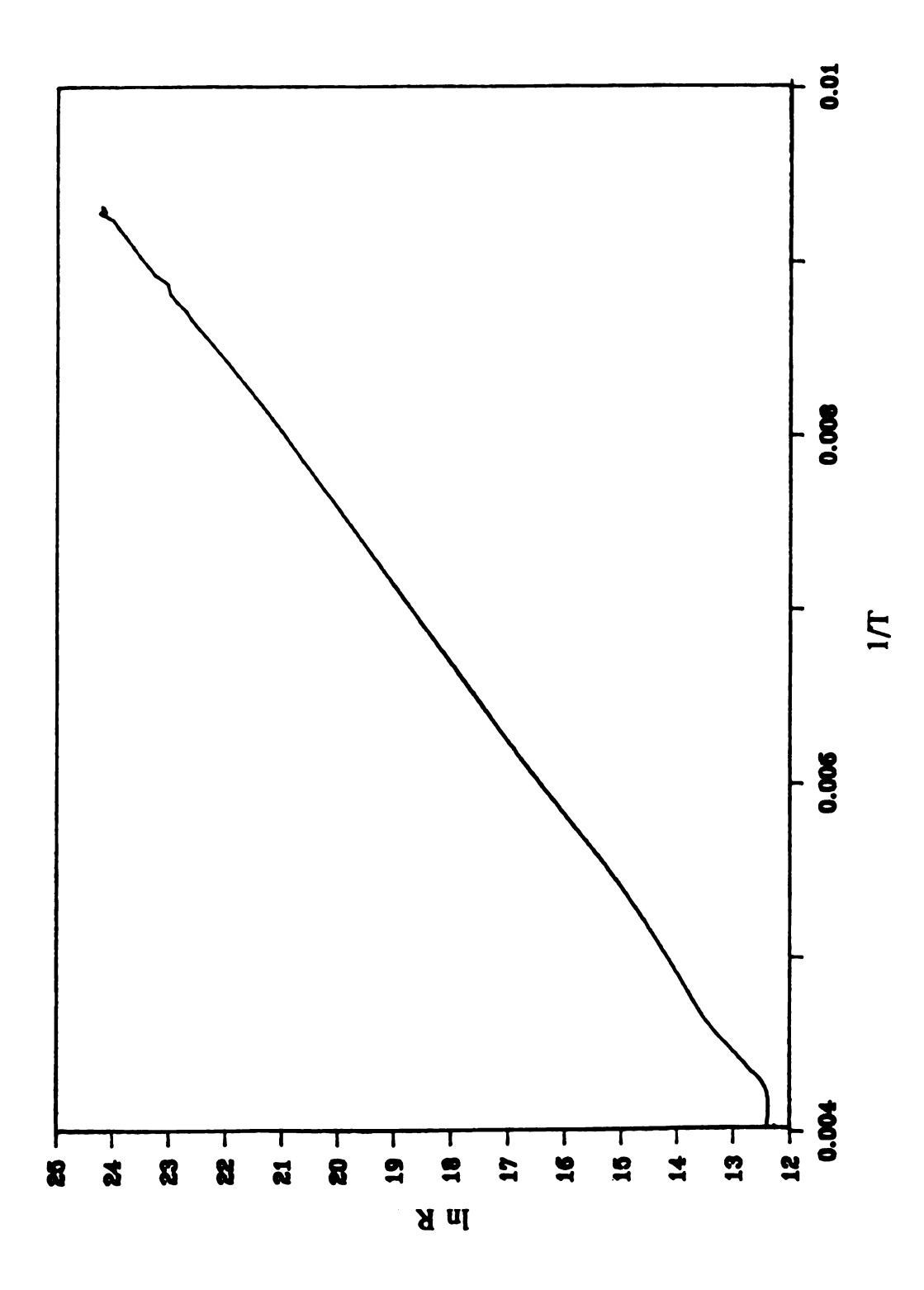


Figure 37: The d.c. conductivity of Cs+(15C5)2Cs-

Cs<sup>0</sup> by the trapped electrons in the system unless they were very tightly bound. One possible mechanism involves the release of Cs<sup>+</sup> from its cage combined with reduction of the Cs<sup>+</sup> to Cs<sup>0</sup> by the electron anion via the reaction:

$$Cs^+(15C5)_2 + e^-t ---> Cs^0 + 2(15C5).$$
 34

where the  $Cs^0$  is located in an anionic cavity of the crystal. From here, the  $Cs^0$  may be transferred to the next anionic center as  $Cs^+$  where it would be reduced by the trapped electron in the second cavity to  $Cs^0$ . This process is outlined in the equations:

$$Cs_{11}^{0} ----> Cs^{+} + e_{11}^{-}$$
 35

$$Cs^+ + e^-_{12} ----> Cs^0_{12}$$
 36

where t1 and t2 denote anionic sites 1 and 2 respectively. Equations 35 and 36 together represent the transfer of Cs<sup>+</sup> in the compound. The transfer of Cs<sup>+</sup> rather than Cs<sup>0</sup> or Cs<sup>-</sup> is more likely due to the much smaller size of Cs<sup>+</sup> compared to these other two species. This mechanism would also account for the lack of significant conductivity in Cs<sup>+</sup>(15C5)<sub>2</sub>I<sup>-</sup> since the electrons play a significant role in the conductivity.

## 3. <u>Cs+(18C6)2e</u>-

Another localized electride for which the structure has been determined is Cs<sup>+</sup>(18C6)<sub>2</sub>e<sup>-</sup>. Each anionic cavity in the crystal

structure has a diameter of ~4 Å and length of ~6 Å.<sup>29</sup> The cavities are interconnected by narrow channels. Optical spectra of thin films of the compound indicate that the electrons are localized in traps of depth >0.5 eV.<sup>11</sup> The magnetic susceptibility indicates that the electrons interact only weakly.<sup>11,27</sup> Early pressed powder conductivity experiments indicated that Cs+(18C6)<sub>2</sub>e<sup>-</sup> is an intrinsic semiconductor with a band gap of 0.9 eV.<sup>11,27</sup>

Attempts to study the impedance spectroscopy of Cs+(18C6)2efailed. The impedances of samples of the compound proved too large to measure with the present instrumentation at any temperature up to the decomposition point of the compound. This was unexpected since the previous d.c. conductivity experiments had indicated a rather high conductivity for the compound. The present d.c. conductivity experiments yielded results drastically different from those obtained previously. In order to verify the present results, the d.c. conductivity of a second sample,84 which had been synthesized for single crystal diffraction studies, was also measured. The second sample showed similar behavior and the results of both experiments The behavior is reminiscent of that of are shown in Figure 38. Cs+(15C5)<sub>2</sub>e<sup>-</sup>, which was attributed to defect electron conductivity at low temperatures and ionic conductivity at high temperatures. Cs+(18C6)<sub>2</sub>e<sup>-</sup> the data yield activation energies of 1.04 and 1.08 eV, respectively, for the two runs in the high temperature region. In the low temperature region, activation energies of 0.17 and 0.13 eV were The crossover between the two activation regions is not associated with any sudden transition which can be resolved by magnetic susceptibility or DSC.

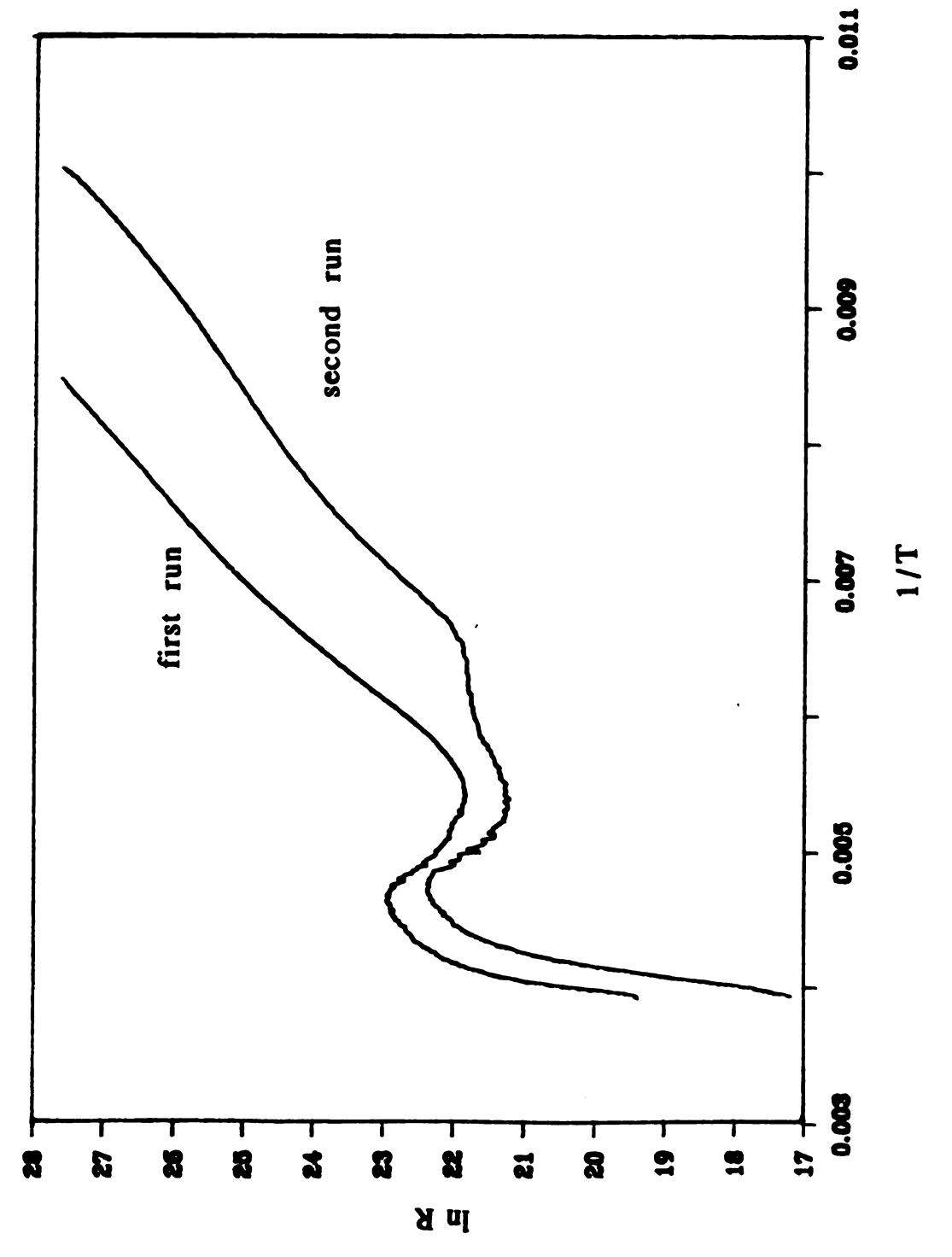


Figure 38: The conductivity of two samples of Cs<sup>+</sup>(18C6)<sub>2</sub>e<sup>-</sup> taken from two different syntheses.

The reason for the increase in the sample resistance before the crossover point is unknown, but was not as pronounced for samples in which the temperature was quickly increased throughout the experiment. <sup>133</sup>Cs NMR of Cs+(18C6)<sub>2</sub>e<sup>-</sup> shows a gradual reversible change of the NMR signal in this region. This change involves the growth of a second <sup>133</sup>Cs peak as the temperature is increased coupled with a decrease of the low temperature peak over a broad temperature range.<sup>46</sup> It is possible that increased motion of the complexant molecules in the crystal structure in this temperature range weaken the cation complex sufficiently to allow ionic conductivity to occur.

Ohm's law plots of the I-V data for Cs+(18C6)<sub>2</sub>e<sup>-</sup> taken in the high temperature region showed some curvature but no time dependence of the current (Figure 39). The lack of time dependence is probably due to the low current flow of these experiments which was, on the average about three orders of magnitude below the current measured in similar experiments on Cs+(15C5)<sub>2</sub>e<sup>-</sup>. If the time dependence for Cs+(15C5)<sub>2</sub>e<sup>-</sup> had been due to depletion, about 3 hours on each bias would have been required for a comparable effect in Cs+(18C6)<sub>2</sub>e<sup>-</sup> to be observed.

When a sample of Cs+(18C6)<sub>2</sub>e- was placed between a steel and a cesium electrode, an electrochemical cell was formed. Current flowed through the cell in the absence of an applied bias and it required ~0.6 V to zero the current. Figure 40 shows an Ohm's law plot for the cell. Another sample placed between two cesium electrodes gave an Ohm's law plot through the origin (Figure 41), although some slight curvature of the plot remained.

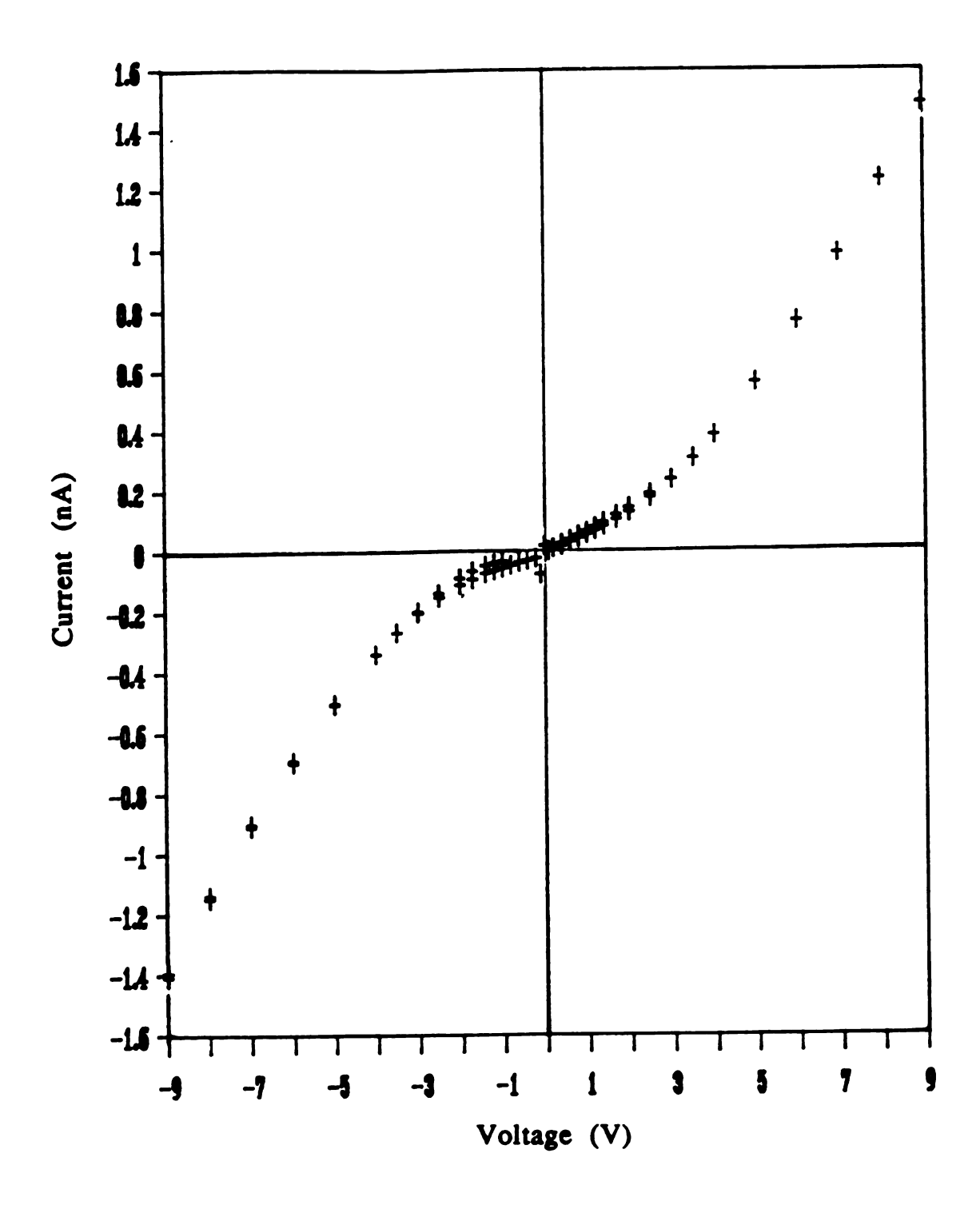


Figure 39: Ohm's law plot for Cs+(18C6)<sub>2</sub>e<sup>-</sup> at -39.2 °C.

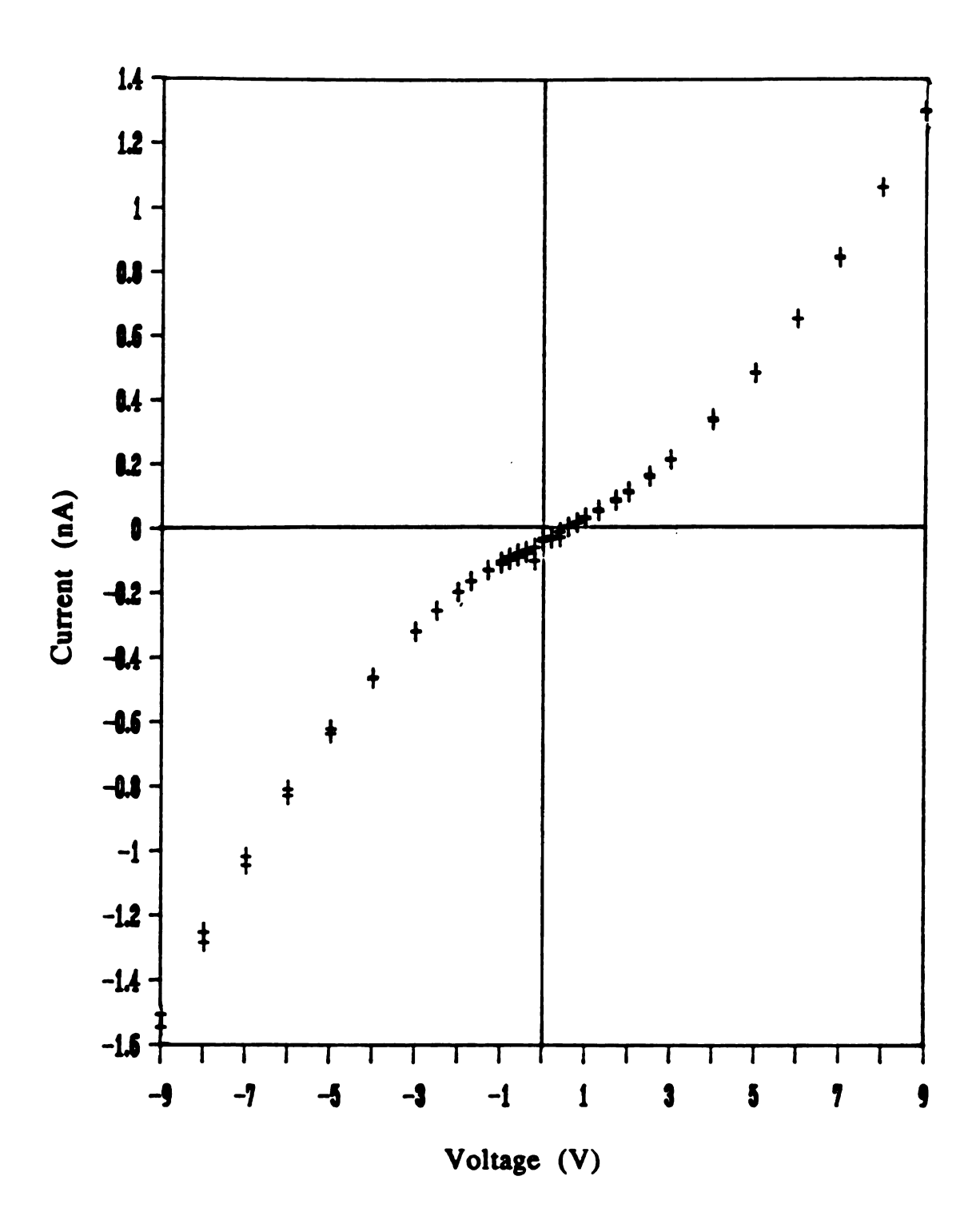


Figure 40: Ohm's law plot of Cs<sup>+</sup>(18C6)<sub>2</sub>e<sup>-</sup> between one steel and one cesium electrode at -33.4 °C and 60 s on bias.

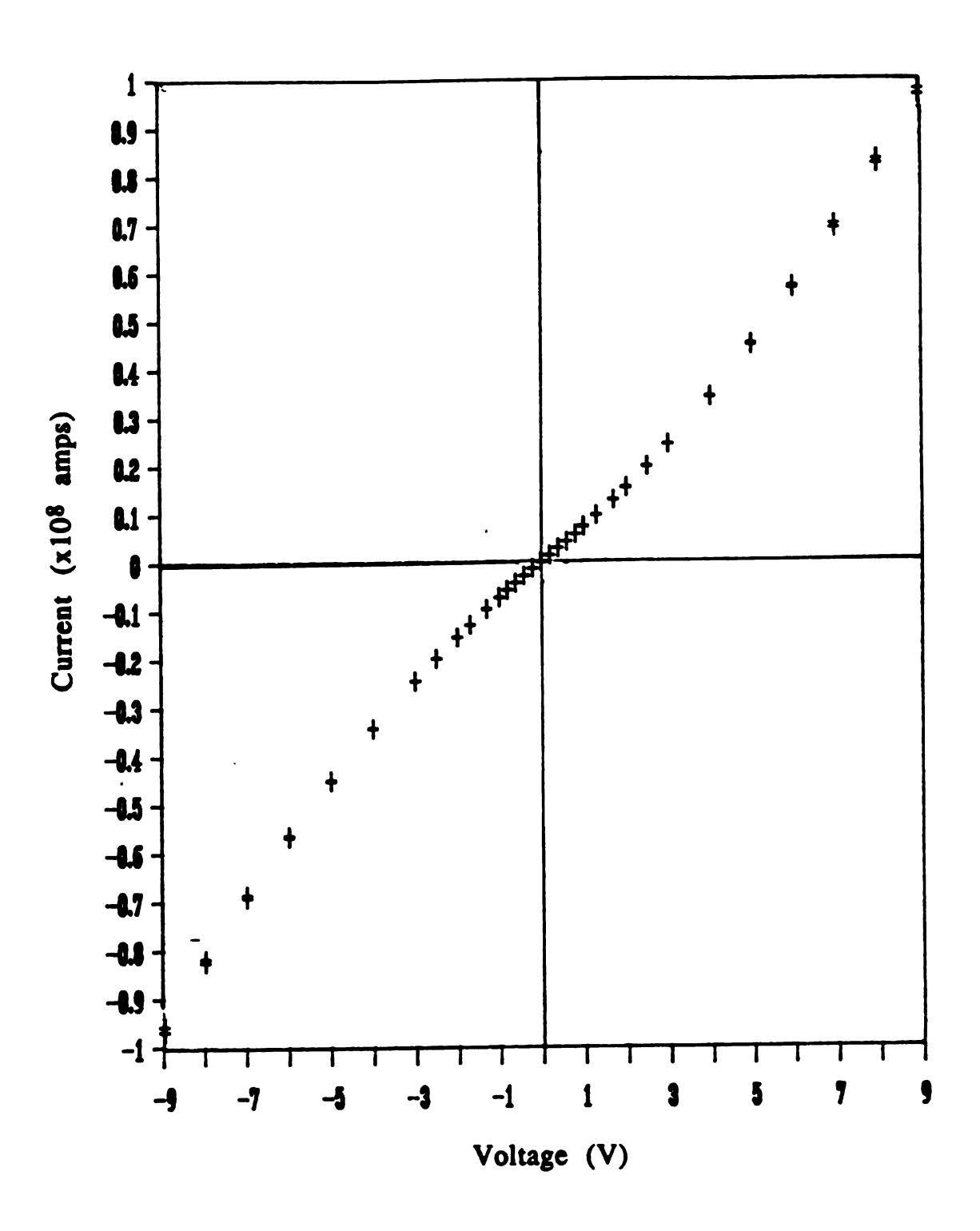


Figure 41: Ohm's law plot for Cs+(18C6)<sub>2</sub>e<sup>-</sup> between two cesium electrodes at -34.4 °C.

The above experiments point to ionic conductivity in Cs+(18C6)<sub>2</sub>e<sup>-</sup>. These results disagree with the previous work which had shown Cs+(18C6)<sub>2</sub>e<sup>-</sup> to be an intrinsic semiconductor. Further studies were required to ascertain the reasons for this difference. Two main possibilities were seen as the cause of this difference. First, since in early conductivity experiments samples had been loaded and temperature cycled at relatively high temperatures, small amounts of decomposition of the sample may have occurred and led to the observed behavior. Secondly, small amounts of alkalide impurity in the early samples may have led to increased electronic conductivity which covered up the ionic conductivity of the system.

In order to test the former possibility, samples of Cs+(18C6)<sub>2</sub>e-were warmed to temperatures between -20 °C and -35 °C for periods of up to 2 hours prior to d.c. conductivity experiments. The results of these experiments varied widely. Although one such experiment did yield an apparent band gap of 0.9 eV, the values of band gaps thus determined ranged from 0.9 to 6.3 eV. In addition, most of these experiments still yielded two activation regions similar to what was seen in the "pure" electride samples. These studies showed that decomposition was probably not the cause of the results obtained previously.

It seemed likely that ceside impurities in samples of Cs+(18C6)<sub>2</sub>e<sup>-</sup> could have affected the conductivity in the previous studies, especially since the conductivity of Cs+(18C6)<sub>2</sub>Cs<sup>-</sup> is higher than that of the electride. The synthesis of electrides has advanced since the early conductivity experiments on Cs+(18C6)<sub>2</sub>e<sup>-</sup> were carried out. Present day synthesis of an electride involves the use of

a small excess of complexant in order to minimize alkalide impurity (as described in Chapter II of this work). When the early conductivity experiments on Cs<sup>+</sup>(18C6)<sub>2</sub>e<sup>-</sup> were performed, however, no excess of complexant was used in the synthesis of electride samples.

Two methods of doping Cs<sup>+</sup>(18C6)<sub>2</sub>e<sup>-</sup> were used for the present work, and gave similar conductivity results. For the first method, 2:1 ratios of complexant to metal were used in the synthesis of the compound as had been done for the previous work. In the second method, a small amount of Cs<sup>+</sup>(18C6)<sub>2</sub>Cs<sup>-</sup> was added to a larger sample of Cs<sup>+</sup>(18C6)<sub>2</sub>e<sup>-</sup> and the mixture was then dissolved and recrystallized. Both methods were described in Chapter II of this It was not possible to determine whether phase separation had occurred as a result of the doping since both the ceside and the electride are black in color. Conductivity results on one such doped sample are shown in Figure 42. The doped samples exhibited increased conductivity over pure Cs<sup>+</sup>(18C6)<sub>2</sub>e<sup>-</sup> samples. The break in conductivity behavior observed in pure samples was not seen in doped samples. When doped samples were placed between one steel and one cesium electrode, no electrochemical cell behavior was observed and the measured current was not time dependent as shown in Figure 43.

Samples of the ceside Cs<sup>+</sup>(18C6)<sub>2</sub>Cs<sup>-</sup> also showed semiconductor behavior as seen in Figure 44. The measured band gap was 0.49 eV and probably resulted from defect electrons in the sample. Magnetic susceptibility measurements on this sample showed the presence of 2.5 % defect electrons. Ohm's law plots for the sample were nearly

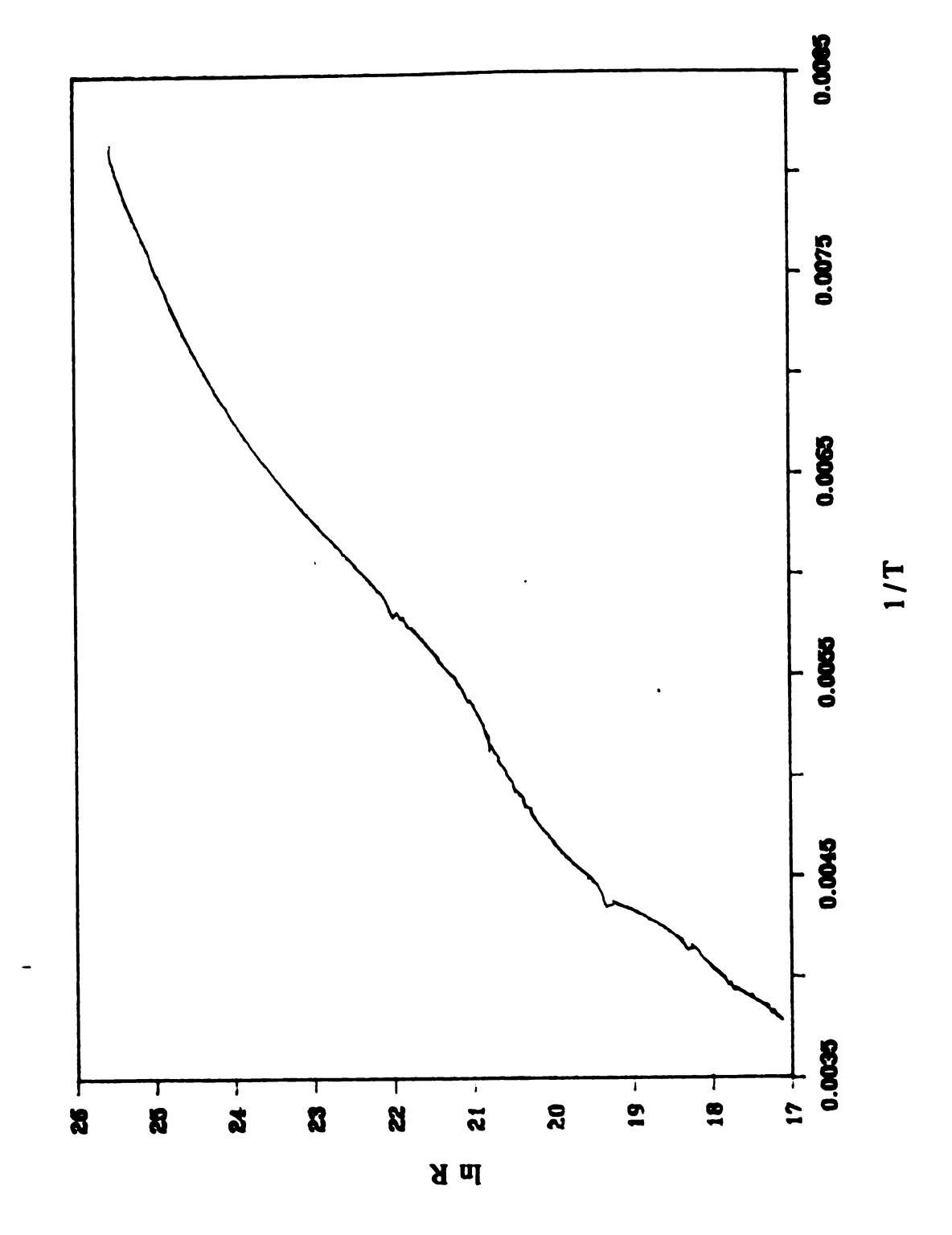


Figure 42: The conductivity of Cs<sup>+</sup>(18C6)<sub>2</sub>e<sup>-</sup> doped with cesium.

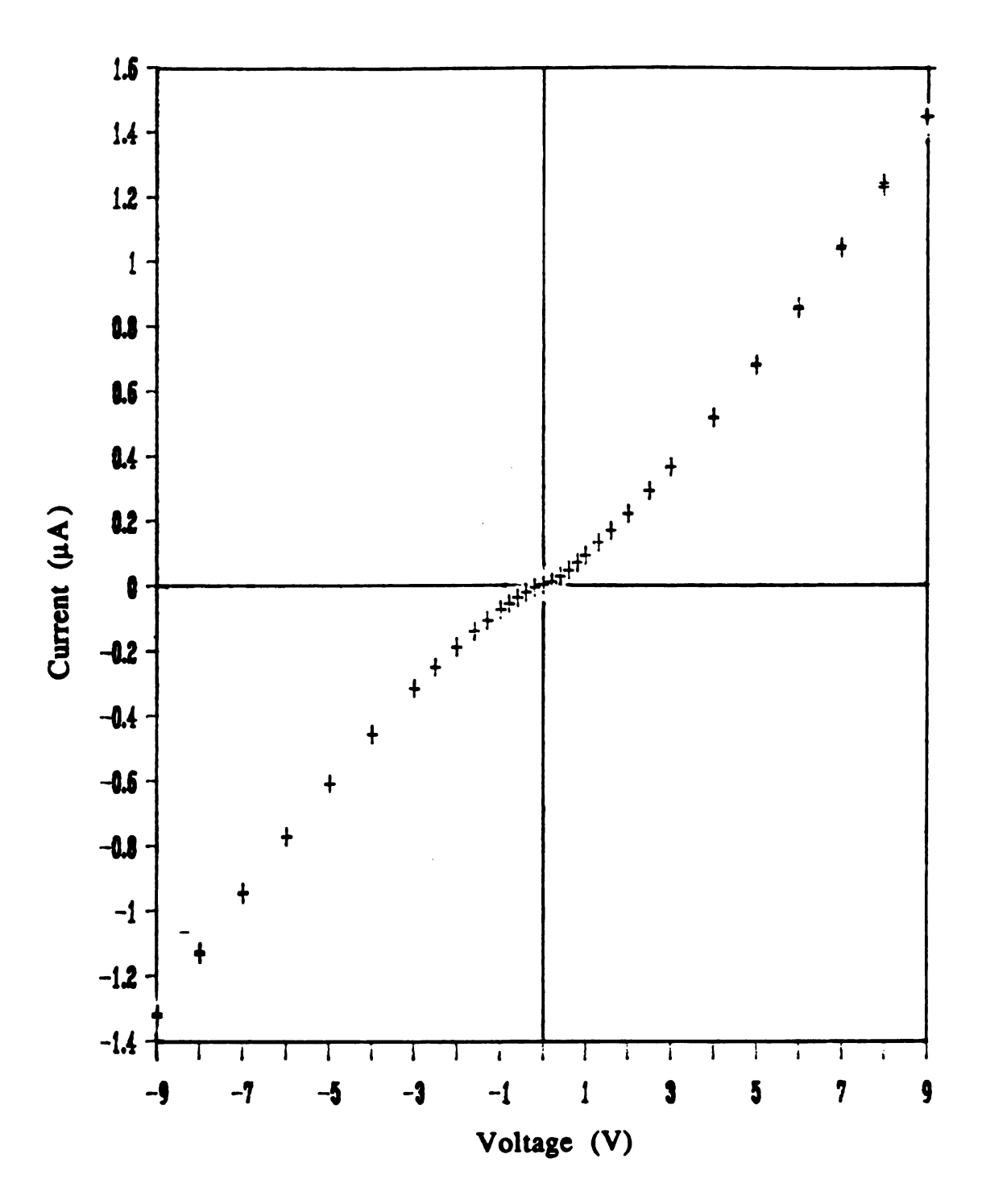


Figure 43: Ohm's law plot for a sample of Cs+(18C6)<sub>2</sub>e- doped with cesium and held between one cesium and one steel electrode at -51 °C.

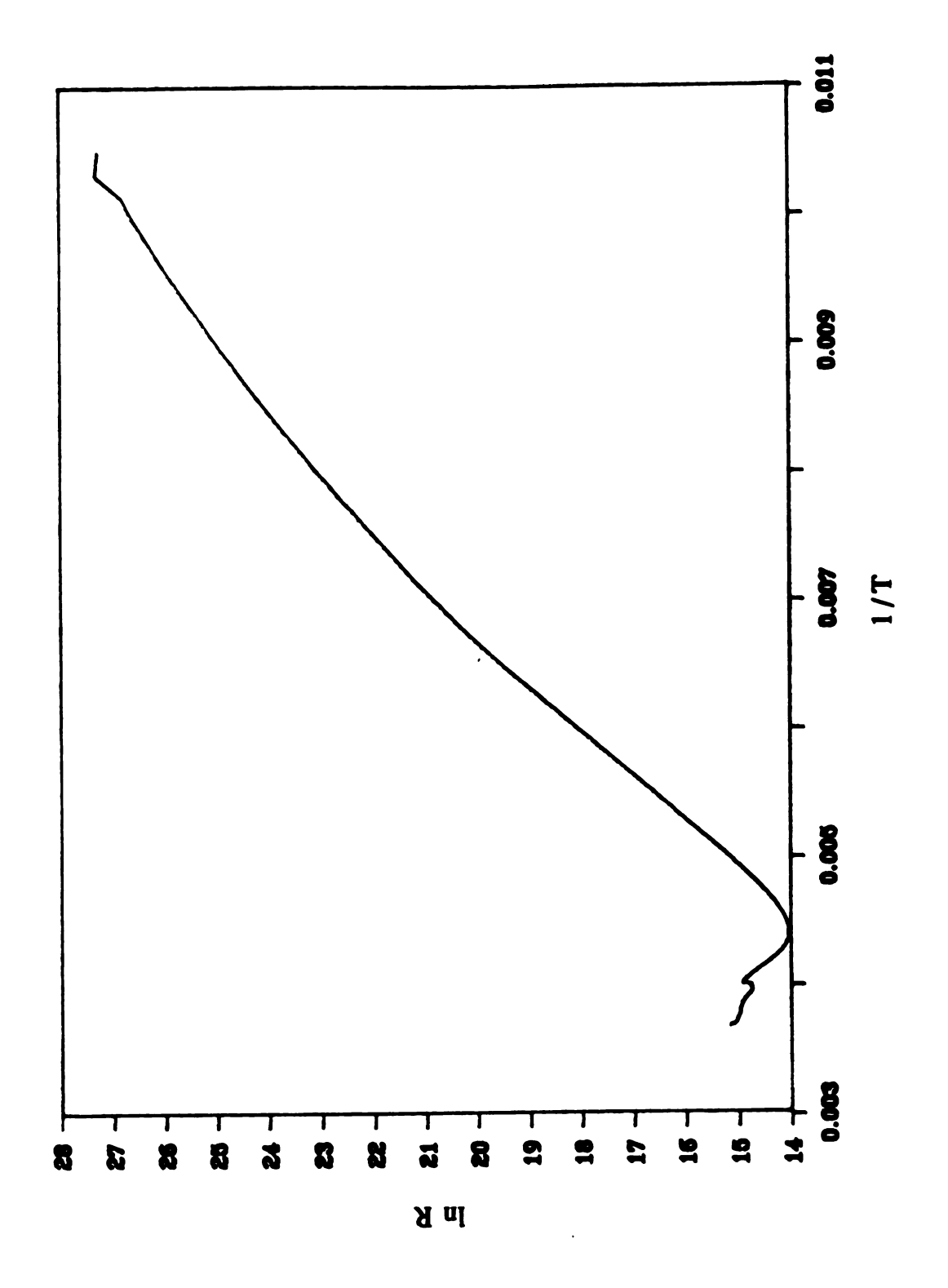


Figure 44: The conductivity of Cs+(18C6)<sub>2</sub>Cs-.

linear and showed no time dependence of the current. As in the doped electride, no electrochemical cell behavior was observed when samples of the ceside were placed between steel and cesium electrodes.

When a sample of Cs<sup>+</sup>(18C6)<sub>2</sub>e<sup>-</sup> was doped with small amounts of sodium, results were quite different. A d.c. conductivity run of the sodium doped electride is shown in Figure 45. Although the sample decomposed prematurely, the conductivity behavior of the sample up to the decomposition point was similar to that of the pure electride.

D.C. conductivity experiments have shown Cs+(18C6)<sub>2</sub>e<sup>-</sup> to be an ionic conductor with an activation energy of 1.0 eV. Once again, the mechanism of conductivity is unknown, but is probably closely related to that of Cs+(15C5)<sub>2</sub>e<sup>-</sup>. If a large part of the activation energy involves the release of Cs+ from its crown ether cage, the observed relation between the activation energies of these two electrides can be understood. Since the cation complex of Cs+(18C6)<sub>2</sub>e<sup>-</sup> is more tightly bound than that of Cs+(15C5)<sub>2</sub>e<sup>-</sup> the increased activation energy of the former may reflect the increased stability of this complex.

The present results have shown that the semiconductor behavior seen previously in samples of Cs+(18C6)<sub>2</sub>e<sup>-</sup> was probably the result of impurity doping of the compound. Intentional doping of electride samples with cesium resulted in increased electronic conductivity of the compound which covered up the effects of ionic conductivity. The doped samples were also more conductive than the pure electride. When sodium was used as the dopant, the

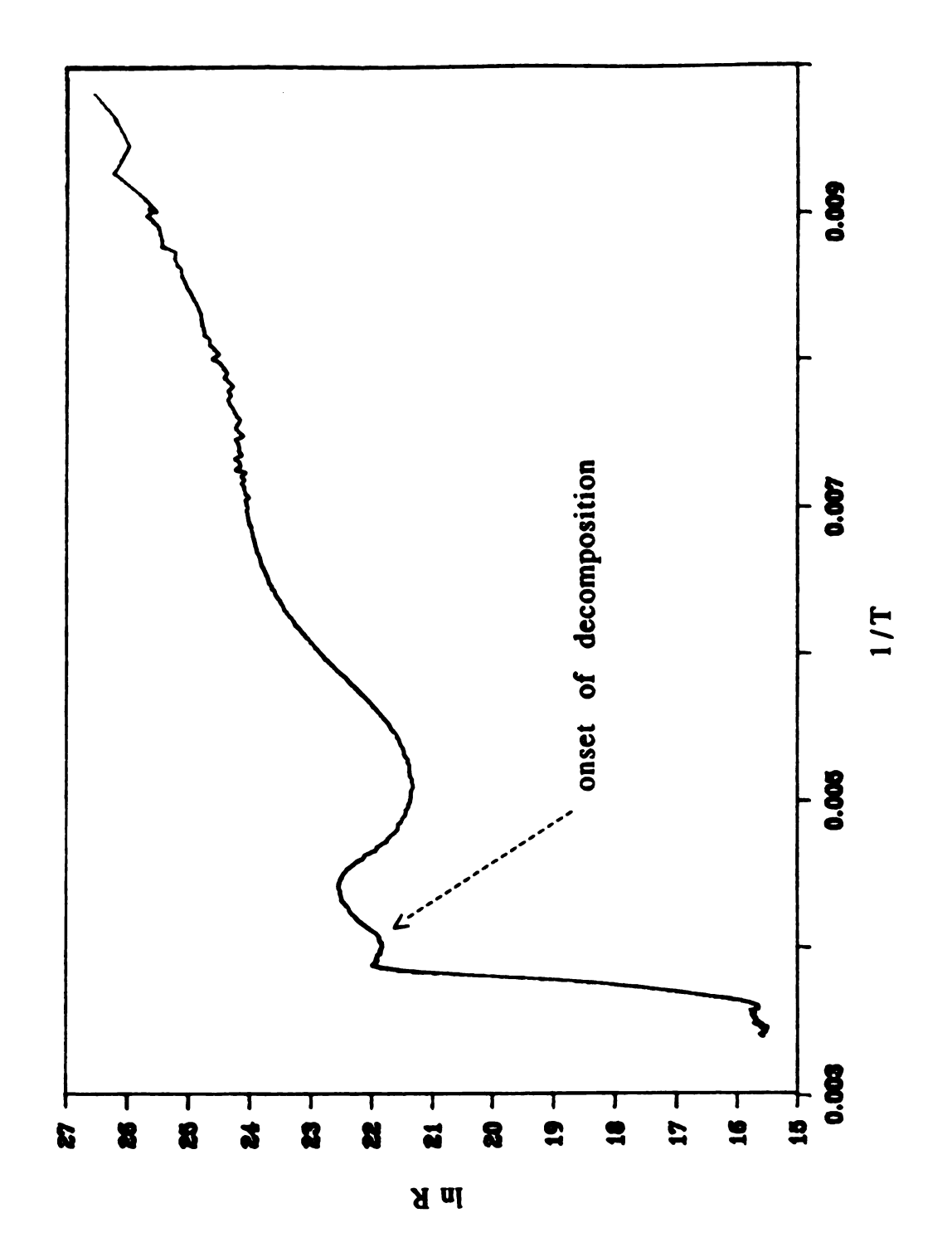


Figure 45: The conductivity of Cs+(18C6)2e- doped with sodium.

conductivity of the sample was virtually the same as that of the pure electride. The reason for the observed difference may lie in the size of the dopant ions. The size of the cesium anion (~7.0 Å in diameter) makes it too large to fit easily into the anionic cavities of Cs+(18C6)2e-. As a result, one of the 6s electrons of Cs- may go into a Rydberg type orbital from which it can be excited into the conduction band of Cs+(18C6)2e-. This would lead to increased electronic conductivity and mask the effects of ionic conductivity in the system. The absence of increased conductivity in the sodium doped system could then also be explained. The diameter of the sodium anion is ~5.0 Å, approximately the same size as the anionic sites in Cs+(18C6)2e- and so would fit more easily into the structure.

Together with the conductivity results from Cs+(15C5)<sub>2</sub>e<sup>-</sup>, the results from Cs+(18C6)<sub>2</sub>e<sup>-</sup> show the need for high purity samples in conductivity experiments. These experiments also point to the need to re-examine the conductivity properties of alkalides and electrides which have been measured in the past. As seen in Cs+(18C6)<sub>2</sub>e<sup>-</sup>, the results of such experiments depend dramatically upon the synthesis methods employed. In particular, ionic conductivity may be much more common in alkalides and electrides than was believed. Further work is needed to determine if this is, in fact, the case.

## 4. Miscellaneous

In addition to the extensive studies of three electrides, there are several compounds for which some electrical measurements have

been made, but which require further study. The results to date on these compounds are presented below.

## a. Li+(PMPCY)e-

Li+(PMPCY)e- was the first electride synthesized which contained an amine complexant.<sup>17</sup> In this case, the complexant is pentamethylpentacyclen (PMPCY), the fully methylated amine analog of 15-crown-5. IS measurements of Li+(PMPCY)e- showed a single slightly depressed impedance arc. D.C. conductivity experiments on the compound showed a sharp break in the conductivity behavior of the compound at a temperature of ~195 K. Figure 46 shows the results of one d.c. experiment on the compound. The sharpness of the observed break suggested that it was the result of a phase Magnetic susceptibility<sup>17</sup> and DSC transition in the solid. experiments later showed evidence of a transition at this temperature. The DSC experiments indicated a reversible endothermic phase transition. The nature of this transition is not known, but the transition may be due to a reordering of the complexant around the lithium cation.

Calculations of a band gap for Li<sup>+</sup>(PMPCY)e<sup>-</sup> from IS and d.c. conductivity experiments led to a range of results. The apparent band gap for samples of Li<sup>+</sup>(PMPCY)e<sup>-</sup> was found to be synthesis dependent, and ranged from 0.14 to 1.06 eV at temperatures above the phase transition. Below the transition, curvature of the data and narrowness of the temperature range prohibited accurate

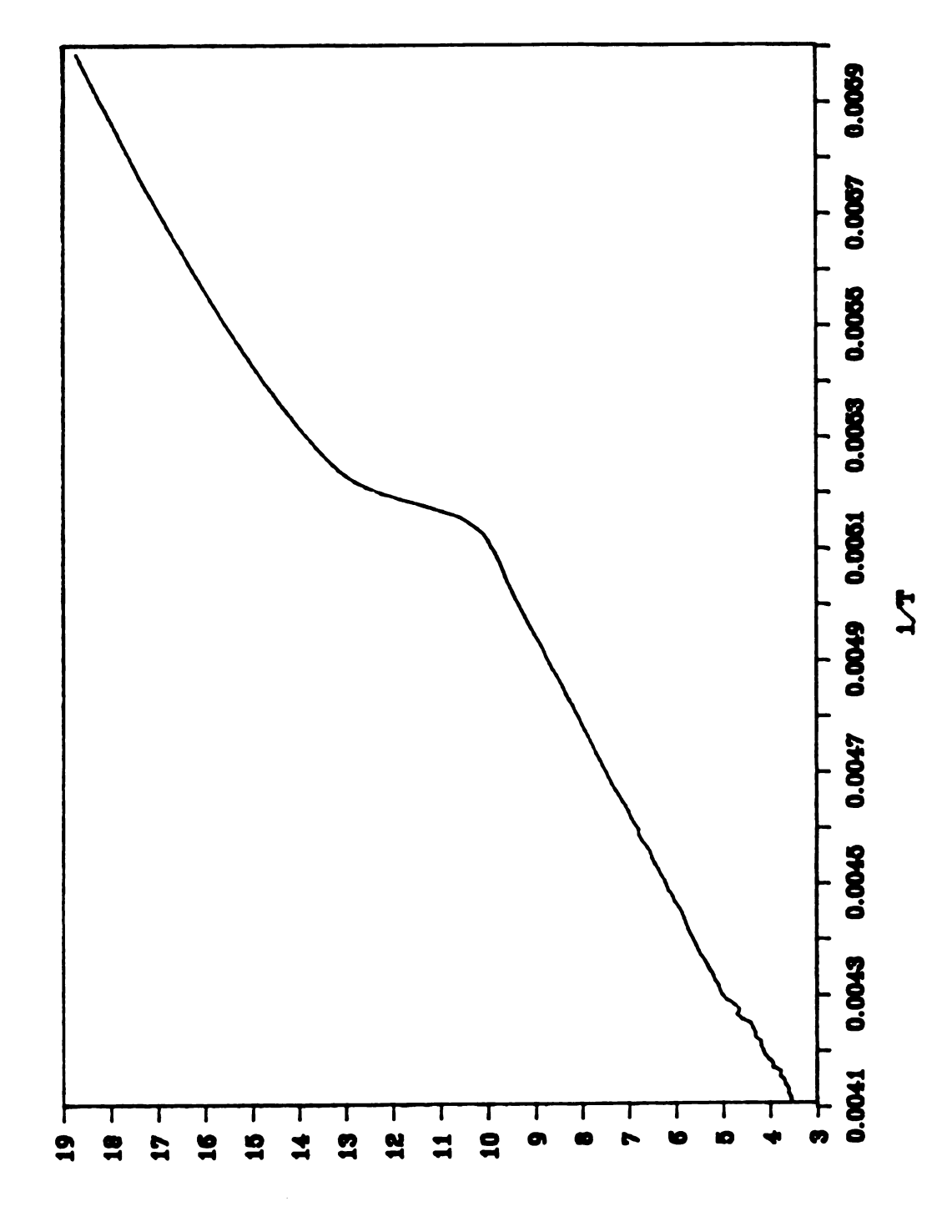


Figure 46: The d.c. conductivity of Li<sup>+</sup>(PMPCY)e<sup>-</sup> showing the break in semiconductor behavior attributed to a solid-solid phase transition.

measurement of a band gap. It is possible that the wide range of band gaps measured for Li<sup>+</sup>(PMPCY)e<sup>-</sup> is due to doping of the compound with lithium. In several of the syntheses of this compound, excess lithium was used. It was for these syntheses that the lowest apparent band gaps were measured.

## b. Li+(TMPAND)e- and Li+(TMPAND)Na-

Two recent compounds in the alkalide/electride class are Li+(TMPAND)e- and Li+(TMPAND)Na-. The complexant in these compounds is a cryptand-like molecule (TMPAND) which contains methylated nitrogens in place of the oxygens of cryptand[1.1.1].<sup>13</sup> In addition, one of the carbon chains in the molecule has been lengthened by two units to increase the cavity size.

The conductivity of Li<sup>+</sup>(TMPAND)e<sup>-</sup> proved impossible to measure via IS or d.c. conductivity methods. The sample resistance was greater than  $10^{13} \Omega$  at all temperatures up to the decomposition point of the compound. Analysis of this sample showed the presence of methylamine left over from the synthesis of the compound.<sup>19</sup> It is uncertain whether the methylamine is incorporated into the structure of the compound or just present as unevaporated solvent. If the solvent is incorporated in the structure, it may expand the lattice sufficiently to cause the high observed resistance.

A sample of Li<sup>+</sup>(TMPAND)Na<sup>-</sup> which had been found to not contain methylamine<sup>19</sup> was also studied by d.c. conductivity methods. This compound had been analyzed previously by DSC and NMR and was found to undergo a solid-solid phase transition at ~-72

°C.85 A plot of the d.c. conductivity results for this compound is shown in Figure 47. As can be seen, the sample resistance is beyond the measurement range of the instrumentation at low temperatures. Above a point which corresponds to the temperature of the phase transition, however, the sample behaves as a semiconductor with a band gap of ~1.2 eV. In order to test for ionic conductivity in the compound, a sample of Li<sup>+</sup>(TMPAND)Na<sup>-</sup> was placed between one sodium and one steel electrode. No electrochemical cell behavior was apparent, and an Ohm's law plot for the cell was symmetrical and passed through the origin of the I-V plane. Since lithium bonds more covalently than other alkali metals, it seemed unlikely that the lithium cation of the compound would be involved in ionic conductivity. It appears, therefore, that Li+(TMPAND)Na- is a semiconductor above the low temperature phase transition with a band gap of 1.2 eV.

# c. Rb+(C222)e-

Rb+(C222)e- is an electride that would be expected to be quite similar to K+(C222)e-. Rubidium and Potassium cations are of similar size, 1.47 and 1.33 Å in radius, respectively. Because of this it would be expected that their cation complexes with cryptand[2.2.2] would be quite similar in size and shape, and would pack similarly in the crystal structure of the two electrides. The crystal structure of Rb+(C222)e- has not been determined so that this idea can be verified. The results of a single d.c. conductivity run performed on Rb+(C222)e- are shown in Figure 48. The behavior of the sample

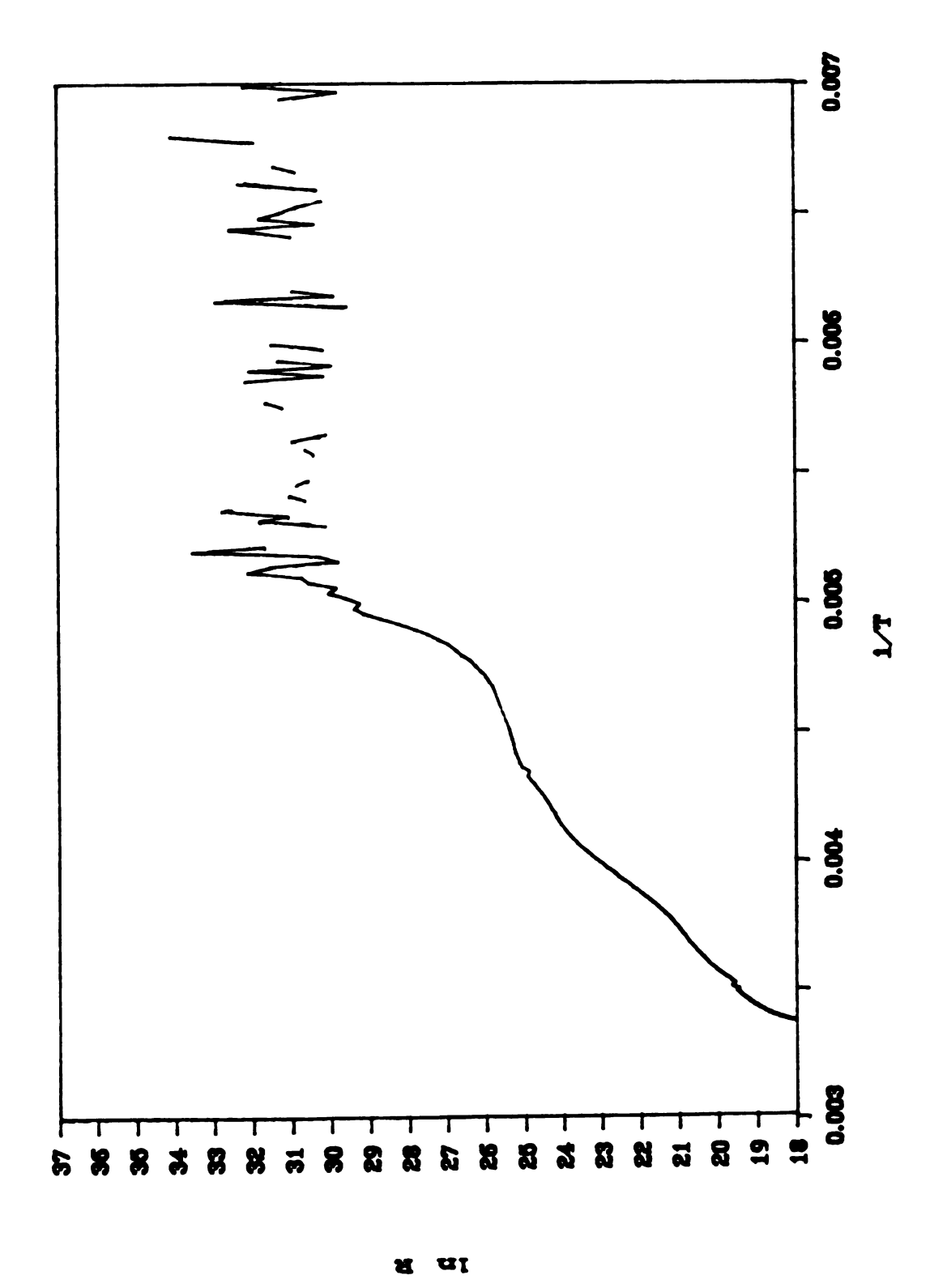


Figure 47: The d.c. condutivity of Li+(TMPAND)Na- showing the onset of conductivity at the solid-solid phase transition.

was, indeed, similar to that of K(C222)e<sup>-</sup>. A band gap of only 0.065 eV was calculated from the data. The relatively high resistance of the sample is probably due to a Schottky barrier at the sample-electrode interface as was observed with K<sup>+</sup>(C222)e<sup>-</sup>.

## d. Others

Samples of the mixed electride Cs+(18C6)(15C5)e-86 and the alkalide Li+(ethylenediamine)<sub>2</sub>Na- were also studied via IS. In both cases, however, results lacked reproducibility. In Cs+(18C6)(15C5)e-, the impedance spectrum consisted of a high frequency arc and a low frequency spike at temperatures as low as -110 °C. After the sample had been warmed briefly to -40 °C, however, its spectrum became a single curved spike. The sample itself retained its original black color throughout the experiment. In Li+(en)<sub>2</sub>Na-, IS resolved a single impedance arc. Several attempts to perform d.c. conductivity measurements, however, indicated that the sample had no apparent resistance.

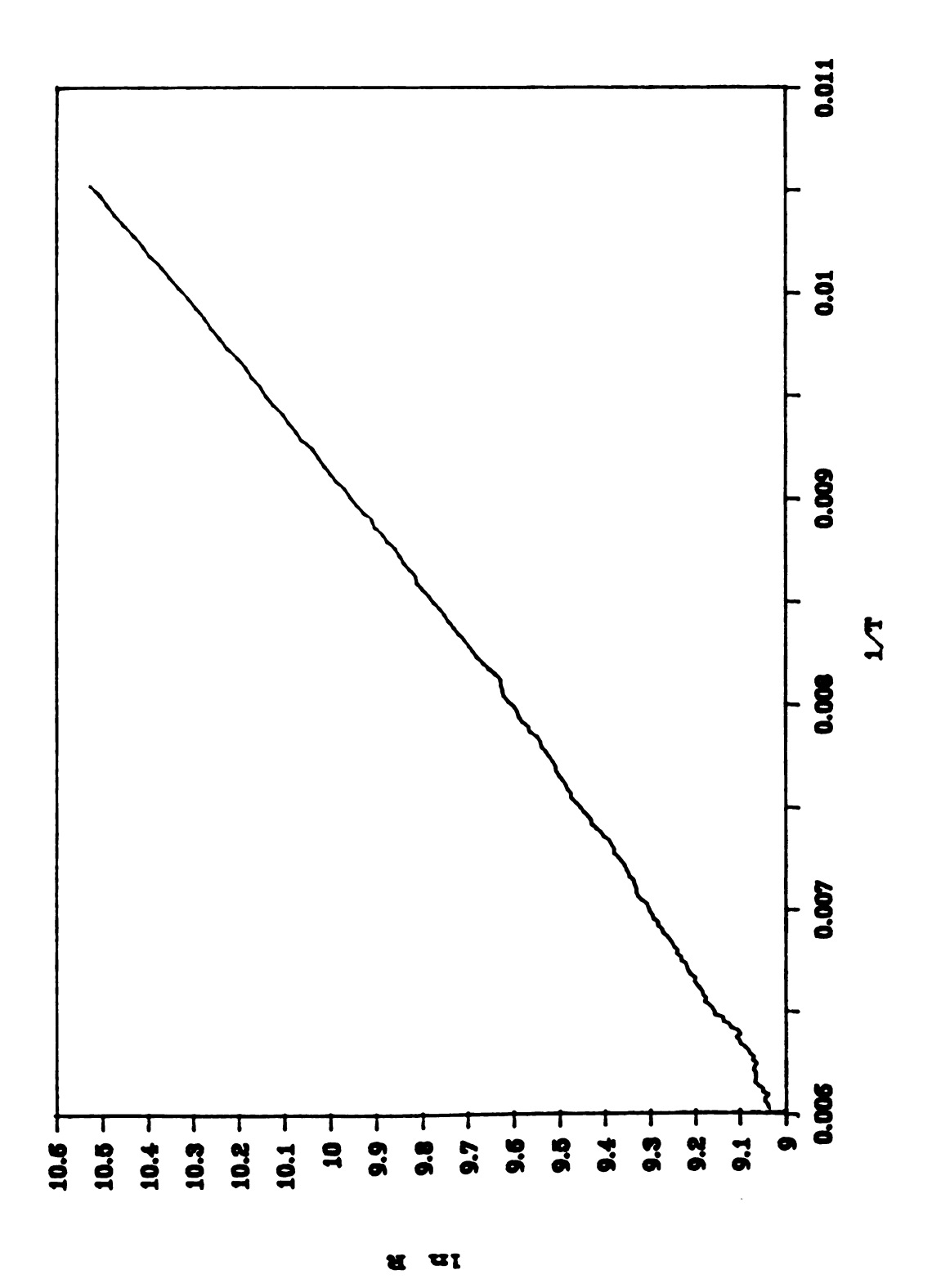


Figure 48: The d.c. conductivity of Rb+(C222)e-.

#### V. CONCLUSIONS AND SUGGESTIONS FOR FURTHER WORK

## V.A. Conclusions

The value of impedance spectroscopy in the separation of electrode effects from the bulk and grain boundary properties of electrides and alkalides has been demonstrated. In particular, the separation of blocking electrode and Schottky barrier impedances from sample properties has been shown. Programs which allow computer control and data acquisition for IS and d.c. conductivity experiments have been developed and used to study the properties of electrides. These programs now allow routine electrical measurements to be made on pressed pellet and powder samples. Methods of coating temperature and air sensitive compounds with reactive alkali metals have been developed.

Electrical measurements on electride samples have uncovered a wide range of behavior in this novel class of compounds. A summary of electrical results on these compounds is given in Table II. It should be noted that since grain boundary impedances have not been separated from the bulk impedances of the compounds in Table 2, the listed resistivities may be orders of magnitude larger than the true resistivities of these compounds.

K+(C222)e- has been shown to be a highly conductive, possibly metallic, compound. The high apparent resistance and non-Ohmic behavior observed in 2-probe measurements of this compound have been shown to be the result of a Schottky barrier at the sample-electrode interface. Through the use of potassium metal as an

electrode material, the barrier height was successfully reduced. This decreased the electrode impedance by four orders of magnitude. IS studies of the related alkalide K+(C222)K- have also shown the presence a Schottky barrier which was eliminated by the use of potassium as an electrode material. An upper limit on the resistivity of K+(C222)e- was obtained through the use of the van der Pauw technique, and an apparent band gap of 0.086 eV for the material was determined. The possibility that the observed band gap of the compound is due to activated transport of electrons across grain boundaries remains.

Table 2: Conductivity data for electrides studied in this work.

	Resistivity upper	Apparent
Compound	limit $(\Omega cm)/temp$ (K)	band gap (eV)
K+(C222)e-	0.189/130	0.086
Cs+(15C5) <sub>2</sub> e-	$4.0 \times 10^{4}/255$	>0.67
Cs+(18C6) <sub>2</sub> e-	$7.0 \times 10^8/255$	>1.0
Li+(PMPCY)e-	3.9 X10 <sup>4</sup> /196	>1.06
Rb+(C222)e-	$3.0 \times 10^4 / 100$	0.065
Li+(TMPAND)e-	large	?

In contrast to the high electronic conductivity of  $K^+(C222)e^-$ , the electrides  $Cs^+(15C5)_2e^-$  and  $Cs^+(18C6)_2e^-$  exhibit very low electronic conductivity but appear to be the first examples of ionically conductive electrides. The mechanism of the ionic conductivity may involve release of the cesium cation from its crown ether cage coupled with its reduction to  $Cs^0$  by an electron anion of the system. Ionic conductivity then results from the transfer of  $Cs^+$ 

between anionic sites in the lattice. A large portion of the activation energy for conductivity in these compounds may be the release of the cation from its crown ether cage. This is supported by the order of the activation energies of the two compounds. Cs+(18C6)<sub>2</sub>e<sup>-</sup>, which should have the higher complex stability, has an activation energy of 1.0 eV as opposed to only 0.7 eV for Cs+(15C5)<sub>2</sub>e<sup>-</sup>. The addition of small amounts of cesium as a dopant in Cs+(18C6)<sub>2</sub>e<sup>-</sup> has been shown to be the probable cause of the semiconductor behavior which was previously recorded for this compound. Attempts to dope Cs+(15C5)<sub>2</sub>e<sup>-</sup> in a similar fashion resulted in phase separation of the synthesis product.

Semiconductor behavior was observed in Li<sup>+</sup>(PMPCY)e<sup>-</sup>. The system appears to be doped with lithium which leads to increased conductivity and a low apparent band gap. Li<sup>+</sup>(TMPAND)e<sup>-</sup>, although not pure, may be the first example of an insulating electride.

The thermal properties of electrides have been found to be equally variable. A method has been developed to examine the stability and decomposition kinetics of electrides at a single temperature through the use of DSC. The application of this method has shown K+(C222)<sub>2</sub>e- to be stable for less than two days at -57 °C, while Li+(PMPCY)e- decomposes only over a period of several days at room temperature. The method shows first-order reaction kinetics for the decomposition of Li+(PMPCY)e- while K+(C222)e- appears to undergo an autocatalytic decomposition. Although the mechanism of decomposition is unknown, these results indicate that two different mechanisms for the decomposition of electrides may exist.

# V.B. Suggestions for Further Work

Much progress has been made in the last several years in the study of alkalides and electrides. Crystal structure determinations and the synthesis of more stable compounds are two of the important strides which have been taken. Together with the results of the present work, several suggestions for further study can be made.

The main push in the study of alkalide and electride conductivity should be the study of single crystals. Recent refinements of the crystal growing technique have resulted in crystals of certain electrides large enough for X-ray diffraction and NMR studies. It should now be possible to grow crystals up to several millimeters in size for conductivity studies. Through the use of single crystals, measurement of the true resistivities, band gaps, and conductivity tensors of electrides should be attainable.

Impedance spectroscopy has proven useful in the separation of electrode impedances from sample impedances for alkalides and electrides. To date, however, we have been unable to separate grain boundary impedances from that of the bulk. Since alkalide and electride samples must be kept in such clean environments to prevent decomposition, they lack many of the impurities and second phases present at the grain boundaries of other compounds. Because of this, the conductivity properties of grain boundaries in alkalides and electrides are probably much closer to those of the bulk and, therefore, much more difficult to separate from the bulk. It may be possible to imbed powdered electride samples in an inert liquid or

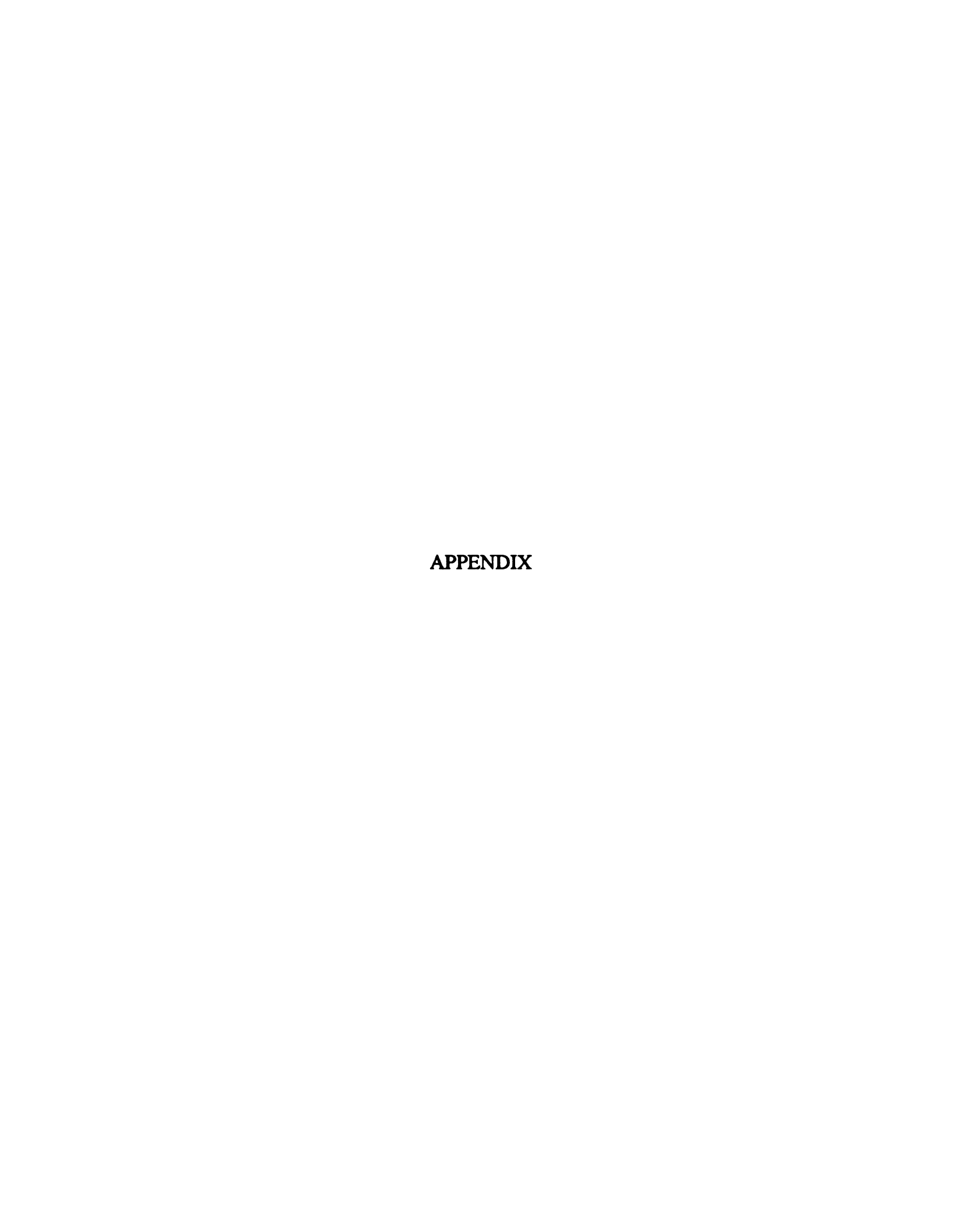
powder matrix which is itself a poor conductor. From such a sample, it may be possible, through the use of IS, to separate the sample impedance into specific arcs due to the electride grains, the matrix material, and the boundary regions between the matrix and the electride.

Thus far, IS studies have been limited by instrumentation to the study of samples which have impedances below 1.3 M $\Omega$ . The adaptation of present instrumentation or use of different instrumentation to measure higher impedance samples would allow more alkalides and electrides to be studied by IS.

Studies of Cs+(18C6)<sub>2</sub>e- have shown the importance of high purity samples for conductivity measurements. Many of the alkalides and electrides for which some electrical data exist were synthesized before current advances in the synthesis of these compounds. As such, they should be re-examined. In particular, checks for ionic conductivity should be made. To date, over 40 alkalides and electrides have been synthesized. A general view of the electrical properties of alkalides and electrides requires that the conductivity of more of these compounds be studied.

Finally, a method of testing the stability of alkalides and electrides has been developed. The use of this method on many alkalides and electrides could prove whether or not two types of decomposition actually exist in these compounds. Coupled with other techniques, likely mechanisms for the decomposition of electrides and alkalides can be determined. Once the mechanisms of decomposition are known, it may be possible to use this knowledge

to design complexants that will allow the synthesis of stable alkalides and electrides.



#### **APPENDIX**

#### DCRUN.bas

20 'PROGRAM DCRUN.BAS 3/6/89

25 PROGRAM TO RUN CONDUCTIVITY USING SQUARE WAVE PULSES OF ALTERNATING 30 POLARITY AND VARIABLE AMPLITUDE. PROGRAM CONTROLS A **KEITHLEY MICRO-**35 'OHMMETER MODEL 580 TO READ THE SAMPLE TEMPERATURE FROM A CARBON/GLASS 40 RESISTANCE THERMOMETER AFTER EACH SAMPLE RESISTANCE READING. 45 'A KEITHLEY MODEL 617 PROGRAMMABLE ELECTROMETER IS **USED BOTH AS THE** 50 CONTROLLABLE VOLTAGE SOURCE AND AS THE AMMETER TO MEASURE THE RESULTING 55 'CURRENT THROUGH THE SAMPLE. 200 DIM DDAT(2500,4) 295 ' 297 ' 300 PRINT 301 PRINT 350 INPUT "INPUT FILE NAME FOR DATA":FILE\$ 400 CLOSE #1 420 OPEN FILES FOR APPEND AS # 1 430 IF LOF(1)=0 THEN CLOSE #1 440 ELSE PRINT "FILE ALREADY EXISTS" :CLOSE #1 499 ' 600 DEF SEG=&HC000 610 CMD\$="SYSCON MAD=3, CIC=1, NOB=1, BA0=&H300" 620 VAR%=0 : FLG%=0 : BRD%=0 : IE488=0 630 CALL IE488(CMD\$, VAR%, FLG%, BRD%) 650 ' 670 ' 680 INPUT "LENGTH OF RUN IN SECONDS":RUNTIME

#### DCRUN.bas (Continued)

```
700 INPUT "POSITIVE BIAS VOLTAGE":PVO
710 INPUT "NEGATIVE BIAS VOLTAGE":NVO
720 INPUT "TIME ON EACH BIAS":WT
730 INPUT"NUMBER OF CYCLES BETWEEN MEASUREMENTS":ZE
735 '
736 '****PLACE INSTRUMENTATION INTO REMOTE OPERATION*******
737 '
740 CMD$="REMOTE 25"
745 CALL IE488(CMD$, VAR%, FLG%, BRD%)
750 CMD$ = "OUTPUT 25[$E]"
755 DVM\$ = "DOX"
760 CALL IE488(CMD$, DVM$, FLG%, BRD%)
770 CMD$="OUTPUT 25[$E]"
775 TON$="01X"
780 CALL IE488(CMD$, TON$, FLG%, BRD%)
800 CMD$="REMOTE 27"
820 CALL IE488(CMD$, VAR%, FLG%, BRD%)
850 CMD$= "OUTPUT 27[$E]"
860 A$="F1X"
870 CALL IE488(CMD$,A$,FLG%,BRD%)
900 X$="X"
920 CMD$="OUTPUT 27[$E]"
930 VON$= "O1X"
940 CALL IE488(CMD$, VON$, FLG%, BRD%)
949 '
951 '
995 COUNT%=0
998 M=0
999 T=TIMER
1000 J=TIMER-T
1001 M = M + 1
1002 PRINT "ELAPSED TIME";J
1010 IF M= ZE THEN COUNT%=COUNT%+1
1100 V$="V"
1200 VO$=V$+STR$(PVO)+X$
1300 CMD$="OUTPUT 27[$E]"
1400 CALL IE488(CMD$, VO$, FLG%, BRD%)
1599 PULSE=0
1600 STTIM=TIMER
1620 WHILE PULSE<WT
```

# DCRUN.bas (Continued) 1640 PULSE=TIMER-STTIM 1645 **WEND** 1160 IF M $\diamond$ ZE THEN GOTO 3000 1679 ' 1680 '\*\*\*\*\*\*\*\*\*\*\*\*COLLECT CURRENT AND TEMPERATURE DATA\*\*\*\* 1681 ' 1700 PAMP\$=SPACE\$(20) 1800 CMD\$="ENTER 27[\$]" 1900 CALL IE488(CMD\$, PAMP\$, FLG%, BRD%) 2000 PRINT PAMP\$ 2020 OHM\$=SPACE\$(20) 2030 CMD\$="ENTER 25[\$]" 2040 CALL IE488(CMD\$, OHM\$, FLG%, BRD%) **2045 PRINT OHM\$** 2050 E11=VAL(MID\$(OHM\$,5,20)) 2060 DDAT(COUNT%,3)=E11 2100 E1=VAL(MID\$(PAMP\$,5,20))2200 DDAT(COUNT%,1)=E1 3000 VO\$=V\$+STR\$(NVO)+X\$ 3100 CMD\$="OUTPUT 27[\$E]" 3200 CALL IE488(CMD\$, VO\$, FLG%,BRD%)3299 PULSE=0 3300 STTIM=TIMER 3320 WHILE PULSE < WT 3330 PULSE=TIMER-STTIM **3340 WEND** 3360 IF M ZE THEN GOTO 1000 3370 M=0 3400 NAMP\$=SPACE\$(20) 3450 CMD\$="ENTER 27[\$]" 3500 CALL IE488(CMD\$, NAMP\$, FLG%, BRD%) 3510 PRINT NAMP\$ 3530 CMD\$="ENTER 25[\$]" 3540 NOHM\$=SPACE\$(20) 3545 CALL IE488(CMD\$, NOHM\$, FLG%, BRD%) 3550 PRINT NOHM\$ 3560 E22=VAL(MID\$(NOHM\$,5,20)) 3570 DDAT(COUNT%,4)=E22 3600 E2=VAL(MID\$(NAMP\$,5,20)) 3700 DDAT(COUNT%,2) = E24000 IF J<RUNTIME GOTO 1000

4199 '

# DCRUN.bas (Continued)

499 '

#### OHMLAW.bas

20 'PROGRAM OHMLAW.BAS 8/16/89 ADAPTED FROM OHMTIME.BAS 25 'PROGRAM TO TAKE DC CONDUCTIVITY DATA AT VARIOUS **VOLTAGES AS A FUNCTION** 30 'OF TIME FOR OHM'S LAW PLOTS 35 USES THE KEITHLEY MODEL 617 PROGRAMMABLE ELECTROMETER AS VOLTAGE SOURCE 40 'AND AS A SENSITIVE OHMMETER. 55 ' 200 DIM DDAT(255.4) 201 DIM PVO(100) 295 ' 297 ' 300 PRINT 301 PRINT 350 INPUT "INPUT FILE NAME FOR DATA":FILE\$ 400 CLOSE #1 420 OPEN FILE\$ FOR APPEND AS # 1 430 IF LOF(1)=0 THEN CLOSE #1 440 ELSE PRINT "FILE ALREADY EXISTS" :CLOSE #1 450 INPUT "LENGTH OF RUN IN SECONDS":RUNTIME

## OHMLAW.bas (continued)

```
501 '
510 OPEN FILES FOR OUTPUT AS #1
600 DEF SEG=&HC000
610 CMD$="SYSCON MAD=3, CIC=1, NOB=1, BA0=&H300"
620 VAR%=0 : FLG%=0 : BRD%=0 : IE488=0
630 CALL IE488(CMD$, VAR%, FLG%, BRD%)
632 K=1
634 K=K+1
635 INPUT "INPUT VOLTAGE, ENTER 999 TO END"; PVO(K)
644 K=K-1
645 FOR J=1 TO K
650 '
652 '
800 CMD$="REMOTE 27"
820 CALL IE488(CMD$, VAR%, FLG%, BRD%)
850 CMD$= "OUTPUT 27[$E]"
860 A$="F1X"
870 CALL IE488(CMD$,A$,FLG%,BRD%)
900 X$="X"
920 CMD$="OUTPUT 27[$E]"
930 VON$= "O1X"
940 CALL IE488(CMD$, VON$, FLG%, BRD%)
995 COUNT%=0
1100 V$="V"
1200 VO$=V$+STR$(PVO(J))+X$
1300 CMD$="OUTPUT 27[$E]"
1350 TIMER1=TIMER
1400 CALL IE488(CMD$, VO$, FLG%, BRD%)
1499 '
1700 PAMP$=SPACE$(20)
1701 COUNT%=COUNT%+1
1800 CMD$="ENTER 27[$]"
1850 TIM=TIMER-TIMER1
1900 CALL IE488(CMD$.PAMP$.FLG%.BRD%)
2000 PRINT PAMP$
```

### OHMLAW.bas (continued)

## **VOLTCHAR.bas**

```
20 'PROGRAM voltcharge.bas ADAPTED FROM OHMLAW.BAS
25 PROGRAM TO APPLY A CONSTANT D.C. VOLTAGE AND MEASURE
    CURRENT FLOW AS
30 'A FUNCTION OF TIME
35 USES THE KEITHLEY MODEL 617 PROGRAMMABLE ELECTROMETER
    AS VOLTAGE SOURCE
40 WRITTEN BY KJM
55 '
200 DIM DDAT(2000,4)
295 '
297 '
300 PRINT
301 PRINT
350 INPUT "INPUT FILE NAME FOR DATA":FILE$
400 CLOSE #1
420 OPEN FILES FOR APPEND AS # 1
430 IF LOF(1)=0 THEN CLOSE #1
440 ELSE PRINT "FILE ALREADY EXISTS" :CLOSE #1
450 INPUT "LENGTH OF RUN IN SECONDS":RUNTIME
499 '
```

## VOLTCHAR.bas (continued)

```
501 '
510 OPEN FILE$ FOR OUTPUT AS #1
600 DEF SEG=&HC000
610 CMD$="SYSCON MAD=3, CIC=1, NOB=1, BA0=&H300"
620 VAR%=0 : FLG%=0 : BRD%=0 : IE488=0
630 CALL IE488(CMD$, VAR%, FLG%, BRD%)
631 PRINT
635 INPUT "INPUT VOLTAGE"; PVO
650 '
800 CMD$="REMOTE 27"
820 CALL IE488(CMD$, VAR%, FLG%, BRD%)
850 CMD$= "OUTPUT 27[$E]"
860 A$="F1X"
870 CALL IE488(CMD$,A$,FLG%,BRD%)
900 X$="X"
920 CMD$="OUTPUT 27[$E]"
930 VON$= "O1X"
940 CALL IE488(CMD$, VON$, FLG%, BRD%)
995 COUNT%=0
1100 V$="V"
1200 VO$=V$+STR$(PVO)+X$
1300 CMD$="OUTPUT 27[$E]"
1350 TIMER1=TIMER
1400 CALL IE488(CMD$, VO$, FLG%, BRD%)
1499 '
1501 '
1700 PAMP$=SPACE$(20)
1701 COUNT%=COUNT%+1
1800 CMD$="ENTER 27[$]"
1850 TIM=TIMER-TIMER1
1900 CALL IE488(CMD$,PAMP$,FLG%,BRD%)
2000 PRINT PAMP$
2100 E1=VAL(MID\$(PAMP\$,5,20))
2200 DDAT(COUNT%,1)=E1
2300 DDAT(COUNT%,2)=TIM
2320 WART=TIMER
2330 PULSE=TIMER-WART
2340 IF PULSE < 5 GOTO 2330
2400 IF TIM<RUNTIME GOTO 1700
```

#### VOLTCHAR.bas (continued)

4800 CMD\$="OUTPUT 27[\$E]"
4820 VO\$="OOX"
4830 CALL IE488(CMD\$, VO\$, FLG%, BRD%)
5100 FOR I=1 TO COUNT%
5200 WRITE #1, DDAT(I,1), DDAT(I,2)
5300 NEXT I
12000 END

#### DCVOLT.bas

10 'PROGRAM DCVOLT.BAS 2/12/90 BY KJM 20 TAKES VOLTAGE READINGS AT PROGRAMMED TIME DELAYS FOR A SAMPLE 190 DIM DDAT(2000,2) 200 INPUT "INPUT FILE NAME FOR DATA":FILE\$ 230 CLOSE #1 250 OPEN FILES FOR APPEND AS #1 260 IF LOG(1)=0 THEN CLOSE #1 270 ELSE PRINT "FILE ALREADY EXISTS": CLOSE #1 300 INPUT "DURATION OF RUN IN SECONDS": RUNTIME 350 ' 352 ' 360 DEF SEG=&HC000 370 CMD\$="SYSCON MAD=3, CIC=1, NOB=1, BA0=&H300" 380 VAR%=0: FLG%=0: VAR%=0: BRD%=0: IE488=0 390 CALL IE488(CMD\$, VAR%, FLG%, BRD%) 550 TON\$="01X" 560 CALL IE488(CMD\$, TON\$, FLG%, BRD%) 600 CMD\$="REMOTE 29" 620 CALL IE488(CMD\$, VAR%, FLG%, BRD%) 630 ' 632 ' 650 COUNT%=1 660 T=TIMER 700 J=TIMER-T 710 PRINT "ELAPSED TIME":J 750 PULSE =0

### DCVOLT.bas (continued)

760 STTIM=TIMER

780 WHILE PULSE<5

800 PULSE=TIMER-STTIM

**820 WEND** 

900 CMD\$="OUTPUT 29[\$E]"

920 A\$="F0X"

940 CALL IE488(CMD\$, A\$, FLG%, BRD%)

950 OHM\$= SPACE\$(20)

960 CMD\$="ENTER 29[\$]"

980 CALL IE488(CMD\$, OHM\$, FLG%, BRD%)

990 PRINT OHM\$

995 TIM=TIMER-T

1000 CMD\$="OUTPUT 29[\$E]"

2040 E1= VAL(MID\$(OHM\$,5,20))

2060 DDAT(COUNT%,1)=E1

2070 DDAT(COUNT%,2)=TIM

2080 COUNT%=COUNT%+1

3000 IF J<RUNTIME GOTO 700

3020 '

3031 '

3040 OPEN FILES FOR OUTPUT AS #1

**3060 FOR I=1 TO COUNT%** 

3080 WRITE #1, DDAT(I,1), DDAT(I,2)

3100 NEXT I

12000 END

#### **DCTIMDEP.bas**

- 20 'PROGRAM DCTIMDEP.BAS 2/90 ADAPTED FROM DCRUN.BAS
  25 'PROGRAM TO MEASURE THE LONG PERIOD TIME DEPENDENCE OF
  SAMPLE CONDUCTIVITY
- 30 'AT A SINGLE TEMPERATURE USING SQUARE WAVE VOLTAGE PULSES OF ALTERNATE
- 35 'POLARITY
- 45 'A KEITHLEY MODEL 617 PROGRAMMABLE ELECTROMETER IS USED BOTH AS THE
- 50 'CONTROLLABLE VOLTAGE SOURCE AND AS THE AMMETER TO MEASURE THE RESULTING

```
DCTIM.bas (continued)
55 'CURRENT THROUGH THE SAMPLE.
200 DIM DDAT(255,4)
295 '
297 '
300 PRINT
301 PRINT
350 INPUT "INPUT FILE NAME FOR DATA":FILE$
400 CLOSE #1
420 OPEN FILE$ FOR APPEND AS # 1
430 IF LOF(1)=0 THEN CLOSE #1
440 ELSE PRINT "FILE ALREADY EXISTS" :CLOSE #1
450 INPUT "LENGTH OF RUN IN SECONDS":RUNTIME
499 '
500 '***************INITIALIZE THE BOARD***************
501 '
600 DEF SEG=&HC000
610 CMD$="SYSCON MAD=3, CIC=1, NOB=1, BA0=&H300"
620 VAR%=0 : FLG%=0 : BRD%=0 : IE488=0
630 CALL IE488(CMD$, VAR%, FLG%, BRD%)
631 PRINT
650 '
652 '
700 INPUT "POSITIVE BIAS VOLTAGE":PVO
710 INPUT "NEGATIVE BIAS VOLTAGE";NVO
720 INPUT "TIME ON EACH BIAS":WT
730 INPUT"NUMBER OF CYCLES BETWEEN MEASUREMENTS":ZE
739 '
740 '********PLACE ELECTROMETER INTO REMOTE OPERATION***
741 '
775 TON$="01X"
780 CALL IE488(CMD$, TON$, FLG%, BRD%)
800 CMD$="REMOTE 27"
820 CALL IE488(CMD$, VAR%, FLG%, BRD%)
850 CMD$= "OUTPUT 27[$E]"
860 A$="F1X"
870 CALL IE488(CMD$, A$, FLG%, BRD%)
900 X$="X"
920 CMD$="OUTPUT 27[$E]"
```

930 VON\$= "O1X"

# DCTIM.bas (continued)

```
940 CALL IE488(CMD$, VON$, FLG%, BRD%)
950 '
952 '
995 COUNT%=0
998 M=0
999 T=TIMER
1000 J=TIMER-T
1001 M=M+1
1010 IF M= ZE THEN COUNT%=COUNT%+1
1100 V$="V"
1200 VO$=V$+STR$(PVO)+X$
1300 CMD$="OUTPUT 27[$E]"
1400 CALL IE488(CMD$, VO$, FLG%, BRD%)
1599 PULSE=0
1600 STTIM=TIMER
1620 WHILE PULSE<WT
1640 PULSE=TIMER-STTIM
1645 WEND
1660 IF M\diamondZE THEN GOTO 3000
1700 PAMP$=SPACE$(20)
1800 CMD$="ENTER 27[$]"
1900 CALL IE488(CMD$,PAMP$,FLG%,BRD%)
2000 PRINT PAMP$
2030 J=TIMER-T
2040 DDAT(COUNT%,3)=J
2100 E1=VAL(MID\$(PAMP\$,5,20))
2200 DDAT(COUNT%,1)=E1
3000 VO$=V$+STR$(NVO)+X$
3100 CMD$="OUTPUT 27[$E]"
3200 CALL IE488(CMD$, VO$, FLG%,BRD%)
3299 PULSE=0
3300 STTIM=TIMER
3320 WHILE PULSE < WT
3330 PULSE=TIMER-STTIM
3340 WEND
3360 IF M\diamondZE THEN GOTO 1000
3370 M=0
3400 NAMP$=SPACE$(20)
3450 CMD$="ENTER 27[$]"
3500 CALL IE488(CMD$, NAMP$, FLG%, BRD%)
```

# DCTIM.bas (continued) 3510 PRINT NAMP\$ 3600 E2=VAL(MID\$(NAMP\$,5,20))3700 DDAT(COUNT%,2) = E24000 IF J<RUNTIME GOTO 1000 4599 ' 4600 '++++++++++++++++++TURN OFF VOLTAGE SOURCE++++++++++++ 4601 ' 4800 CMD\$="OUTPUT 27[\$E]" 4820 VO\$="O0X" 4830 CALL IE488(CMD\$, VO\$, FLG%, BRD%) 4849 ' 4851 ' 4900 CLOSE #1 5000 OPEN FILES FOR OUTPUT AS #1 **5100 FOR I=1 TO COUNT%** 5200 WRITE #1, DDAT(I,1), DDAT(I,2), DDAT(I,3) 5300 NEXT I

#### **INTERMIT.bas**

12000 END

20 'PROGRAM INTERMIT.BAS 2/28/90 25 PROGRAM TO RUN CONDUCTIVITY USING SQUARE WAVE PULSES OF ALTERNATING 30 'POLARITY AND VARIABLE AMPLITUDE. gIVES INTERMITTANT **PULSES AT TIMED** 35 'DELAYS DESIGNED TO OPERATE AT A SINGLE TEMPERATURE 45 'A KEITHLEY MODEL 617 PROGRAMMABLE ELECTROMETER IS **USED BOTH AS THE** 50 'CONTROLLABLE VOLTAGE SOURCE AND AS THE AMMETER TO MEASURE THE RESULTING 55 CURRENT THROUGH THE SAMPLE. 60 WRITTEN 3/6/89 BY KJM AND A. EINSTEIN DFY 200 DIM DDAT(2500.4) 297 ' 300 PRINT

### INTERMIT.bas (continued)

```
301 PRINT
350 INPUT "INPUT FILE NAME FOR DATA":FILE$
400 CLOSE #1
420 OPEN FILE$ FOR APPEND AS # 1
430 IF LOF(1)=0 THEN CLOSE #1
440 ELSE PRINT "FILE ALREADY EXISTS" :CLOSE #1
450 INPUT "LENGTH OF RUN IN SECONDS":RUNTIME
499 '
501 '
600 DEF SEG=&HC000
610 CMD$="SYSCON MAD=3, CIC=1, NOB=1, BA0=&H300"
620 VAR%=0 : FLG%=0 : BRD%=0 : IE488=0
630 CALL IE488(CMD$, VAR%, FLG%, BRD%)
631 PRINT
650 '
652 '
700 INPUT "POSITIVE BIAS VOLTAGE";PVO
710 INPUT "NEGATIVE BIAS VOLTAGE":NVO
720 INPUT "TIME ON EACH BIAS"; WT
730 INPUT"TIME BETWEEN POINTS"; ZE
750 '
751 '**************************PLACE INSTRUMENTATION INTO REMOTE***
752 '
800 CMD$="REMOTE 27"
820 CALL IE488(CMD$, VAR%, FLG%, BRD%)
850 CMD$= "OUTPUT 27[$E]"
860 A$="F1X"
870 CALL IE488(CMD$,A$,FLG%,BRD%)
900 X$="X"
950 '
952 '
995 COUNT%=0
998 LONG = TIMER
999 T=TIMER
1000 J=TIMER-T
1002 COUNT%=COUNT%+1
1003 P=0
1010 M=TIMER
```

# INTERMIT.bas (continued)

1020 WHILE P<ZE

1030 P=TIMER-M

**1040 WEND** 

1050 CMD\$="OUTPUT 27[\$E]"

1060 VON\$="01X"

1070 CALL IE488(CMD\$, VON\$, FLG%, BRD%)

1100 V\$="V"

1200 VO\$=V\$+STR\$(PVO)+X\$

1300 CMD\$="OUTPUT 27[\$E]"

1400 CALL IE488(CMD\$, VO\$, FLG%, BRD%)

1599 PULSE=0

1600 STTIM=TIMER

1620 WHILE PULSE<WT

1640 PULSE=TIMER-STTIM

**1645 WEND** 

1700 PAMP\$=SPACE\$(20)

1800 CMD\$="ENTER 27[\$]"

1900 CALL IE488(CMD\$,PAMP\$,FLG%,BRD%)

2000 PRINT PAMP\$

2020 OHM\$=SPACE\$(20)

2030 CMD\$="ENTER 25[\$]"

2040 CALL IE488(CMD\$, OHM\$, FLG%, BRD%)

2045 PRINT OHM\$

2050 E11=VAL(MID\$(OHM\$,5,20))

2060 DDAT(COUNT%,3)=E11

2100 E1=VAL(MID\$(PAMP\$,5,20))

2200 DDAT(COUNT%,1)=E1

2210 LL = TIMER - LONG

2220 DDAT(COUNT%,3)=LL

2230 PRINT "ELAPSED TIME";LL

3000 VO\$=V\$+STR\$(NVO)+X\$

3100 CMD\$="OUTPUT 27[\$E]"

3200 CALL IE488(CMD\$, VO\$, FLG%,BRD%)

3299 PULSE=0

3300 STTIM=TIMER

3320 WHILE PULSE < WT

3330 PULSE=TIMER-STTIM

3340 WEND

3370 M=0

3400 NAMP\$=SPACE\$(20)

3450 CMD\$="ENTER 27[\$]"

#### INTERMIT.bas (continued)

```
3500 CALL IE488(CMD$, NAMP$, FLG%, BRD%)
3510 PRINT NAMP$
3530 CMD$="ENTER 25[$]"
3540 NOHM$=SPACE$(20)
3545 CALL IE488(CMD$, NOHM$, FLG%, BRD%)
3550 PRINT NOHM$
3560 E22=VAL(MID$(NOHM$,5,20))
3570 DDAT(COUNT%,4)=E22
3600 E2=VAL(MID$(NAMP$,5,20))
3700 DDAT(COUNT%.2) = E2
4800 CMD$="OUTPUT 27[$E]"
4820 VO$="O0X"
4830 CALL IE488(CMD$, VO$, FLG%, BRD%)
4850 IF J<RUNTIME GOTO 1000
4870 '
4872 '
4900 CLOSE #1
5000 OPEN FILES FOR OUTPUT AS #1
5100 FOR I=1 TO COUNT%
5200 WRITE #1, DDAT(I.1), DDAT(I.2), DDAT(I.3)
5300 NEXT I
12000 END
```

#### KIRP.bas

### KIRP.bas (continued)

```
30 CMD$ = "SYSCON MAD=3, CIC = 1, NOB=1, BA0=&H300"
35 VAR%=0: FLG%=0: BRD%=0: IE488=0
40 CALL IE488(CMD$, VAR%, FLG%, BRD%)
41 CMD$ = "REMOTE 17"
42 CALL IE488(CMD$, VAR%, FLG%, BRD%)
45 INPUT "INPUT OSCILLATOR VOLTAGE IN VOLTS": OSC
50 BI\$ = "OL+"
55 WORK$ = "ENEX"
60 VOLT$ = BI$ + STR$(OSC)+ WORK$
70 CMD$ = "OUTPUT 17[$E]"
75 IF OSC>1.1 GOTO 11900
76 IF OSC< .005 GOTO 11900
80 CALL IE488(CMD$, VOLT$, FLG%, BRD%)
100 INPUT "STARTING FREO FOR LOG DATA IN kHz":STARTLOG
110 INPUT "ENDING FREQ FOR LOG DATA IN kHz"; ENDLOG
120 MKEV = FIX(LOG(STARTLOG)/LOG(1.25))
130 \text{ KKEV} = \text{FIX}(\text{LOG}(\text{ENDLOG})/\text{LOG}(1.25))
135 \text{ COUNT\%} = 0
140 \text{ FOR N} = \text{MKEV TO KKEV}
150 X = 1.25 ^ N
160 \text{ COUNT\%} = \text{COUNT\%} + 1
200 '***********
201 'INITIALIZE THE BOARD
202 '************************
250 DEF SEG = &HC000
275 CMD$ = "SYSCON MAD = 3, CIC = 1, NOB = 1, BA0 = &H300"
300 \text{ VAR\%} = 0: FLG% = 0: BRD% = 0: IE488 = 0
325 CALL IE488(CMD$, VAR%, FLG%, BRD%)
350 PLACE 4192A INTO REMOTE OPERATION
375 CMD$ = "REMOTE 17"
400 CALL IE488(CMD$, VAR%, FLG%, BRD%)
410 VAR$="C2ENEX"
415 CMD$="OUTPUT 17[$E]"
420 CALL IE488(CMD$, VAR$, FLG%, BRD%)
426 TELL 4192A TO MEASURE IZI AND PHASE
450 VAR$ = "A1ENB1ENEX"
475 \text{ CMD} = "OUTPUT 17[$E]"
```

#### KIRP.bas (continued)

```
500 CALL IE488(CMD$, VAR$, FLG%, BRD%)
510 'SET OPERATING FREOUENCY
511 '*********************
525
    MM$ = "FR+"
550 WORK$ = "ENEX"
575 MAR$ = MM$ + STR$(X) + WORK$
600
    CMD$ = "OUTPUT 17[E$]"
625 CALL IE488(CMD$, MAR$, FLG%, BRD%)
     READ THE DATA AND PRINT IT OUT ON THE SCREEN
650'************************
     GIVE AN INSTRUMENT RESPONSE TIME
660 \text{ TIMER}1 = \text{TIMER}
662 \text{ TIM} = \text{TIMER}
664 IF TIM<TIMER1+1 GOTO 662
675 DVM$ = SPACE$(45)
700 \text{ CMD} = "ENTER 17[$]"
725 CALL IE488(CMD$, DVM$, FLG%, BRD%)
750 PRINT "FREO="; X; " "; DVM$
800 E1 = VAL(MID\$(DVM\$,5,20))
825 IMPDAT(COUNT%,1) = E1
850 E2 = VAL(MID\$(DVM\$,21,20))
875 IMPDAT(COUNT\%.2) = E2
925 IMPDAT(COUNT%,11) = X
950 NEXT N
990 '********
995 WRITE DATA TO THE CORRECT FILE
1050 INPUT "PLEASE INPUT SAMPLE TEMP AND UNITS": TEMP$
1060 INPUT "PLEASE INPUT SAMPLE TEMPERATURE DRIFT": UNC$
1100 OPEN FILE$ FOR OUTPUT AS #1
1199 \text{ SPC} = SPACE$(10)
1200 WRITE #1, TEMP$, OSC
1210 WRITE #1, UNC$
1220 WRITE #1, SPC$
1230 WRITE #1, "FREQ(kHz)", " |Z|", " PHASE", " Re Z", " -Im Z"
1300 FOR I = 1 TO COUNT%
1400 WRITE #1, IMPDAT(I,11), IMPDAT(I,1), IMPDAT(I,2)
1500 NEXT I
2000 END
```

# KIRP.bas (continued)

5000 '

5002 '

**5025 PRINT** 

**5030 PRINT** 

5050 PRINT "WHAT DATA FILE WOULD YOU LIKE TO CREATE?"

5100 INPUT "PLEASE INPUT ITS FULL NAME"; FILE\$

5125 CLOSE #1

5150 OPEN FILE\$ FOR APPEND AS #1

5175 IF LOF(1) = 0 THEN CLOSE #1 :RETURN

5200 PRINT " "

5225 PRINT " "

**5230 PRINT** 

5250 PRINT "THIS FILE ALREADY EXISTS AND CONTAINS DATA"

5275 INPUT "PLEASE INPUT 'Y' TO MAKE IT CURRENT (DATA WILL BE OVERWRITTEN"; YES\$

5300 IF YES\$ = "Y" THEN CLOSE #1 :RETURN

5310 IF YES\$ = "y" THEN CLOSE #1 :RETURN

5400 IF YES\$ <>"Y" THEN CLOSE #1:GOTO 5000

11900 PRINT "OSCILLATOR VOLTAGE MUST BE LESS THAN 1.1V AND GREATER THAN .005v"

12000 END

#### LIST OF REFERENCES

- 1 W. Weyl, Annalen der Physik und Chemie, 197, 601 (1864).
- 2 J.L. Dye, Pure & Appl. Chem., 49, 3 (1977).
- J.C. Thompson, "Electrons in Liquid Ammonia", Clarendon Press (Oxford) (1976).
- 4 C.J. Pedersen, J. Am. Chem. Soc., 89, 7017 (1967).
- 5 B. Dietrich, J.M. Lehn, and J.P. Sauvage, *Tet. Letters*, <u>34</u>, 2885 (1969).
- B. Dietrich, J.M. Lehn, and J.P. Sauvage, *Tet. Letters*, <u>34</u>, 2889 (1969).
- J.L. Dye, M.G. DeBacker, and V.A. Nicely, J. Am. Chem. Soc., <u>92</u>, 5225 (1970).
- J.L. Dye, M.T. Lok, F.J. Tehan R.B. Coolen, N. Papadakis, J.M. Ceraso, and M.G. DeBacker, *Ber. Bunsenges. Phys. Chem.*, 75, 659 (1971).
- J.L. Dye, J.M. Ceraso, M.T. Lok, B.L. Barnett, and F.J. Tehan, J.
   Am. Chem. Soc., 96, 608 (1974).
- 10 F.J. Tehan, B.L. Barnett, and J.L. Dye, J. Am. Chem. Soc., <u>96</u>, 7203 (1974).
- 11 A.S. Ellaboudy, P.B. Smith, and J.L. Dye, J. Am. Chem. Soc., <u>105</u>, 6490 (1983).
- 12 A.G.M. Barrett, C.R.A. Godfrey, D.M. Hollinshead, P.A. Prokopiou, D.H.R. Barton, R.B. Boar, L. Joukhadar, J.F. McGhie, and S.C. Misra, J. Chem. Soc. Perkins Trans. 1, 1981, 1501.

- 13 A. Bencini, A. Bianchi, M. Ciampolini, E. Garcia-Espana, P. Dapporta, M. Micheloni, P. Paoli, J.A. Ramirez, B. Valtancoli, J. Chem. Soc. Chem. Commun., 1989, 701.
- 14 R. Concepcion and J.L. Dye, J. Am. Chem. Soc., 109, 7203 (1987).
- 15 J.L. Dye, J. Phys. Chem., 88, 3842 (1984).
- 16 J.L. Dye, J. Phys. Chem., <u>84</u>, 1084 (1980).
- 17 Mark E. Kuchenmeister, Ph.D. Dissertation, Michigan State University, (1989).
- 18 M.E. Kuchenmeister, and J.L. Dye, J. Am. Chem. Soc., 111, 935 (1989).
- 19 J.L. Eglin, and E.P. Jackson, unpublished results, this laboratory.
- 20 Mary L. Tinkham, Ph.D. Dissertation, Michigan State University, (1985).
- 21 Ahmed S. Ellaboudy, Ph.D. Dissertation, Michigan State University, (1984).
- 22 A.L. Wayda, and J.L. Dye, J. Chem. Educ., 62, 356 (1985).
- 23 J.M. Ceraso, and J.L. Dye, J. Chem. Phys., 61, 1585 (1974).
- 24 J.L. Dye, C.W. Andrews, and J.M. Ceraso, *J. Phys. Chem.*, <u>79</u>, 3076 (1975).
- A.S. Ellaboudy, M.L. Tinkham, B. Van Eck, J.L. Dye, and P.B. Smith, J. Phys. Chem., 88, 3853 (1984).
- 26 S.B. Dawes, A.S. Ellaboudy, and J.L. Dye, J. Am. Chem. Soc., <u>108</u>, 3534 (1986).
- D. Issa, A.S. Ellaboudy, R. Janakiraman, and J.L. Dye, *J. Phys. Chem.*, 88, 3847 (1984).
- 28 S.B. Dawes, D.L. Ward, O. Fussa-Rydel, R.H. Huang, and J.L. Dye, *Inorg. Chem.*, 28, 2132 (1989).

- 29 S.B. Dawes, D.L. Ward, R.H. Huang, and J.L. Dye, J. Am. Chem. Soc., 108, 3534 (1986).
- 30 M.G. DaGue, J.S. Landers, H.L. Lewis, and J.L. Dye, *Chem. Phys. Letters*, <u>66</u>, 169 (1979).
- 31 J.L. Dye, M.G. DaGue, M.R. Yemen, J.S. Landers, and H.L. Lewis, J. *Phys. Chem.*, <u>84</u>, 1096 (1980).
- 32 S. Jaenicke, M.K. Faber, J.L. Dye, and W.P. Pratt Jr., *J. Solid State Chem.*, 68, 239 (1987).
- 33 L.D. Le, D. Issa, B. Van Eck, and J.L. Dye, J. Phys. Chem., <u>86</u>, 7 (1982).
- 34 J.S. Landers, A. Stacy, M.J. Sienko, and J.L. Dye, J. Phys. Chem., 85, 1096 (1981).
- 3.5 R.S. Bannwart, S.A. Solin, M.G. DeBacker, and J.L. Dye, J. Am. Chem. Soc., 111, 5552, (1989).
- J. Papaioannou, S. Jaenicke, and J.L. Dye, J. Solid State Chem., 67, 122 (1987).
- 37 J.L. Dye, Prog. Inorg. Chem., <u>32</u>, 327 (1984).
- 38 J.L. Dye, and M.G. DeBacker, Ann. Rev. Phys. Chem., 38, 271 (1987).
- Mei-Tak Lok., Ph.D. Dissertation, Michigan State University (1973).
- Michael R. Yemen, Ph.D. Dissertation, Michigan State University (1982).
- 41 Margaret K. Faber, Ph.D. Dissertation, Michigan State University (1985).
- 42 F. Nomouinde Tientega, M.S. Dissertation, Michigan State University (1984).
- Dheeb Issa, Ph.D. Dissertation, Michigan State University (1982).

- Odette Fussa, Ph.D. Dissertation, Michigan State University (1986).
- 45 J.L. Dye and A. Ellaboudy, Chem. in Britain, 20, 210 (1984).
- 46 Unpublished results, this laboratory.
- 47 Steven B. Dawes, Ph.D. Dissertation, Michigan State University (1986).
- 48 L.J. van der Pauw, *Phil. Res. Repts.*, <u>13</u>, 1 (1958).
- 49 L.J. van der Pauw, Phil. Tech. Rev., 20, 220 (1958).
- 50 J.L. Dye, Pure & Appl. Chem., 61, 1555 (1989).
- 51 A. Maercker, Angew. Chem. Int. Ed. Engl., 26, 972 (1987).
- M.E. Brown, "Introduction to Thermal Analysis", Chapman and Hall, London 1988.
- 53 P. Murray and J. White, Trans. Brit. Ceram. Soc., <u>54</u>, 151 (1955).
- 54 H.E. Kissinger, J. Res. Nat. Bur. Stand., <u>57</u>, 217 (1956).
- 55 H.E. Kissinger, Anal Chem., 29, 1702 (1957).
- 56 T. Ozawa, Bull. Chem. Soc. Japan, 38, 1881 (1965).
- G. Krien, "3rd Symposium on the Chemical Problems Associated with the Stability of Explosives", ed. J. Hansson, Ystad, May 1973.
- R.G. Patel and M.M. Chaudri, "4th Symposium on the Chemical Problems Associated with the Stability of Explosives", Molle, May 1976.
- 59 R.G. Patel and M.M. Chaudri, *Thermochim. Acta*, <u>25</u>, 247 (1978).
- 60 A.A. Van Dooren and B.W. Muller, *Thermochim. Acta*, <u>65</u>, 257 (1983).

- R.H. Huang, M.K. Faber, K.J. Moeggenborg, D.L. Ward, and J.L. Dye, *Nature*, 331, 6157 (1988).
- G. Goodman, "Advances in Ceramics vol. 1", The American Ceramic Society, Columbus OH 1981 pg 215.
- 63 S.S. Villiamil, H.Y. Lee, and L.C. Burton, *IEEE Trans. Compon.*, *Hybrids, Manuf. Technol.*, CHMT-10, 482 (1987).
- 64 G.E. Pike and C.H. Seager, J. Appl. Phys., <u>50</u>, 3414 (1979).
- 6.5 S.M. Sze, "Physics of Semiconductor Devices", John Wiley & Son, New York 1981.
- 66 B.L. Sharm, "Metal-Semiconductor Schottky Barrier Junctions and Their Applications", Plenum Press, New York 1984.
- 67 W. Schottky, Naturwissenschaften, 26, 243 (1938).
- 68 D.H. Navon, "Semiconductor Microdevices and Materials", Holt, Rinehart and Winston, New York 1986.
- 69 L.J. van der Pauw., Phil. Res. Repts., 16, 187 (1961).
- 70 J.D. Wasscher, *Phil. Res. Repts.*, <u>16</u>, 301 (1961).
- 71 H.C. Montgomery, J. Appl. Phys., <u>42</u>, 2971 (1971).
- 72 B.F. Logan, S.O. Rice, and R.F. Wick, *J. Appl. Phys.*, <u>42</u>, 2975 (1971).
- 73 J.E. Bauerle, J. Phys. Chem. Solids, <u>30</u>, 2657 (1969).
- 74 J.R. MacDonald, "Impedance Spectroscopy", John Wiley & Sons, New York 1987.
- 75 J.R. MacDonald and J.A. Garber, J. Electrochem. Soc., <u>124</u>, 1022 (1977).
- J.R. MacDonald, J. Schoonman, and A.P. Lehnen, J. Electroanal. Chem., 131, 77 (1982).
- 77 J. Papaioannou, unpublished results, this laboratory.

- 78 M.P. Lepselter and S.M. Sze, Bell Syst. Tech. J., <u>47</u>, 195 (1968).
- 79 J.M. Andrews and F.B. Koch, Solid State Elect., 14, 901 (1971).
- 80 D.L. Ward, R.H. Huang, and J.L. Dye, *Acta Cryst. C*, <u>C44</u>, 1374 (1988).
- 8.1 S.B. Dawes, J.L. Eglin, K.J. Moeggenborg, J. Kim, and J.L. Dye, To Be Published.
- 82 R.H. Huang, M.E. Kuchenmeister, D.L. Ward, and J.L. Dye, *Acta. Cryst.*, In Press.
- 83 I.M. Hodge, M.D. Ingram, and A.R. West, *J. Electroanal. Chem.*, 74, 125 (1976).
- 84 Sample provided by R.H. Huang.
- 85 J.L. Eglin, unpublished results.
- 86 Sample provided by J.L. Eglin.

MICHIGAN STATE UNIV. LIBRARIES 31293008914388